

# Final Report for Creative 3D Plant Optimization (C3PO) System

eXploration Systems and Habitation (X-Hab) 2018 Academic Innovation Challenge

## Advisors

Timothy Taylor, PhD  
Biological Engineering  
Utah State University

Scott Jones, PhD  
Plants, Soils, and Climate  
Utah State University

Ryan Summers, PhD  
Chemical Engineering  
University of Alabama

Jackson Graham, M.S.  
Mechanical Engineering  
Utah State University

Iren Bencze, M.A.  
Biological Engineering  
Utah State University

## List of Participants

Shelby Berrett  
Biological Engineering  
Utah State University

Camille Daniels  
Biological Engineering  
Utah State University

Cameron LeBaron  
Biological Engineering  
Utah State University

Carter Bodnar  
Chemical Engineering  
University of Alabama

Amanda Dennis  
Chemical Engineering  
University of Alabama

Nicholas Narrell  
Chemical Engineering  
University of Alabama

Joanna Boyd  
Mechanical Engineering  
Utah State University

Jaci Fielding  
Biological Engineering  
Utah State University

Ty Nicholas  
Biological Engineering  
Utah State University

Jake Brockwell  
Chemical Engineering  
University of Alabama

Crystal Fowler  
Biological Engineering  
Utah State University

Adreann Peel  
Biological Engineering  
Utah State University

Rebecca Brown  
Mechanical Engineering  
Utah State University

Dallin Gividen  
Biological Engineering  
Utah State University

Andrew Poulos  
Chemical Engineering  
University of Alabama

Emily Burgett  
Biological Engineering  
Utah State University

Camren Hansen  
Mechanical Engineering  
Utah State University

David Redd  
Biological Engineering  
Utah State University

Kaitlin Burnash  
Chemical Engineering  
University of Alabama

Skyler Heiner  
Biological Engineering  
Utah State University

Joshua Wallace  
Biological Engineering  
Utah State University

Logan Crawford  
Chemical Engineering  
University of Alabama

Brandon Furman  
Mechanical Engineering  
Utah State University

# Contents

<b>1</b>	<b>TEAM GOAL .....</b>	<b>1</b>
1.1	PROPOSAL .....	1
1.2	PREVIOUS EFFORTS .....	1
1.3	VEGGIE.....	1
1.4	CONCEPT OF DESIGN.....	2
1.5	IDENTIFICATION OF THE CUSTOMER .....	2
1.6	TARGET END USER .....	2
1.7	REQUIREMENTS .....	2
1.8	OTHER GOALS AND DESIRED OBJECTIVES .....	3
1.9	END DELIVERABLE .....	3
1.9	ISSUES OF PRIMARY CONCERN .....	3
<b>2</b>	<b>TEAM STRUCTURE AND COMMUNICATIONS.....</b>	<b>3</b>
2.1	ORGANIZATIONAL AND WORK BREAKDOWN.....	3
2.2	GANTT CHART .....	5
2.3	GOVERNING STANDARDS .....	5
2.4	ENVIRONMENTAL AND SOCIETAL IMPACT .....	5
2.5	SAFETY.....	5
2.6	FINANCIAL BUDGET.....	7
<b>3</b>	<b>SUBSTRATE DESIGN.....</b>	<b>8</b>
3.1	CONCEPTUAL ANALYSIS OF THE BLOCK.....	8
3.2	IMPROVEMENTS UPON PREVIOUS EFFORTS .....	8
	3.2.1 <i>Printing Procedures</i> .....	8
	3.2.2 <i>Printing Schedule</i> .....	10
3.3	VARIOUS PORE SIZES.....	10
3.4	VARIOUS INTERNAL GEOMETRIES .....	10
	3.4.1 <i>Crosshatched Design</i> .....	11
	3.4.2 <i>Swiss Cheese Design</i> .....	11
	3.4.3 <i>Microchannel Design</i> .....	11
	3.4.4 <i>Control Block</i> .....	11
3.5	HYDROPHOBIC AND HYDROPHILIC CHANNELS.....	12
3.6	COMPOSITE BLOCKS.....	12
3.7	CHEMICAL LEACHING .....	12
3.8	OFF GASSING .....	15
3.9	OFF GASSING PROCEDURES.....	16
3.10	OFF GASSING RESULTS .....	16
3.11	SUBSTRATE OVERSATURATION .....	16
3.12	FAVORABLE WATER/AIR RATIOS.....	17
3.13	WATER RETENTION CURVES .....	17
3.14	TESTING PROCEDURES.....	19
3.15	PORE SIZE COMPARISON.....	20
	3.15.1 <i>The 2 mm Comparison</i> .....	20
	3.15.2 <i>The 2.5 mm Comparison</i> .....	20
	3.15.3 <i>The 3 mm Comparison</i> .....	21
3.16	DESIGN COMPARISON .....	22

3.16.1	Crosshatched Comparison .....	22
3.16.2	Microchannel Comparison.....	22
3.16.3	Swiss Cheese Comparison.....	23
3.16.4	Control Comparison.....	23
3.17	FINAL DESIGN.....	24
<b>4</b>	<b>SUBSTRATE SIMULATION .....</b>	<b>24</b>
4.1	PRELIMINARY INFORMATION .....	24
4.1.1	Motivation .....	24
4.1.2	The Boltzmann Equation .....	25
4.1.2	The Lattice Boltzmann Method .....	26
4.2	ALGORITHM .....	27
4.2.1	Variable Initialization .....	27
4.2.2	Streaming Step (Begin Loop) .....	27
4.2.3	Macroscopic Variables.....	28
4.2.4	Cohesive & Adhesive Forces .....	28
4.2.5	Equilibrium Distribution.....	29
4.2.6	Collision Step (Restart Loop).....	30
4.3	SIMULATION CHARACTERIZATION, PARAMETERIZATION, AND VALIDATION .....	30
4.3.1	Surface Tension .....	30
4.3.2	Contact Angle .....	31
4.3.3	Capillary Intrusion .....	32
4.4	SUBSTRATE SIMULATION.....	33
4.4.1	Geometry.....	33
<b>5</b>	<b>PLANTS .....</b>	<b>35</b>
5.1	GERMINATION .....	35
5.2	PLANT GROWTH .....	36
5.3	POTENTIAL ISSUES .....	36
5.4	WATER AND NUTRIENT DELIVERY .....	36
5.5	HYDROGELS/AGAR .....	37
5.6	PORE GEOMETRY .....	37
5.7	SEED PLANTING PROCEDURE .....	37
5.8	SCHEDULE.....	37
5.9	GROWTH CHAMBER/HOUSING .....	38
5.10	OPTIMAL SUBSTRATE DESIGN .....	38
<b>6</b>	<b>HOUSING DESIGN.....</b>	<b>38</b>
6.1	MANUFACTURING PLAN .....	38
6.2	CHECK VALVE .....	39
6.3	SINTERED POROUS PLATE .....	39
6.4	RESERVOIR.....	39
6.5	SOLIDWORKS DESIGN .....	40
6.6	MATERIAL CHOSEN.....	41
6.7	PROTOTYPE.....	42
6.8	ACQUISITION OF PARTS .....	42
6.9	FUTURE MANUFACTURE OF COMPONENTS.....	42
6.10	ASSEMBLY.....	42
6.11	SPECIFIC CHALLENGES.....	42

6.12	FUTURE WORK.....	43
6.13	SCHEDULE .....	43
<b>7</b>	<b>LOW GRAVITY TESTING .....</b>	<b>43</b>
7.1	PURPOSE .....	43
7.2	AIRFOIL DESIGN .....	44
7.3	AIRFOIL MATERIAL .....	44
7.4	FILMING .....	45
7.5	DRONE .....	45
7.6	RESERVOIR AND TEST BLOCKS.....	46
7.7	TESTING PROCEDURE .....	46
7.8	DATA .....	47
<b>8</b>	<b>OUTREACH.....</b>	<b>48</b>
8.1	OUTREACH OVERVIEW .....	48
8.2	OUTREACH TO STUDENTS.....	48
8.3	SOCIAL MEDIA.....	49
<b>9</b>	<b>CONCLUSION.....</b>	<b>50</b>
9.1	LESSONS LEARNED .....	50
9.2	SOCIETAL IMPACT .....	50
9.3	GUIDELINES FOR THE NEXT ITERATION .....	51
9.4	SUBSTRATE .....	51
9.5	SIMULATION.....	51
9.6	PLANTS .....	52
9.7	LOW GRAVITY TESTING.....	52
9.8	HOUSING.....	53
9.9	OUTREACH.....	53
	<b>REFERENCES .....</b>	<b>54</b>
	<b>APPENDICES .....</b>	<b>56</b>
A	GANTT CHART .....	56
B	HOW TO MAKE A 3D SUBSTRATE WITH GLOBAL VARIABLES.....	57
C	SUBSTRATE DRAWINGS.....	67
D	DROP TEST DRAWINGS.....	72
E	HOUSING DRAWINGS .....	76
F	OUTREACH POSTER.....	79

## List of Figures

Figure 1.	Project organizational structure.....	4
Figure 2.	3D printing schedule.....	8
Figure 3.	pH of control media and the sample media after exposure to various matrices.....	12
Figure 4.	Surface tension measured for each sample.....	13
Figure 5.	Microgravity experiment for a nylon and two PLA substrates. (a) The onset of microgravity (b) 0.4 seconds later.....	14
Figure 6.	Typical water retention curve [3] .....	15
Figure 7.	Water retention testing apparatus.....	17
Figure 8.	Water retention curves for substrates with 2 mm pores.....	18
Figure 9.	Water retention curves for substrates with 2.5 mm pores.....	18
Figure 10.	Water retention curves for substrates with 3 mm pores.....	19
Figure 11.	Water retention curves for the crosshatched design.....	19
Figure 12.	Water retention curves for the microchannel design.....	20
Figure 13.	Water retention curves for the swiss cheese design.....	20
Figure 14.	Water retention curves for the control.....	21
Figure 15.	3-dimensional 19 direction lattice structure .....	24
Figure 16.	Microscopic density distribution before and after streaming.....	25
Figure 17.	(a) Typical pressure distribution throughout the domain of a bubble. (b) A linear fit to the pressure difference vs. inverse radius graph.....	29
Figure 18.	Contact angle vs. Gadh for droplets on a flat plate.....	29
Figure 19.	Simulation and analytic results for capillary rise in a tube of radius 20.....	30
Figure 20.	Simulated capillary array geometry.....	31
Figure 21.	Fluid rise in a square capillary with rough walls and hydrophobic air channels.....	32
Figure 22.	Labelled housing diagram .....	38
Figure 23.	Prototype housing.....	40
Figure 24.	Housing design schedule.....	41

## List of Figures (continued 1)

Figure 25. NACA 0018 airfoil design in SolidWorks.....	43
Figure 26. Completed drop box for low gravity testing.....	43
Figure 27. SolidWorks view of low gravity testing assembly.....	45
Figure 28. Group photo.....	46
Figure 29. Social media post.....	47
Figure A.1. Gantt chart.....	54
Figure B.1. Global variables step 1.....	55
Figure B.2. Global variables step 2.....	55
Figure B.3. Global variables step 3.....	56
Figure B.4. Global variables step 4.....	56
Figure B.5. Global variables step 5.....	57
Figure B.6. Global variables step 6.....	57
Figure B.7. Global variables step 7.....	58
Figure B.8. Global variables step 8.....	58
Figure B.9. Global variables step 9.....	58
Figure B.10. Global variables step 10.....	59
Figure B.11. Global variables step 11.....	59
Figure B.12. Global variables step 12.....	60
Figure B.13. Global variables step 13.....	60
Figure B.14. Global variables step 14.....	61
Figure B.15. Global variables step 15.....	61
Figure B.16. Global variables step 16.....	62
Figure B.17. Global variables step 17.....	63
Figure B.18. Global variables step 18.....	63
Figure B.19. Global variables step 19.....	64
Figure C.1. Crosshatched design drawing.....	65
Figure C.2. Microchannel design drawing.....	66
Figure C.3. Swiss cheese design drawing.....	67
Figure C.4. Control design drawing.....	68
Figure C.5. Final design drawing.....	69
Figure D.1. Drop test assembly.....	70
Figure D.2. Drop test sample.....	71
Figure D.3. Drop test reservoir.....	72
Figure D.4. Drop test reservoir.....	73
Figure E.1. Housing drawing.....	74
Figure E.2. Bottom housing drawing.....	75

**List of Figures (continued 2)**

Figure E.3. Top housing drawing.....76  
Figure F.1. Outreach poster.....77

**List of Tables**

Table 1. Financial budget.....6  
Table 2. Printer settings for PLA and Nylon.....8  
Table 3. Surface tension measurements for the different liquids sampled.....13  
Table 4. Drop test schedule.....45  
Table 5. The scheduled outreach events.....46

# **1 Team Goal**

## **1.1 Proposal**

Utah State University (USU) and the University of Alabama's (UA) X-Hab design project created a 3D printed substrate to facilitate plant growth in a microgravity environment. The design team proposed a 3D printed substrate that would allow the plants to have a root support matrix, necessary oxygen flow, and a passive water and nutrient delivery system. This substrate was designed to easily integrate into NASA's Veggie and Advanced Plant Habitat platforms. 3D printed components are easily replaceable at a relatively low cost. In addition, since research and development has moved to using 3D printers in space, any needed garden components for the blocks could be easily re-printed while in orbit.

## **1.2 Previous Efforts**

A number of different designs have been created and employed by the varying space programs which are a part of the international space station. Though they have seen success, certain qualities of the past systems, and that currently in use, have led to further work to develop different systems for plant growth in microgravity. This project specifically looked to continue the work begun by the 2016 USU X-Hab team, which initially suggested the plants be grown in a 3D printed matrix. The previous team successfully created a block design, based upon 3D printing using varying percentages of infill, which could support plant growth through triangular capillaries. It was determined that triangular capillaries would provide maximum water wicking, providing the most water for the plants. Nylon bridge was chosen as the material for printing, as it is a frequently used, hydrophilic material that can be readily 3D printed. However, the blocks were essentially non-reproducible, as the sizes of triangles varied with each print depending upon the printer specifications and the infill percentage used. Another problem that was faced involved the integration of the 3D printed block into a larger system that could support total plant growth. A set of check valves were proposed to allow water to flow to the block—not to flow backwards—depending upon the matric potential. However, the valves clogged and were never rendered successful, thus disabling the possibility of total integration into the comprehensive system to allow for passive growth.

## **1.3 Veggie**

Veggie is the current plant growth module being used on board the space station. Veggie was envisioned as a passive system intended to minimize the time spent by astronauts caring for plants. The water wicking system, or “pillows,” used by Veggie was unable to meet the water content requirements for proper plant growth on the space station. Furthermore, the wicking system also had mold growth issues, and plants were often over watered. The astronauts on board the space station have not been required to take a more active role in watering the plants on board the space station [1].



## **1.4 Concept of Design**

The goal of this project was to create an entirely passive system of water and nutrient delivery to plants grown in a microgravity environment. To do this, the team decided to utilize 3D printing to create a 3D matrix or substrate. This substrate would deliver the necessary nutrients to the roots of the plant through capillary action, which still holds in a microgravity environment. The main problem to overcome was oversaturation of the plant roots. Due to previous issues seen in the Veggie system, astronauts are currently using a syringe to manually give the plants water and nutrients. Our design hopes to eliminate that necessity by creating a passive system that will deliver the correct amount of nutrient solution to the plant roots while avoiding oversaturation.

## **1.5 Identification of the Customer**

NASA provided the funding for the project and the main facilitator was Dr. Timothy Taylor who is a faculty member of the Biological Engineering Department at Utah State University (USU).

## **1.6 Target End User**

The target end users are scientists and engineers at the National Aeronautics and Space Administration's (NASA) Kennedy Space Center (KSC).

## **1.7 Requirements**

Design requirements are broken down into four categories: Fluid Transfer, Biological, Manufacturing, Control and Containment. The following is the list of requirements:

### Fluid Transfer

- Supports nutrient solution transfer in microgravity
- Does not over-saturate plant roots
- Fluid transfer is characterized and understood
- Provides proper air mixture for plant roots

### Biological

- Capable of germinating plants within substrate
- Substrate meets an acceptable porosity for plant growth
- Substrate pores will constrict root size

### Manufacturing

- Substrate will be 3D printed
- Substrates will be reusable and integrated into Veggie
- Substrate will not leach chemicals into nutrient solution
- Substrate will meet ISS outgassing standards

## Control and Containment

- System will be passive, requiring minimal intervention from the operator
- System will control matric potential appropriate for plant growth
- Water retention will meet the needs required for plant growth

## 1.8 Other Goals and Desired Objectives

The overall goal for the C3PO system is to create a modular, passive, 3D printed system that would allow for the growth of plants in space. The main hope and desired objective is that this system would allow substrates to be optimized and 3D printed based upon the needs of a given plant species. This way an astronaut would be able to 3D print substrates as needed in orbit. As improvements are made in 3D printing in orbit, this ability to print substrates as a soil substitute will be of great benefit to the overall objective of NASA's Journey to Mars. It is also hoped that this system will be available for testing on the space station. That testing will help to design and optimize a housing unit that controls the flow of nutrients to the plant system using the substrates.

## 1.9 End Deliverable

To deliver a functional 3D printed matrix system (substrate) that will allow plants to grow in microgravity. The matrix will be reusable and integratable into the Veggie growth platform to meet all of the requirements stated in the solicitation. Also, to design the 3D printed matrix system to allow experiments and models to be developed to better understand the challenges and physics of delivering water and nutrients to plants in a microgravity environment. (The new and improved 3D substrate that goes from a 2 mm triangle size to a 3 mm triangle size.)

## 1.9 Issues of Primary Concern

The following are primary areas of concern during the design and testing of this system:

- Substrates and system meet the required water retention necessary to sustain plant growth
- Substrates allow for seeds to germinate within the blocks
- Roots have room to grow and expand within the printed pores
- Substrates will not allow for plant roots to become oversaturated and drown
- Oxygen will be provided to plant roots
- Overall system will be a passive system with little interaction required
- Matric potential will be controlled, preventing oversaturation of roots

## 2 Team Structure and Communications

### 2.1 Organizational and Work Breakdown

The C3PO team is interdisciplinary across two universities: Utah State University and the University of Alabama. The engineering disciplines present on the team are mechanical, biological, and chemical. For sake of ease of coordination between departments/universities, a

lead engineer was assigned to each of the engineering disciplines, with a Point of Contact (POC) being in regular touch with the Integrated Team Coordinator who ensured smooth communication between the overall student team, the PI, and NASA; especially when preparing for the SDR, PDR, CDR, and the Checkpoint Review; as seen on Figure 1a. The initial plan was that team leadership will be rotated periodically, however, this rotation was not implemented after all; for various reasons, some of which may be traced back to personal preference or reserve.

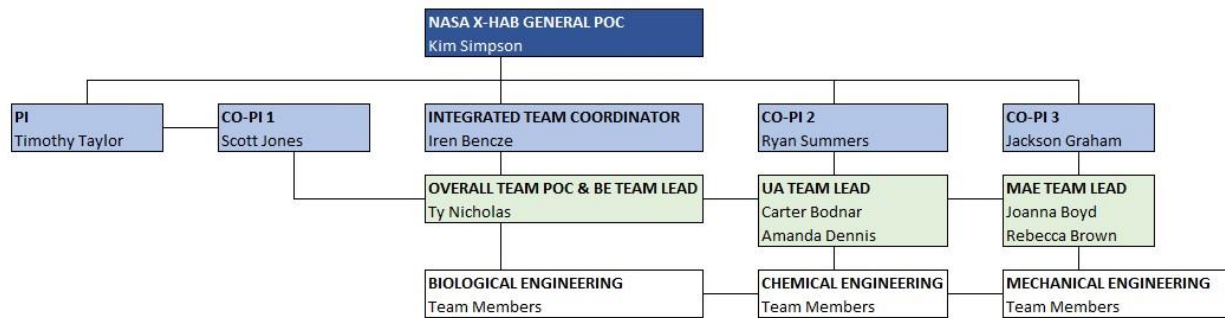


**Figure 1a. Project organizational structure**

The above organizational layout ensured that the C3PO team’s weekly overall meetings (face-to-face at USU, plus UA tuning in through Skype) ran smoothly; and that agenda items, decisions, tasks, and responsible individuals were documented. Furthermore, the closed loop of the system ensured that even if someone was unable to attend a meeting, this did not affect the information flow to them. (Or if there was a lag in the fill in, everyone knew whom to contact to be brought up to date.) Team leaders coordinated with each other at least once a week, before the overall meeting; and all team members kept in touch with each other throughout the week face-to-face or through GroupMe.

For meeting agendas and notes, a modified Stephen Covey Meeting Planner was used, in Excel; see examples in separately attached document. While working in Excel made note-taking somewhat clumsy, this method made it possible to save all overall meeting records throughout the duration of the project in one easily navigable document; and it allowed the team leadership to assess meeting efficiency and project progress straightforwardly.

Given the wide scope of the project, departmental team members were distributed into interdisciplinary groups working on various aspects of the design, as seen in Figure 1b.

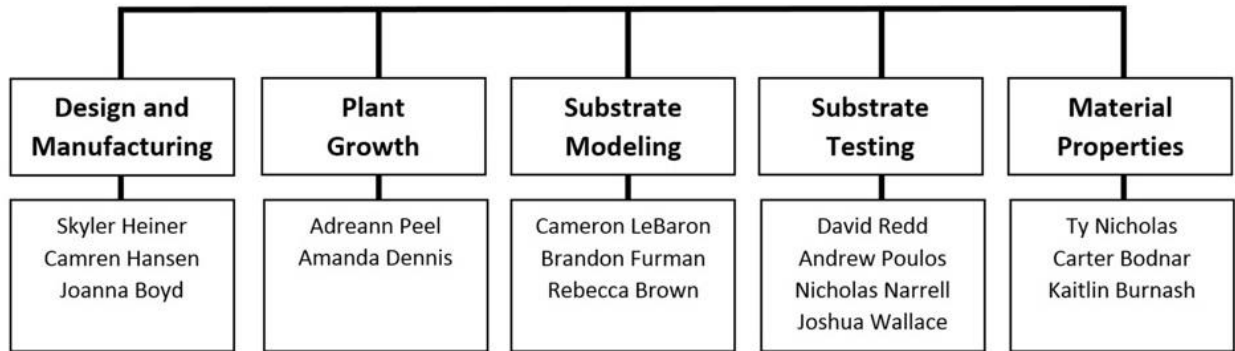


**Figure 1b. Subgroups by tasks, Fall 2017**

## 2.2 Gantt Chart

A Gantt chart was used to schedule all aspects of the project to ensure program progression. See Fig. A.1.

## 2.3 Governing Standards

C3PO is designed in compliance to the American National Standards Institute (ANSI) and NASA requirements for the International Space Station.

## 2.4 Environmental and Societal Impact

The aim of the substrate design is to allow plant growth in the space station with minimal impact on the valuable time of the astronauts. Plant growth in space would create a better environment for the astronauts to live in as well as provide a greater variety of food to eat. The substrate itself would be able to be reused and reprinted, which would minimize waste on the ISS and on other missions. There is possible off-gassing of the material and leaching into the nutrient solution, which is further discussed in this paper. The societal impact includes possible uses of the substrate design in hydroponics. The efficiency of plant growth in microgravity will increase the possibility of longer flights and better endurance of humans when traveling in space.

## 2.5 Safety

Safety has been one of the important considerations moving forward in this research, both for the researchers and those who would use the proposed design for plant growth in microgravity. As such, care has been taken to conduct experiments in well ventilated and clean areas. The work performed in laboratories has been done with accordance to the university's standards of appropriate lab attire and personal protective equipment (PPE), as necessary. Regarding the safety of plants obtained from the proposed design for consumption, the following factors were considered: the risks associated with using printed Nylon, including FDA requirements, chemical leaching and off-gassing of the substrates, along with the risks associated with interactions of the water, hydrosol, calcium nitrate, plants and the substrate. Further research is desired to assess the

addition of the hydrogel layer for germination, and its potential effects on plant growth and human consumption.

The nylon being used is not currently FDA approved for direct food or drink contact and is potentially UL 94 HB flammable. Also, according to NASA's materials database, nylon did not pass its off-gassing requirements of maximum concentration limits of (in parts-per-million by volume) carbon monoxide (0.5), carbon dioxide (0.3), total hydrocarbons: methane (0.1), halogenated compounds (0.5), water (0.7), and nitrogen dioxide (0.005). These results were replicated using a similar protocol as presented by NASA, and further research will be conducted to consider treatment methods for the nylon in order to pass the set guidelines. Testing was completed previously to determine chemical leaching that may occur from the 3D printed substrates. The analysis included changes in pH and surface tension using a tensiometer, dynamic light scattering (DLS), and a pH meter. The data obtained showed that there were particles leaching into the plant growth media. However, based on particle size alone it is difficult to determine the exact materials being leached, especially considering that HPLC Mass Spectroscopy requires a known material for analysis. Additional research would be required to ensure the safety of the nylon substrates for use in plant growing for human consumption.

The water, plants, and nutrient media are not known to be caustic or poisonous on their own, and there have been no observable adverse reactions when these materials are in contact with each other. During plant growth, some media has been seen to evaporate off the top surface of the printed substrates, leaving behind a layer of salt buildup. This buildup may present stress on germinating seeds, because of the high concentrations of salts present. To date no research has been conducted regarding a hydrogel germination layer or its associated risks.

## **3 Substrate Design**

### **3.1 Conceptual Analysis of the Block**

The previous design was built upon utilizing the material infill produced by the 3D printer. The infill percent was managed to execute a specific wall thickness in the substrate. Setting the print to 100% infill would ensure that any designed space would continue to be completely solid, whereas setting the print to 0% infill would ensure that any solidly designed space would be turned into negative space. Any infill setting in between would demonstrate the compatibility between solid space and negative space in the solidly designed space. The default infill design of the printer were triangles. This was beneficial because of the desire to use a triangle shape to take advantage of capillary action. This year, the goal of the 3D substrate was to create a design that contained global variables.

### **3.2 Improvements Upon Previous Efforts**

Global variables is a term used in SolidWorks that deemed a variable name a specific dimension. This variable can be used throughout a SolidWorks design. This variable can be changed once and any dimension attached to that specific variable name will change instantly. The use of global variables ensured that the design could be manipulated quickly with only changing a few variable specifications. This would in turn propagate throughout the substrate and create a smaller, bigger, taller, or shorter design instantly.

*Implementation of Global Variables* Printing with global variables ensured that each design variation could be manipulated perfectly. The variation of pore sizes and the variation of length that became crucial characteristics to each substrate could all be changed without having to redesign the substrate. Not only does the use of global variables save time when making small manipulations to the design in the future, but the variation between blocks is minimized immensely. The infill was not consistent, which caused variation. We wanted to create something that could be printed repeatedly with accuracy and precision.

A step by step process to create a 3D printed substrate using global variables and maximizing the constraint function is shown in Appendix B.

#### *3.2.1 Printing Procedures*

The Ultimaker 3 (S/N: BPP-004712-031213) was the 3D printer used for printing the substrates. The software Cura 3.2.1 was used to manage settings for the printer and import our designs from a STL file. After the program finished slicing a print, the gcode could be saved to repeat the print without having to import another STL file. The material in the printer was changed according to how the printer instructed. Before printing, the bed was cleaned with 70% ethanol and Kimwipes, the nozzle was cleaned, and hair spray was applied to the bed to hold down the prints and prevent warping. When a print was finished, it was removed and the bed was again cleaned.

Printing Results and Settings The two materials used for printing were PLA (MatterHackers Pro series, 3 mm Light Blue) and Bridge Nylon (Taulman3D, 2.85 mm Black). The settings below, in Table 2, were most often used for the prints after testing a few different settings. Other settings not shown in the table were kept at the default settings, as shown in the Cura program for the respective materials.

**Table 2. Printer settings for PLA and Nylon**

	PLA	Nylon
Head Temperature (°C)	205	255
Bed Temperature (°C)	60	50
Flow (%)	100	100
Wall Thickness (mm)	1	0.6
Infill Density (%)	100	100
Layer Height (mm)	0.2	0.2
Brim (mm)	-	7

There were no issues when printing with PLA. When beginning to print with nylon, there were problems with stringing and poor print quality. One member of the team made changes to the flow rate, layer height, wall thickness, bed temperature, head temperature and print speed to find the best combination to obtain a clean print from nylon. The nylon was initially printed with the bed temperature off, but warping within the prints soon became an issue and so it was turned back on to 50 °C. Even with the bed temperature on, warping of the nylon has still been an issue. It was noted that when there were multiple objects being printed at once, the warping was markedly worse than when just one object was being printed. There was also some stringing of the nylon, so the printer speed was adjusted, but soon put back to the default settings, after there was no improvement.

### 3.2.2 Printing Schedule

The print schedule can be seen in Fig. 2.

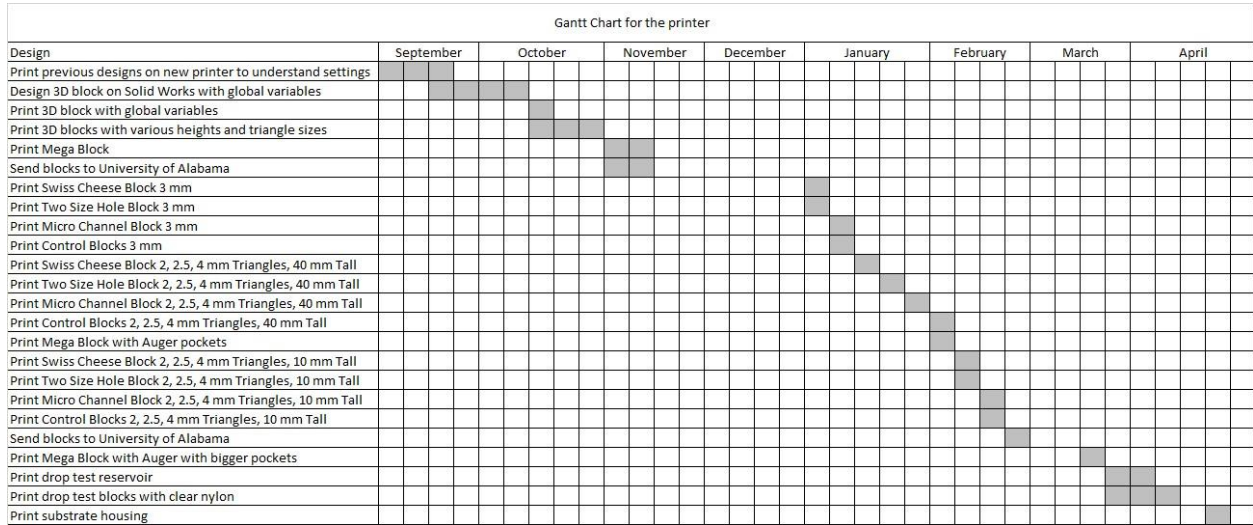


Figure 2. 3D printing schedule

### 3.3 Various Pore Sizes

In order to further understand the variables influencing capillary action in a 3D printed substrate, various block designs were proposed and tested. These tests focused on two main things, namely pore size and internal geometry. The four pore sizes originally chosen for testing were 2 mm, 2.5 mm, 3 mm, and 4 mm, where the length measurement refers to one side of the equilateral triangle of a single capillary channel. These pore sizes were selected based on the hypothesis that smaller triangles would yield better water retention but also restrict plant root growth. Therefore, it was necessary to determine the best balance between retaining water and not choking the plant root. Based on plant growth experiments described later on in this report, the largest plant root diameter for the different plant species we have been examining was approximately 2 mm, therefore, a triangle of 4 mm would allow for maximum root growth. This gave us our upper pore size limit. Plants with root diameters that were below 1 mm (which would correspond with the 2 mm triangular pore size) were determined to be unhealthy, and therefore it was unnecessary to design below this lower pore size limit. Upon further research, and due to time restrictions, it was eventually determined to drop the 4 mm pore size design. In a gravity situation, such large pore sizes did not retain barely any water at all and therefore it became difficult to characterize such blocks using the established testing methods.

### 3.4 Various Internal Geometries

Changing the internal geometry was the second item of variability that was selected for block testing. The three designs that were tested were nicknamed “Crosshatched”, “Microchannel” and “Swiss Cheese”, and will be described shortly. The basic concept between all of these designs was to try to create an environment in which both water and oxygen can be dispersed properly in



microgravity. The goal was to find a design that will allow sufficient nutrient solution to nourish the plant but also allow oxygen to reach the roots and avoid drowning.

### *3.4.1 Crosshatched Design*

The Crosshatched design was chosen for purposes of continuity. That is, the previous group (X-Hab 2016) to work on this project used this particular design for most of their testing, and they chose this design to incorporate into their final project, which they called EDEN. We decided it would be useful to continue this design and use it to test new designs against. It consists of the triangular capillary tubes in the lateral direction with a set of 2 mm diameter oxygen inlet holes running perpendicular to the capillary tubes and a larger set of 4.2 mm diameter oxygen inlet holes running at a 90-degree angle from the first set of holes. The CAD Drawing for this design is shown in Fig. C.1.

### *3.4.2 Swiss Cheese Design*

The Swiss Cheese design is similar to the Varied Air Hole design in that there are sets of oxygen inlet holes running perpendicular to the capillary channels. However, in the Swiss Cheese design an element of randomness is introduced because, rather than only two different hole diameters, there are a large number of different sizes. Also, these holes are distributed randomly throughout the block, creating an external topography that resembles swiss cheese (hence the nickname). The hope was that this randomness would create a chaotic internal geometry that more closely resembles the soil-based systems that plants are accustomed to growing in. The CAD Drawing for this design is shown in Fig C.3

### *3.4.3 Microchannel Design*

The Microchannel design was selected based on the substantiated assumption that hydrophobic/hydrophilic interactions would be the dominating factor in fluid movement through the block in microgravity. This design is slightly more complex than the first two, and the void space is significantly greater. Like the other designs, it consists of an array of triangular capillary channels. However, unlike the other designs, these triangular channels are not continuous on all sides but rather have a side missing, resulting in an X-fashioned cross-sectional shape. The concept behind this design is that due to the hydrophilic nature of the nylon material, the aqueous nutrient solution will “stick” to the solid material and rise to the plant roots, while the channels of void space in between the solid material will allow oxygen to also be present within the block. The CAD Drawing for this design is shown in Fig. C.2.

### *3.4.4 Control Block*

A control block was selected for the different block designs to be compared against. This design consists of simply an array of triangular capillary channels with no perpendicular air channels or any variability of internal geometry. Again, it’s important to note that all four of the designs discussed above (including the control blocks) were tested at the three different pore sizes,

resulting in a total of twelve blocks being tested. The CAD Drawing for this Design is shown in Fig. C.4.

### **3.5 Hydrophobic and Hydrophilic Channels**

The initial idea was to have perpendicular air channels run through the block, but with all channels being naturally hydrophilic, water would flood those as well. Since printing multiple materials together had proved unsuccessful in the past, the idea to coat the air channels in a hydrophobic layer was suggested. This was inspired by the Teflon coatings on cookware, as it was already safe for preparing food; but it ended up not being applicable by virtue of a spray-on Teflon coating not being commercially available. Other methods of spray-on Teflon coatings are being considered, but none have been tested for their health concerns. Instead, other hydrophobic coatings are being tested, the forefront among them being Rain-X and commercially available seam sealers. These seam sealers are composed of polyurethane and silicone-based hydrophobic plastics dissolved in volatile solvents. These are produced for use on tents, many of which are made of nylon, so they should easily adhere to our nylon blocks. The plan originally was to apply them with a pipe cleaner, but if the tubes are too narrow for application in this manner, we may simply dip the edges of the channels into the coating. This allows the edges to be hydrophobic, increasing the amount of air allowed to the plant roots.

### **3.6 Composite Blocks**

One idea to control the amount of the nutrient solution to the plants was different layers of materials that would act differently to the solution. Once the hydrophilic nylon would pull the solution into the capillaries, layer or layers of a hydrophobic material would hinder or slow the movement of water through the pore, to prevent the roots of the plants from flooding. This plan was tested by printing a nylon block and adding a polylactic acid polymer (PLA) layer to the top of the block with a height of about 3 mm. The layer did print correctly, but with the major differences in composition of the two different polymers, the layers separated from each other with a low amount of force. If the multilayer idea was to be repeated, then either using an adhesive that is safe for the plants and humans to adhere the layers together or using a different hydrophobic material that has a better interaction to the nylon is advised.

### **3.7 Chemical Leaching**

The material properties of nylon and PLA have been assessed to determine any potential hazards or safety concerns within the system. To extract any possible chemicals that will leach from the 3D printed substrate, the following protocol was followed. For each material, three blocks were placed in a Soxhlet extractor with 200 proof ethanol for 24 hours. The blocks were removed, and the ethanol from each Soxhlet run was sampled and analyzed for any change in pH or surface tension due to leachables. The next three blocks of each material were placed in a beaker filled with double-deionized water and boiled for 3.5 hours. Blocks were removed and the water from each was sampled and analyzed for any change in pH or surface tension due to leachables. The final three blocks of each material were left untreated as a control. The solution was thoroughly

mixed using a stir plate. The blocks from each treatment group were placed in jars with 250 mL of nutrient media and sealed. Containers were placed on a shaker and left for 12 days at 100 rpm. Chemicals with the possibility of leaching out of the 3D printed substrate while in contact with the nutrient solution is being assessed through HPLC mass spectrophotometry. This process requires ionization methods and methodology for the HPLC. These are usually determined based on the knowledge of what is being analyzed. With manufacturing companies of these 3D printed filaments keeping the specifics under secret under copyright, determining the correct methods will take trial and error. Methods to test these unknown need further consideration.

The following are the results of the tests performed on the solution for extraction. PH measurements yielded unexpected data. It was previously believed that PLA was not a viable plant matrix material because it degrades into lactic acid, which has a pH of 2.3. In contrast, the data that were obtained show an increase in pH instead of an increase in acidity. The initial pH of the growth media was 5.0. The media from the untreated nylon matrices had the highest pH and lowest acidity at 6.69, followed by the Soxhlet treated PLA matrices, boiled nylon, and Soxhlet treated nylon. The media from the untreated and boiled PLA matrices had lower pH values than the others, at 5.82 and 5.66, respectively. All media samples were less acidic after exposure to the various matrices than before, as seen in Fig. 3. It would appear that the matrices are acting either as mild bases or as buffers, though further testing would be required to draw more definitive conclusions. If the matrices are acting as buffers, it is possible that over time, as the PLA degrades, the solution could become significantly more acidic. It is worth noting that the untreated and boiled PLA matrices raised the media pH the least. However, if acidity is the cause of root damage and plant death, the matrices do not appear to be the problem based on this short term study.

The surface tension, as measured by the tensiometer was found for each different sample, and measured nine times for each sample to ensure that the results were accurate. Pure ethanol, double deionized water, and mixed nutrient media were used as controls, and each liquid that came into contact with the 3D printed matrices were tested for possible changes in surface tension due to leachables during the different treatments. Double deionized water was used, which untreated has a surface tension of 78 mN/m. The boiling of the nylon matrix resulted in a lowering of the surface tension to an average of 75 mN/m, while the boiling of the PLA matrices raised the surface tension by an equal amount to that of 81 mN/m. Both samples of water changed very slightly, only 3 mN/m for both types of matrix. 200 proof Ethanol was found to have a surface tension of 25 mN/m, with little change for the ethanol that was used in the Soxhleting process. The ethanol that was used in the Soxhlet extraction process for the PLA only differed from pure ethanol by 1 mN/m on average, and that of the Soxhlet extraction for nylon was not different at all.

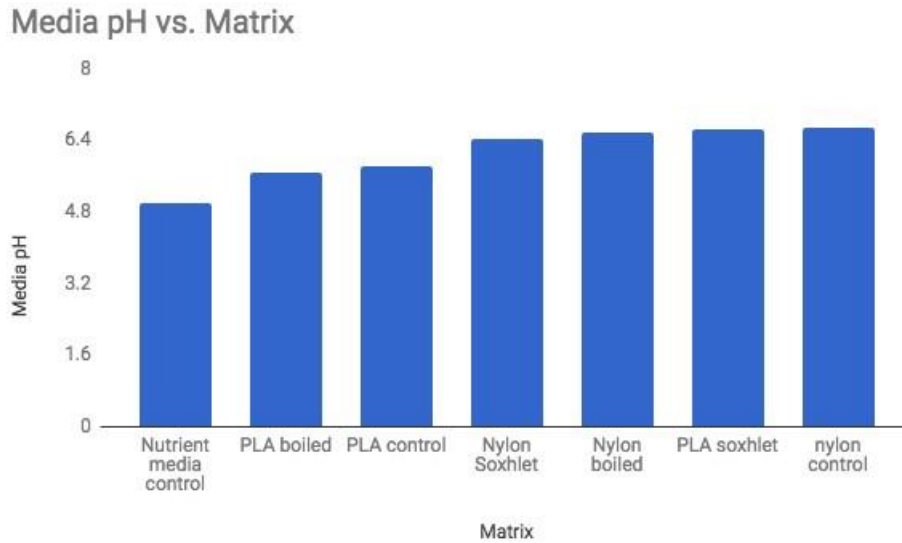


**Figure 3. pH of control media and the sample media after exposure to various matrices**

The unused nutrient media was tested and the control found to have a surface tension of 78. The nutrient media samples that had the nylon matrices in them ranged from 58 mN/m - 68 mN/m, and those which contained PLA matrices had surface tension that ranged from 69 - 82 mN/m. The average measurements for each sample, along with corresponding standard deviations, are found in Table 3, with Fig. 4 showing those measurements in a bar chart for visual comparison. As is noted in the data, there was very little change for the surface tension of the water used in the boiling treatment as well as the ethanol used in the Soxhlet treatment. This would imply that a significant amount had not leached out of the materials in order to cause a change in surface tension. The nutrient media, however, was what the focus of the experiment was on, and the surface tension was much more variable after placing the matrices in the media on the orbital shaker. Both matrices, when placed in the media, lowered the surface tension of the media, implying leachables from the matrices that were introduced into the media solution. The media from the nylon matrices had much lower surface tensions on average, being about 16.67 mN/m lower, on average, than the original media, and the media from the PLA matrices was only about 5 mN/m lower on average. Thus it appears that, from the tensiometer data, there are leachables from both materials that have an effect on the surface tension of the media. This, however, was not observed for the water and ethanol from the treatment methods, as they all had very similar surface tensions to the control liquid.

**Table 3. Surface tension measurements for the different liquids sampled.**

Sample	Average (mN/m)	SD
DD Water	78	0.93
Pure Ethanol	25	0.32
Nutrient Media	78	2.41
Nylon Control	58	1.66
Nylon Soxhlet	58	2.96
Nylon Soxhlet Ethanol	25	0.45
Nylon Boil	68	3.11
Nylon Post Boil	75	1.77
PLA Control	69	6.07
PLA Soxhlet	69	8.37
PLA Soxhlet Ethanol	26	0.54
PLA Boil	82	0.69
PLA Post Boil	81	0.43

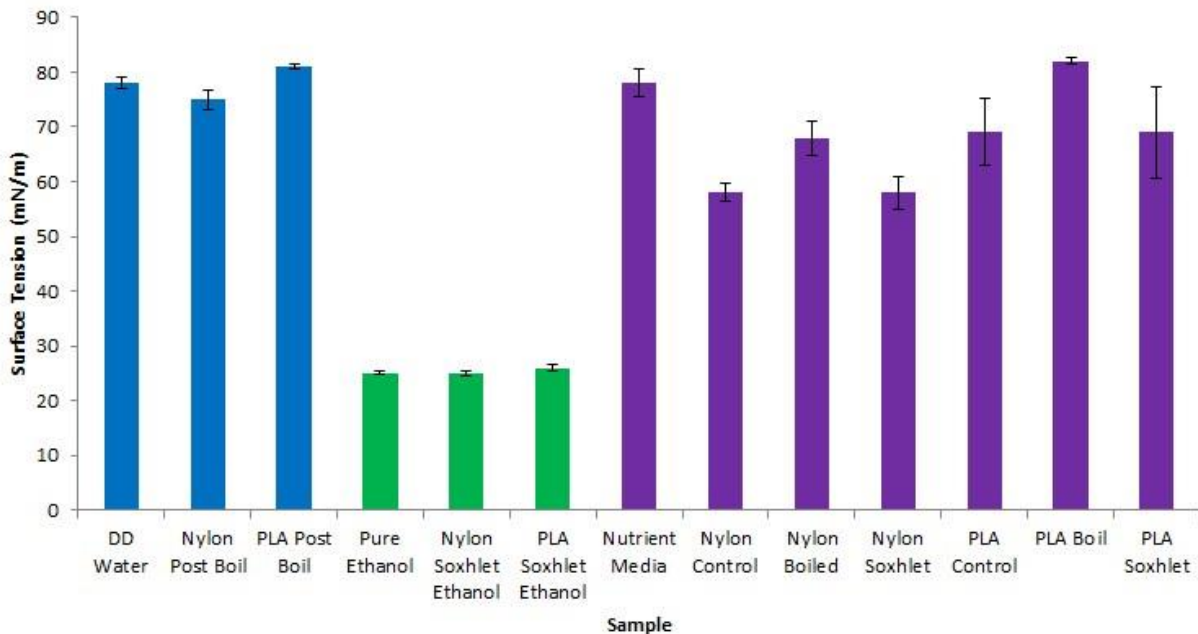


**Figure 4. Surface tension measured for each sample.**

### 3.8 Off Gassing

When it comes to testing the material, the safety of the astronauts is the number one priority. The gas coming off of the material must remain within the allowable limits of the International Space Station. According to NASA's materials database, the off-gassing maximum concentration limits are (in parts-per-million by volume) carbon monoxide (0.5), carbon dioxide (0.3), total

hydrocarbons: methane (0.1), halogenated compounds (0.5), water (0.7), and nitrogen dioxide (0.005). When tested by NASA, Bridge Nylon did not pass these concentration limits.

### 3.9 Off Gassing Procedures

As stated by NASA testing procedures, NASA-STD-6001, the test for off gassing of material should be as follows: the sample should be set in an environmental chamber of  $49 \pm 3$  °C and  $\pm 0.5$  psi of ambient pressure for  $72 \pm 1$  hours. The carrier gas used in this situation is about 20.9 percent oxygen, with the balance being nitrogen.

This test will be conducted with a TCD/HIC gas chromatograph. The thermal conductivity detector carrier gas will be helium and will allow the team to determine when off gassing of the substrate block should be analyzed. The helium ionization concentration gas chromatograph will analyze the gases given off at the times determined by the TCD testing, and the team will study the data to determine how the Bridge nylon does not fit NASA's results.

### 3.10 Off Gassing Results

Off gassing results will guide the team to determine what needs to be changed about the material. Several different sealant types will be tested to determine what aids in decreasing the concentration of the gases given off of the nylon material.

### 3.11 Substrate Oversaturation

In general, any substrate made of a hydrophilic material will encounter the issue of oversaturation. On Earth, gravity provides a limit to how much fluid can be present in a substrate. This means that there will naturally be some air-filled pores within the substrate. In microgravity, however, this limit does not exist. Any fluid that comes into contact with the substrate will immediately and rapidly be drawn into it. Fluid will continue to be drawn until either the liquid reservoir empties or the substrate is 100% filled with fluid. This can be seen in a video of a drop test done at Glenn Research Center. Figure 5a shows a nylon substrate (left) and two PLA substrates (right) at the onset of a microgravity environment. Figure 5b shows the same substrates 0.4 seconds later. It can be seen that the fluid has already made it entirely through the nylon substrate and is halfway through the PLA substrates.

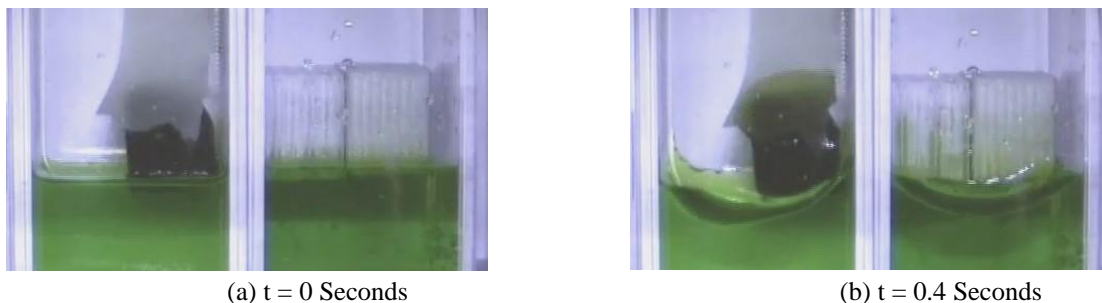


**Figure 5. Microgravity experiment for a nylon and two PLA substrates.**

**(a) The onset of microgravity (b) 0.4 seconds later**

The proposed design attempts to overcome the saturation problem by applying suction to the substrate via a check valve. The goal of the subsequent sections is to determine how much suction needs to be applied to the base of the substrate to maintain the substrate at an optimum water level.

### **3.12 Favorable Water/Air Ratios**

Since the substrate is non-specific for a certain plant type, it will ideally hold 40-60% volumetric water content, which encompasses the needs for the majority of plants. The matric potential at those values will be obtained through the water retention testing, in order to adjust the check valve which will maintain that specific water content range in the substrate. Because of the small range of pressures that allow for the range of the volumetric water content, the wider range of 40-60% was chosen. As specific plants are grown, the system could be adjusted to optimize the growth by narrowing the range and fine-tuning the check valve for the individual plant species.

### **3.13 Water Retention Curves**

Water retention curves are traditionally used to define the relationship between soil suction and soil water content. This relationship is important because it provides information about the water that is available for plant consumption as well as the water that is unavailable to a plant due to the tight bonding between the soil particles and the water molecules i.e. hygroscopic water. Water retention curves also provide other important information. For example, they can tell us information about the soil such as the field capacity (maximum water available to a plant after gravitational drainage), moisture diffusivity (D), hydraulic conductivity (K), hydraulic permeability (k). They also help us to determine the wilting coefficient (minimum moisture required by a plant before wilting) of a plant. An example of a typical soil water retention curve is shown in Fig. 6.

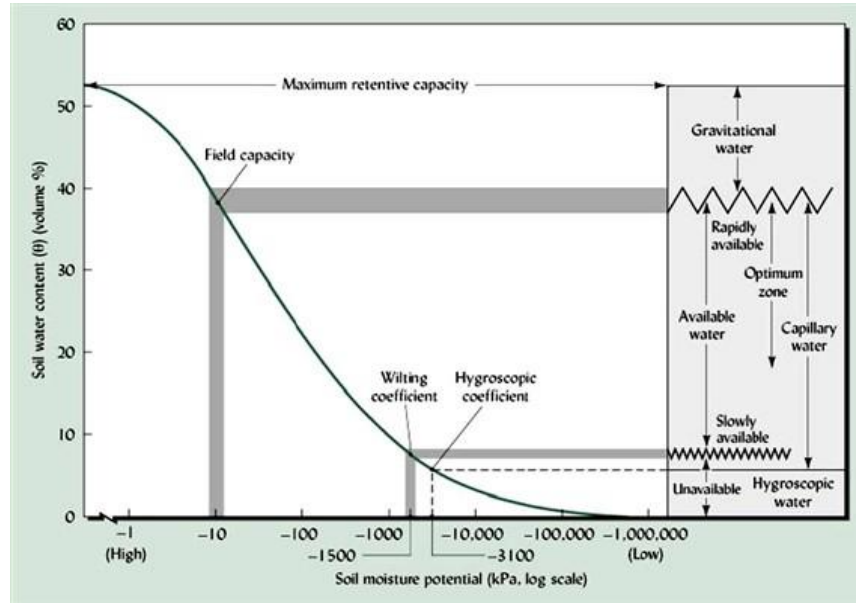


**Figure 6. Typical water retention curve [3]**

The values gleaned from the water retention curve are helpful because they can be used to determine further characteristics about the soil/water/root system. For example, Darcy's Law can be used to describe the volumetric flux of a liquid through a solid, porous medium [2]

$$n^v = -K \frac{\delta \mathcal{H}}{\delta s} \quad (1)$$

$$H = h + z \quad (2)$$

Where  $n^v$  is the volumetric flux,  $K$  is the hydraulic conductivity,  $s$  is the distance the liquid travels in the direction of the flow, and  $H$  is the sum of the pressures causing the liquid to flow, namely matric potential ( $h$ ) and gravitational potential ( $z$ ). In a matrix with a bundle of capillary tubes such as is the case with our particular design, the volumetric flux can be more accurately approximated using the following equation:

$$Q_i = -\frac{\pi r_i^4 \rho g \delta h}{8\mu \delta s} \quad (3)$$

$$n^v = \frac{\sum_i \omega_i Q_i}{A} \quad (4)$$

Where  $Q$  is the volumetric discharge,  $\omega$  is the number of pores (circular tubes) in a particular size class with radius  $r$ ,  $A$  is the total cross-sectional area,  $\mu$  is the viscosity of the liquid,  $\rho$  is the density of the liquid and  $g$  is the gravitational constant. Thus, the volumetric flux is a function of the properties of both the matrix and the liquid flowing through it. Many other important characteristics can be determined from water retention curves; volumetric flux is just an example used to demonstrate the importance of establishing reliable water retention curves for our particular block substrate designs.



The water retention curve and the equations developed above, were done so in the presence of gravity. In a microgravity environment some important differences must be noted. For example, referring back to Fig. 6, all of the curve above the soils' field capacity will be removed because there will be no natural drainage due to gravity, no matter how much water mass the sample is initially saturated with. After that point on the curve, gravitational forces are inconsequential even on earth so it is doubtful that there will be a difference in the liquid/matrix behavior in microgravity. Also, it is important to note that in microgravity the only pressure acting on the liquid and causing it to flow will be the soil matric potential ( $h$ ), the root potential of the plant and any additional pressure added to the system by the input of energy. In other words, the gravitational potential ( $z$ ) will essentially equate to zero.

### 3.14 Testing Procedures

In order to obtain the water retention curves for our 3D printed block substrates, a novel apparatus had to be assembled. A sintered stainless steel plate was epoxied together with a plastic housing block. Tygon tubing was used to connect a water channel from the bottom of the sintered plate to a pipette tip with 1 mL gradations. This pipette tip was loosely attached in parallel to a yard stick with 1 mm gradations. Before testing, the apparatus had to be calibrated by syringing a large amount of water into the pipette tip and applying a film of water on top of the sintered plate, in order to remove all air bubbles that would interfere with the water conductivity through the sintered plate. Once this was accomplished, the system was allowed to equilibrate, and any excess water that remained on top of the sintered plate was removed with a paper towel. The system was then ready for testing. A photo of the apparatus can be found in Fig. 7.

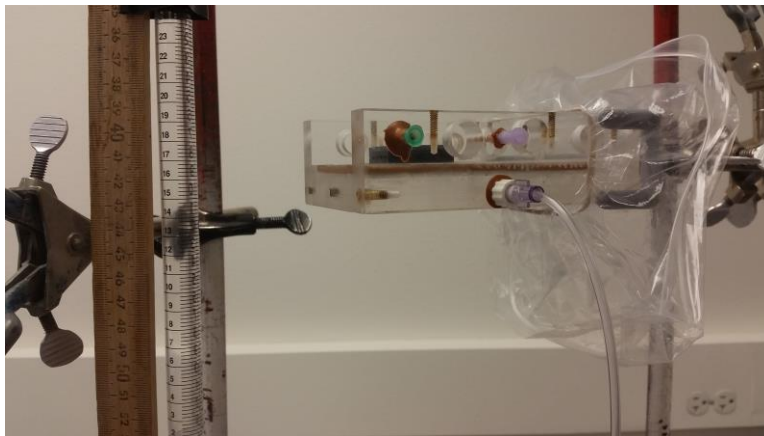


**Figure 7. Water retention testing apparatus**

The blocks were prepared for testing by fully immersing them in a container of water and shaking them sufficiently to remove any air bubbles trapped within the internal geometry of the block. Once fully saturated, the blocks were placed on top of the sintered plate with the capillary tubes running perpendicular to the contact surface. At this point the system was again allowed to equilibrate. Once equilibrium had been achieved, the pipette was dropped by 0.5 cm, in order to apply a minute amount of suction pressure to the block. After ten minutes the water level in the pipette was measured and recorded in mL (corresponding to the water content in the block) and

in cm (corresponding to the pressure head/suction). This was repeated until all or most of the water had been sucked out of the block.

### 3.15 Pore Size Comparison

Due to the sensitivity of the testing methods it was often difficult to obtain reliable data for these figures. Better testing methods are currently being examined for future work.

#### 3.15.1 The 2 mm Comparison

Fig. 8 shows the WRC for the 2 mm pore size block designs. It can be observed that the Varied Air Hole design appeared to retain water significantly better than the other three designs. However, the starting saturation percentage was above 100%, which may give rise to doubts as to how reliable the measurements were. Also from this figure, the 2 mm control block appeared to have a “step” where a large amount of water was removed from the block with very little suction being applied. A similar curve was expected for most of the blocks, because it was expected that the middle column of water within each triangular channel would drain quickly once sufficient suction was applied, and then drainage would occur more slowly as the water from the hydrophilic sides of the triangle was pulled off the block.

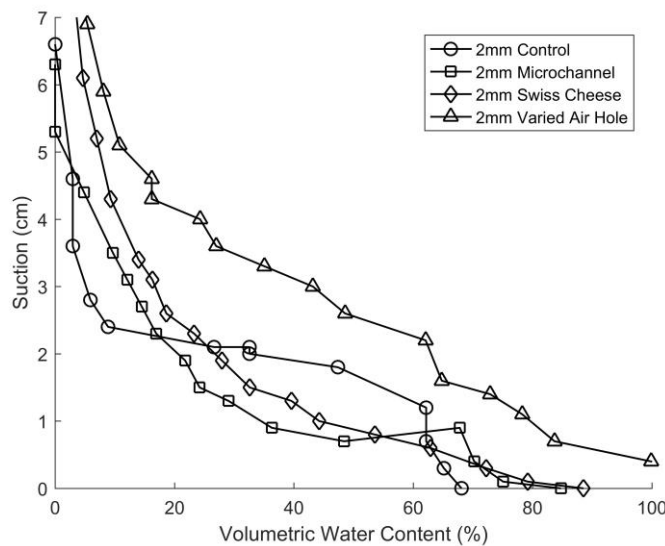


**Figure 8. Water retention curves for substrates with 2 mm pores**

#### 3.15.2 The 2.5 mm Comparison

Fig. 9 shows the WRC for the 2.5 mm pore size block designs. It appears that the Swiss Cheese design retains the water best when suction is applied.

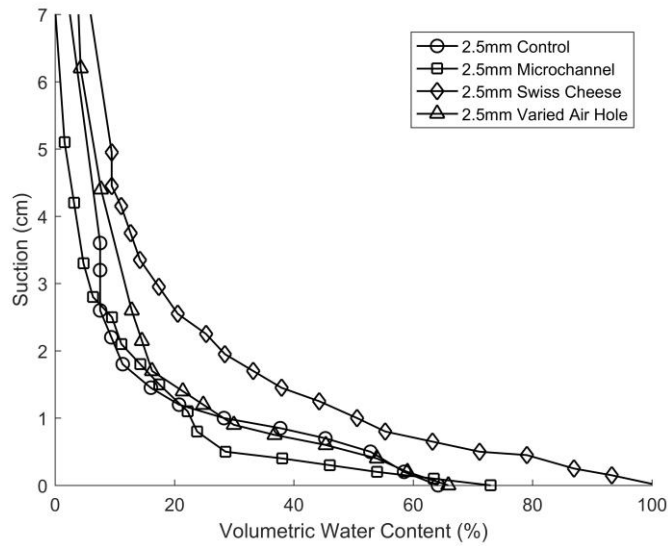


**Figure 9. Water retention curves for substrates with 2.5 mm pores**

### 3.15.3 The 3 mm Comparison

Fig. 10 shows the WRC for the 3 mm pore size block designs. A comparison of the designs at this pore size is difficult as they all appear to follow very close to the same curves. This may be due to the same problem that occurred with the 4 mm blocks, where the capillary forces were negligible in the presence of gravity, and therefore gravitational drainage occurs too quickly to measure dependably.

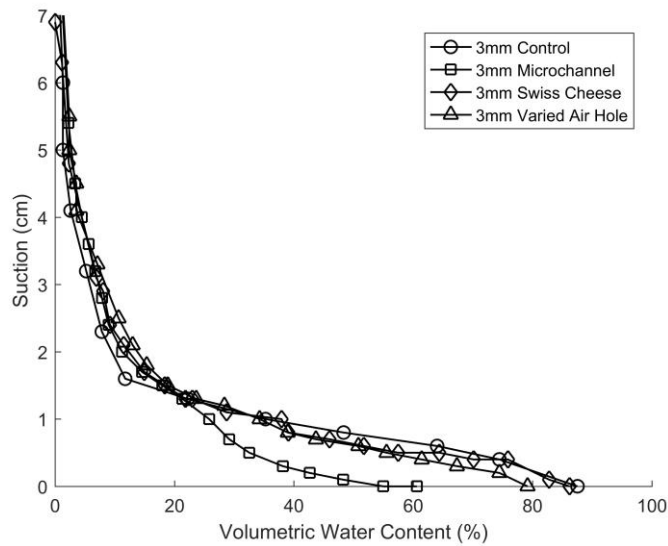


**Figure 10. Water retention curves for substrates with 3 mm pores**

### 3.16 Design Comparison

#### 3.16.1 Crosshatched Comparison

Fig. 11 shows the WRC for the Crosshatched design for different pore sizes. As expected, the smallest pore size retained water the best while the other two pore sizes were too similar to differentiate.

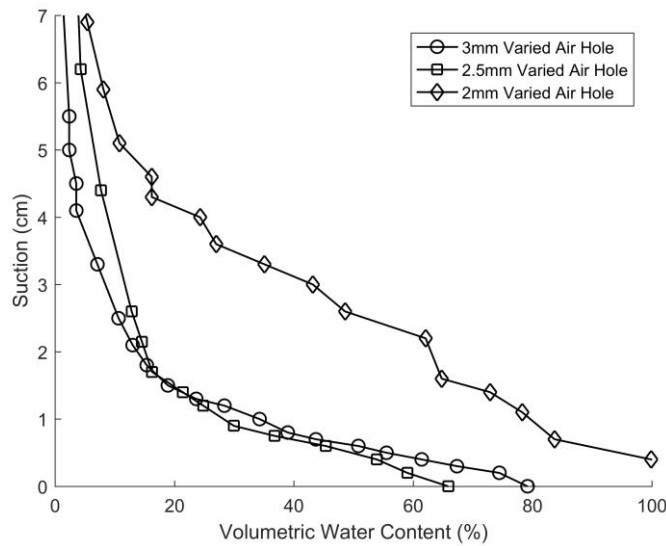


**Figure 11. Water retention curves for the crosshatched design**

#### 3.16.2 Microchannel Comparison

Fig. 12 shows the WRC for the Microchannel design for different pore sizes. Again, the 2 mm pore size retained water the best, as expected. The 2 mm pore size also reached 0% water content much more quickly than the other two, due to its smaller overall volume.

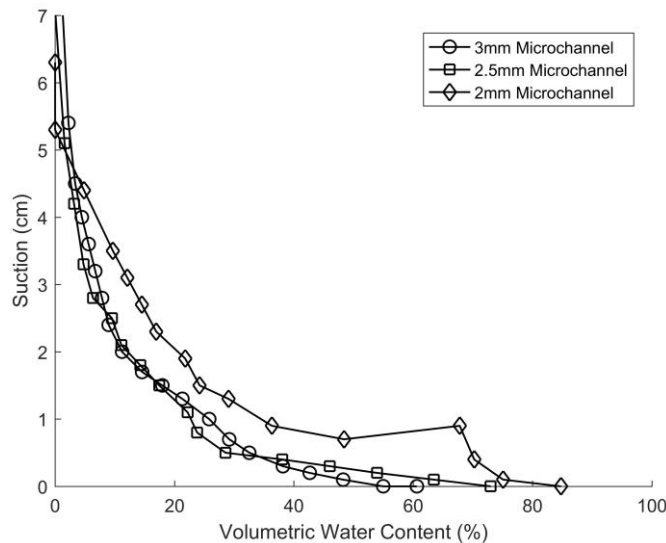


**Figure 12. Water retention curves for the microchannel design**

### 3.16.3 Swiss Cheese Comparison

Fig. 13 shows the WRC for the Swiss Cheese design for different pore sizes. The 2.5 mm and 2 mm pore sizes retained water very similarly while the 3 mm pore size drained much more quickly, as expected.

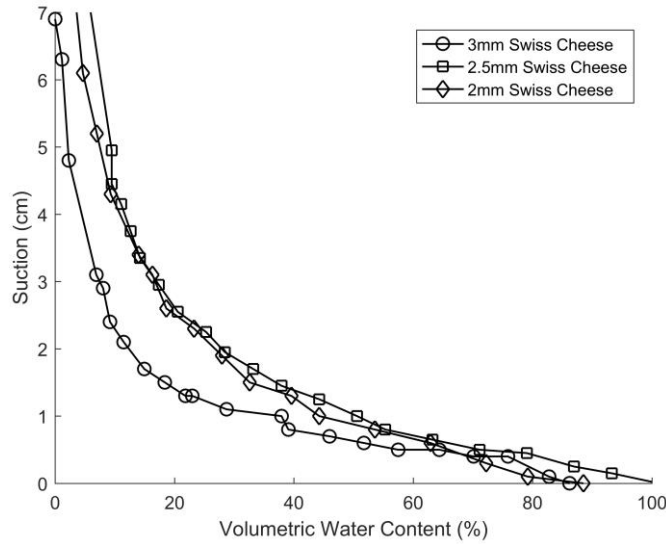


**Figure 13. Water retention curves for the swiss cheese design**

### 3.16.4 Control Comparison

Fig. 14 shows the WRC for the Control block design for different pore sizes. The 2 mm pore size appeared to retain water the best from about 1 to 2.5 cm of suction.

However, at suction values greater than 2.5 cm, all three pore sizes behaved very similarly.

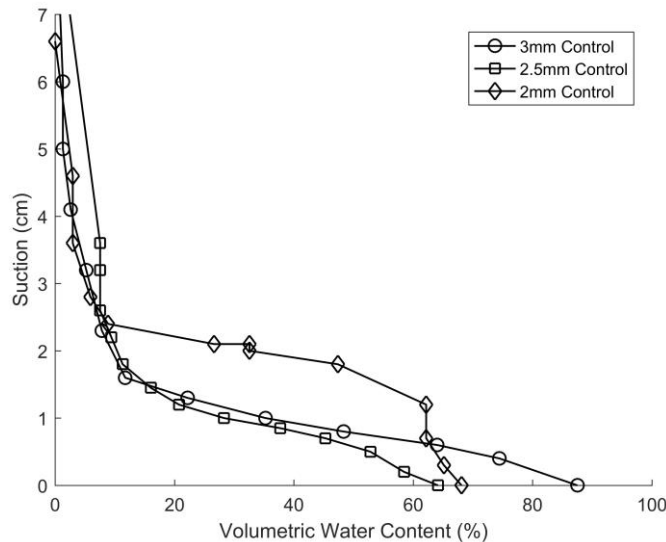


**Figure 14. Water retention curves for the control**

### **3.17 Final Design**

Based on the water retention curves, there seems to not be much of a difference between the different designs when comparing across the board for each similar triangle size. However, there is a difference between the different triangle sizes applied to each block as discussed above. Theoretically, having a block that contains multiple triangle sizes throughout its design may be the appropriate direction to go. This would allow the block to encapsulate every part of the water retention curve and give the plant enough nutrients throughout its growing process as it gets bigger and bigger. The initial design that captures this idea gradually goes from a 2 mm triangle design to a 3 mm triangle design. The design is shown in Fig. C.5. This design would need to be tested to see if this is an appropriate representation of what we think is going to happen.

## **4 Substrate Simulation**

The purpose of this section is to discuss simulations that were done to analyze key design features and constraints of a 3D printed substrate. In particular, the artificial roughness introduced by the 3D printing process and the effectiveness of air channels coated in a hydrophobic material at preventing oversaturation of the substrate.

### **4.1 Preliminary Information**

#### *4.1.1 Motivation*

In the early stages of the project sizable effort was put into determining the fluid uptake rate of the substrate. It was hoped that by determining an analytic formula for the uptake rate it would be possible to determine an ideal geometry for plant growth. After several months it was determined that analytic solutions to the problem of fluid flow within the substrate were infeasible due to the complex nature of the design.

It is worth noting that the problem of capillary action in corners is a well understood problem [4–6]. There are two fundamental issues with these solutions, however. The first issue is that 3D printing creates capillary walls that are non-smooth. For large capillary sizes the roughness of the wall is small enough with respect to the pore size to be considered negligible. For small capillary sizes, however, the roughness can cause significant fluctuations in the pore size. In this case the roughness might be a non-negligible component of the final solution and should be included in the model. A second issue with analytic solutions is caused by the inclusion of air channels in the substrate. In particular, analytic solutions present no feasible way to deal with interruptions in the pore boundaries that the air channels cause.

It is apparent that computational techniques are necessary to resolve these issues. A technique known as the Lattice Boltzmann Method (LBM) is used in this report to model the capillary action in the substrate. At its core, the LBM simulates collisions between macroparticles. This is in contrast to more “standard” techniques that solve the Navier–Stokes Equation.

There are two primary benefits to using the LBM. The first is its ability to easily model fluid flow through complex geometries without performance penalty, loss of accuracy, or significant

pre-processing. This ability allows for the easy inclusion of rough capillary walls and air channels. The second benefit of the LBM is the ability to easily include adhesive and cohesive effects for the fluid. Whereas traditional methods require adding terms to track the fluid/gas interface, the LBM handles this easily with the inclusion of a forcing term on each node [7]. It has been shown that LBM is capable of accurately modeling circular, square, and triangular pores [8,9].

For this project we have developed our own LBM code. Open source alternatives could have included Palabos or OpenLB [10,11]. There are two primary benefits to using one of the open source solutions. The first benefit is computation time. Both open source solutions are extremely well optimized and are likely to be an order of magnitude faster than our own code. The second benefit is a guarantee to correct implementation of the LBM.

Both of these options are lacking in two regards, however. The first issue is scarce documentation on the aspects of the simulation that are relevant to this project. In particular, the methods used to calculate adhesive and cohesive properties could not be found. The second issue relates to the idea of the air channel. In our design it has been proposed that the air channels be either made of a hydrophobic material or coated with a hydrophobic coating. Accurate simulations involving the air channels would therefore need a way to incorporate vastly different surface properties throughout the solid. In addition, it would be desirable for the surface properties to be able to change with time (to simulate wear to the hydrophobic coating, for instance). Existing solutions do not appear to have an easy way to accomplish the aforementioned properties (or it is not well documented).

For these reasons LBM code was developed that uses well documented techniques that are effective at simulating capillary phenomena and allows for varying surface properties throughout the solid.

#### 4.1.2 The Boltzmann Equation

Before discussing the LBM, a brief derivation of the Boltzmann Equation, which the LBM is based on, is given. Let  $f(x,p,t)$  be a distribution function that gives the probability of finding a particle at a location  $x$  with momentum  $p$  at a time  $t$ . Under this definition the expected number of particles in a region  $x \pm dx$  with momentum  $p \pm dp$  is given by  $f(x,p,t)dx dp$ . Now suppose the existence of some force  $F$  that acts on all particles in the region  $x \pm dx$ . At a time  $t + dt$  we must have  $x_{t+dt} = x_t + v dt = x_t + dx$  and  $p_{t+dt} = p_t + F dt = p_t + dp$ . Thus, at a time  $t + dt$  we have Eq. 5.

$$f(x + dx, p + dp, t + dt) dx dp = f(x, p, t) dx dp \quad (5)$$

Due to collisions, some particles that start with  $(x,p)$  will not arrive at  $(x + dx, p + dp)$ . Similarly, some particles that do not start with  $(x,p)$  may end up arriving at  $(x + dx, p + dp)$ . Let  $\Gamma(+)$   $dx dp dt$  be the number of extra particles that arrive at  $(x + dx, p + dp)$  and  $\Gamma(-)$   $dx dp dt$  be the number of particles that do not arrive at  $(x + dx, p + dp)$ . These quantities can be added to Eq. 5 to yield Eq. 6.

$$f(\mathbf{x} + d\mathbf{x}, \mathbf{p} + d\mathbf{p}, t + dt)d\mathbf{x}d\mathbf{p} = f(\mathbf{x}, \mathbf{p}, t)d\mathbf{x}d\mathbf{p} + [\Gamma(+)-\Gamma(-)]d\mathbf{x}d\mathbf{p}dt \quad (6)$$

At this point the LHS of Eq. 6 can be expanded via Taylor series to find the traditional form of the Boltzmann Equation. However, for the purposes of the LBM it will be more convenient to divide Eq. 6 by  $d\mathbf{x}d\mathbf{p}$ . This yields Eq. 7.

$$f(\mathbf{x} + d\mathbf{x}, \mathbf{p} + d\mathbf{p}, t + dt) = f(\mathbf{x}, \mathbf{p}, t) + [\Gamma(+)-\Gamma(-)]dt \quad (7)$$

#### 4.1.2 The Lattice Boltzmann Method

The Lattice Boltzmann Method is a discretization of the Boltzmann equation. The Boltzmann Equation describes a physical situation where particles can be located anywhere in space, and momentum can be oriented in any direction. In the Lattice Boltzmann Method particles are confined to nodes on a cubic lattice and momentum transfer is only allowed to happen in a finite number of directions.

There are three lattice structures in common use. They are designated by D3Q15, D3Q19, and D3Q27. The D3 means that the lattice is 3-dimensional and the Qxx designates how many directions there are for momenta transferal. In this report a D3Q19 lattice structure is used. This means that the lattice is 3-dimensional (3D) and that there are 19 directions that momentum can travel during collisions and streaming (Q19). A diagram of this lattice structure is shown in Fig. 15.

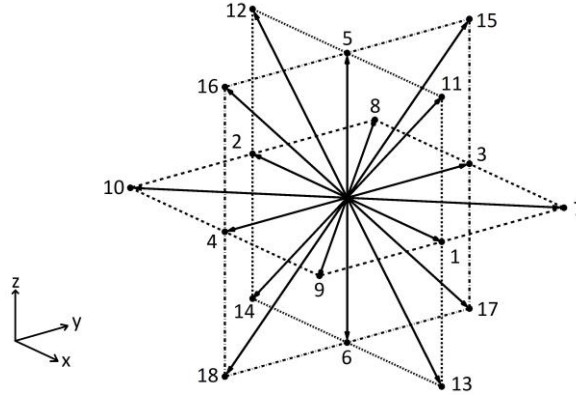


**Figure 15. Three-dimensional 19 direction lattice structure**

For this report the Boltzmann Equation is discretized using the basic Bhatnagar-Gross-Krook (BGK) approximation [12]. The discretized form of Eq. 7 is given by Eq. 8.

$$f_i(\mathbf{x} + \mathbf{e}_i\Delta t, t + \Delta t) = f_i(\mathbf{x}, t) + \frac{[f_i^{eq}(\mathbf{x}, t) - f_i(\mathbf{x}, t)]}{\tau} \quad (8)$$

Where  $f_i(\mathbf{x}, t)$  is analogous to  $f(\mathbf{x}, \mathbf{p}, t)$  in the Boltzmann equation and  $[f_i^{eq}(\mathbf{x}, t) - f_i(\mathbf{x}, t)]/\tau$  is analogous to  $[\Gamma^{(+)} - \Gamma^{(-)}] dt$  in the Boltzmann equation. In the discrete form the  $i$  subscript denotes the direction of momenta travel and corresponds to the numbering in Fig. 15.



## 4.2 Algorithm

The following subsections describe the algorithm and the calculations involved in exactly the order it is programmed. In general, this report will follow the steps outlined by Sukop, unless otherwise noted [7]. Because the algorithm is circular, in many cases terms will not be defined until subsequent sections.

### 4.2.1 Variable Initialization

In general, it is desirable to specify an initial density distribution,  $\rho(x,0)$ , and velocity distribution,  $u(x,0)$ . However, at  $t = 0$  data for  $f_i(x,t)$  does not yet exist. This data can be approximated by setting  $f_i(x,0) = f_{ieq}(x,0)$ .

### 4.2.2 Streaming Step (Begin Loop)

The streaming (propagation) step directly follows the collision step and is the point at which microscopic densities are redistributed throughout the computational domain. At every node in the domain microscopic densities “explode” outwards along each direction of the lattice structure. See Fig. 16 for a two-dimensional example.

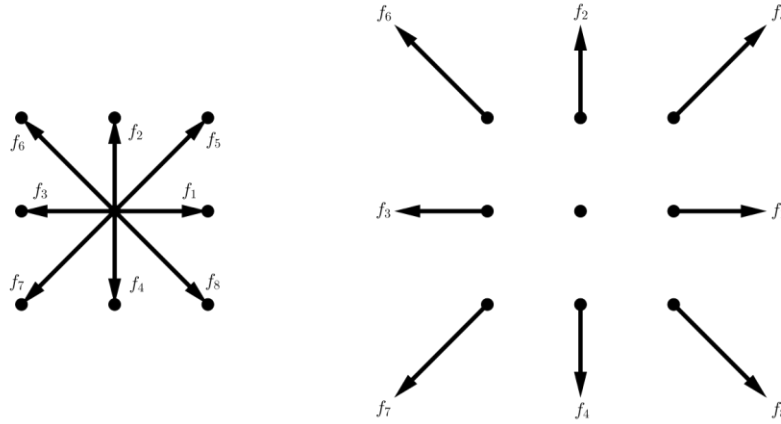


**Figure 16. Microscopic density distribution before and after streaming.**

The streaming step can be written as shown in Eq. 9

$$f_i^*(\mathbf{x} + \mathbf{e}_i \Delta t, t + \Delta t) = f_i(\mathbf{x}, t) \quad (9)$$

Where  $f_i(x,t)$  is the microscopic density distribution after the collision step,  $x$  is the location of a node and  $\mathbf{e}_i$  is a discrete velocity vector whose direction corresponds to the numbering in Fig. 15. During the streaming step periodic (wrap around) boundary conditions are enforced. For this type of boundary condition, opposite faces of the computational domain are treated as if they

were adjacent. This type of boundary condition cleanly resolves the issue of missing data at the edges of the computational domain, but usually requires that the domain be oversized.

#### 4.2.3 Macroscopic Variables

The macroscopic density of each node can be calculated by summing the microscopic direction-specific fluid densities after streaming, as shown in Eq. 10.

$$\rho(\mathbf{x}, t) = \sum_{i=0}^{18} f_i^*(\mathbf{x}, t) \quad (10)$$

The macroscopic fluid velocity is simply the sum of the microscopic fluid velocities weighted by the direction-specific fluid densities after streaming, as shown in Eq. 11.

$$\mathbf{u}(\mathbf{x}, t) = \frac{1}{\rho(\mathbf{x}, t)} \left( \sum_{i=0}^{18} f_i^*(\mathbf{x}, t) \mathbf{e}_i \right) \quad (11)$$

#### 4.2.4 Cohesive & Adhesive Forces

Phase separation and surface tension effects are induced in the fluid via a cohesive force between particles. The cohesive force is calculated using the nearest-neighbor model originally introduced by Shan and Chen [13]. The cohesive force at a node  $\mathbf{x}$  is given by Eq. 12.

$$\mathbf{F}_{coh}(\mathbf{x}, t) = -G_{coh} \psi(\mathbf{x}, t) \sum_{i=1}^Q w_i \psi(\mathbf{x} + \mathbf{e}_i \Delta t, t) \mathbf{e}_i \quad (12)$$

Where  $G_{coh}$  is an arbitrary constant,  $w_i$  are the lattice weights (defined later), and  $\psi(\mathbf{x}, t)$  is the interaction potential (also called the effective mass) defined by the equation of state (EOS). The interaction potential is related to the pressure of the fluid by Eq. 13 [14].

$$p = c_s^2 \rho(\mathbf{x}, t) + \frac{c_0}{2} G_{coh} [\psi(\mathbf{x}, t)]^2 \quad (13)$$

Where  $p$  is the pressure,  $c_s$  is the lattice sound speed (defined later), and  $c_0$  is a constant related to the type of lattice structure used. For a D3Q19 lattice structure  $c_0 = 6$ . Work done by Yuan and Schaefer showed that the Carnahan-Starling EOS yielded the lowest spurious currents at liquid-gas interfaces and allowed for high density ratios [14]. The Carnahan-Starling EOS has an interaction potential given by Eq. 14.

$$\psi(\mathbf{x}, t) = \sqrt{\frac{2 \left( \rho(\mathbf{x}, t) RT \frac{1+b\rho(\mathbf{x},t)/4+(b\rho(\mathbf{x},t)/4)^2-(b\rho(\mathbf{x},t)/4)^3}{(1-b\rho(\mathbf{x},t)/4)^3} - a\rho(\mathbf{x}, t)^2 - \frac{\rho(\mathbf{x}, t)}{3} \right)}{G_{coh} c_0}} \quad (14)$$

Where  $T$  is the temperature,  $R$  is the ideal gas constant,  $a$  is the attraction parameter, and  $b$  is the repulsion parameter. For the purposes of convenience  $R = 1$ ,  $a = 1$ , and  $b = 4$  are usually picked [14]. A value of  $T = 0.08$  is picked for the simulations that follow because it results in a density ratio between the liquid and gas phases of 10 and exhibits good numerical stability [15]. Note that when calculating  $F_{coh}$ ,  $G_{coh}$  will vanish for all values of  $G_{coh}$ . Thus, the only purpose of  $G_{coh}$  is to ensure the quantity in the square root of  $\psi(\mathbf{x}, t)$  does not become negative. A value of  $G_{coh} = -1$  is sufficient to achieve this.

Note that calculating the adhesive force at a node,  $F_{adh}$ , requires densities from all of the surrounding nodes. This presents a technical challenge near solid nodes because this density data will not exist. If this data is not supplanted in some form, fluid will always exhibit repulsion effects near walls. For the simulations that follow, missing density data at solid nodes is approximated by taking the weighted average density of all surrounding fluid nodes. This provides relatively good results at little to no performance penalty.

In order to induce a non-90° contact angle between the liquid phase of the fluid and solid nodes, an adhesive force is required. The adhesive force between fluid nodes and solid nodes is given by Eq. 15.

$$\mathbf{F}_{adh}(\mathbf{x}, t) = -\psi(\mathbf{x}, t) \sum_{i=1}^Q w_i G_{adh}(\mathbf{x} + \mathbf{e}_i \Delta t) \mathbf{e}_i \quad (15)$$

Where  $G_{adh}(\mathbf{x}, t)$  is an arbitrary constant that affects the contact angle between the fluid and the walls of the capillary. For the purposes of this report  $G_{adh}$  is given by Eq. 16.

$$G_{adh}(\mathbf{x}) = \begin{cases} 0 & \text{if } \mathbf{x} \text{ is a fluid node} \\ a_1 & \text{if } \mathbf{x} \text{ is a type 1 solid node} \\ \vdots & \\ a_n & \text{if } \mathbf{x} \text{ is a type n solid node} \end{cases} \quad (16)$$

By making  $G_{adh}$  a function of space, the contact angle can be changed throughout the capillary. This will allow for the simulation of a hydrophobic coating in the air channels of the substrate.

#### 4.2.5 Equilibrium Distribution

The adhesive and cohesive forces are incorporated into the model by modifying the velocity term and computing the equilibrium distribution with the new velocity. In particular, we have Eq. 17.

$$\mathbf{u}^{eq}(\mathbf{x}, t) = \mathbf{u}(\mathbf{x}, t) + \Delta \mathbf{u}(\mathbf{x}, t) = \mathbf{u}(\mathbf{x}, t) + \frac{\tau \mathbf{F}(\mathbf{x}, t)}{\rho(\mathbf{x}, t)} \quad (17)$$

Where  $F(\mathbf{x},t) = F_{coh} + F_{adh}$  and  $\tau$  is the relaxation time (defined later). Collisions between particles is considered a relaxation towards equilibrium [7]. For the D3Q19 lattice structure the equilibrium distribution is given by Eq. 18.

$$f_i^{eq}(\mathbf{x}, t) = w_i \rho(\mathbf{x}, t) \left[ 1 + 3 \frac{\mathbf{e}_i \cdot \mathbf{u}^{eq}(\mathbf{x}, t)}{c^2} + \frac{9}{2} \frac{(\mathbf{e}_i \cdot \mathbf{u}^{eq}(\mathbf{x}, t))^2}{c^4} - \frac{3}{2} \frac{(\mathbf{u}^{eq}(\mathbf{x}, t) \cdot \mathbf{u}^{eq}(\mathbf{x}, t))}{c^2} \right] \quad (18)$$

Where  $c$  is the lattice speed defined as  $c = \Delta x / \Delta t$  and  $w_i$  are the lattice weights given by Eq. 19.

$$w_i = \begin{cases} 1/3 & \text{if } i = 0 \\ 1/18 & \text{if } i = 1, \dots, 6 \\ 1/36 & \text{if } i = 7, \dots, 18 \end{cases} \quad (19)$$

For the purposes of this report  $\Delta x = 1 \text{ lu}$  and  $\Delta t = 1 \text{ ts}$ , so  $c = 1 \text{ lu/ts}$ .

#### 4.2.6 Collision Step (Restart Loop)

The collision step simulates collisions between all the particles in the lattice. Essentially, the collision step recalculates the densities of each node. For fluid nodes, the collision step is written as Eq. 20.

$$f_i(\mathbf{x}, t) = f_i^*(\mathbf{x}, t) - \frac{1}{\tau} (f_i^*(\mathbf{x}, t) - f_i^{eq}(\mathbf{x}, t)) \quad (20)$$

where  $\tau$  is called the relaxation time and it is related to the kinematic viscosity of the fluid by  $\nu = c_s^2 \Delta t (\tau - \frac{1}{2})$ . The quantity  $c_s$  is called the lattice sound speed and is related to the lattice speed by  $c_s = c / \sqrt{3}$ . For the simulation that follow a relaxation time of  $\tau = 1$  is chosen, which results in a kinematic viscosity of  $\nu = 1/6$ .

For solid nodes the collision step is handled with the midplane bounceback technique. This method consists of reflecting all incoming microscopic densities back to their original fluid nodes, but in the opposite direction (i.e. a f15 would become a f18). This type of bounce back replicates no-slip conditions along walls and is reasonably accurate [7].

### 4.3 Simulation Characterization, Parameterization, and Validation

In this section the LBM code developed for this project will be tested. The surface tension of the simulated fluid will be characterized and the relationship between  $G_{adh}$  and contact angle will be parameterized. The code will be validated by simulating capillary action in a circular tube and comparing the results to an analytic solution.

#### 4.3.1 Surface Tension

Similarity between the simulation and the real world can be achieved via dimensionless numbers. For most common dimensionless numbers, the surface tension of the fluid is required. Surface

tension is not a property explicitly given by the EOS and must be measured. The surface tension can be measured by generating droplets of varying sizes and measuring the pressure inside and outside the droplet. The Young-Laplace Equation can then be used to estimate the surface tension [7,15]. The Young-Laplace Equation is given by Eq. 21.

$$\Delta P = \frac{\sigma \cos(\theta)}{r} \quad (21)$$

Where  $\Delta P$  is the difference in pressure between the inside and outside of the droplet,  $\sigma$  is the surface tension,  $\theta$  is the contact angle, and  $r$  is the radius of the droplet. The radius of the droplet is approximated by  $r = \sqrt[3]{(3/(4\pi))V}$  where  $V$  is the volume of fluid in the droplet. Fluid is considered as part of the droplet if its density is larger than 99% of the maximum density that occurs within the droplet. The contact angle for a droplet is  $\theta = 0$ , thus, for a droplet, the surface tension can be estimated by the slope of the  $\Delta P$  vs.  $1/r$  graph. This graph is shown in Fig. 17b. The surface tension of the fluid is measured to be  $\sigma = 0.00483 \text{ mu/ts}^2$ .

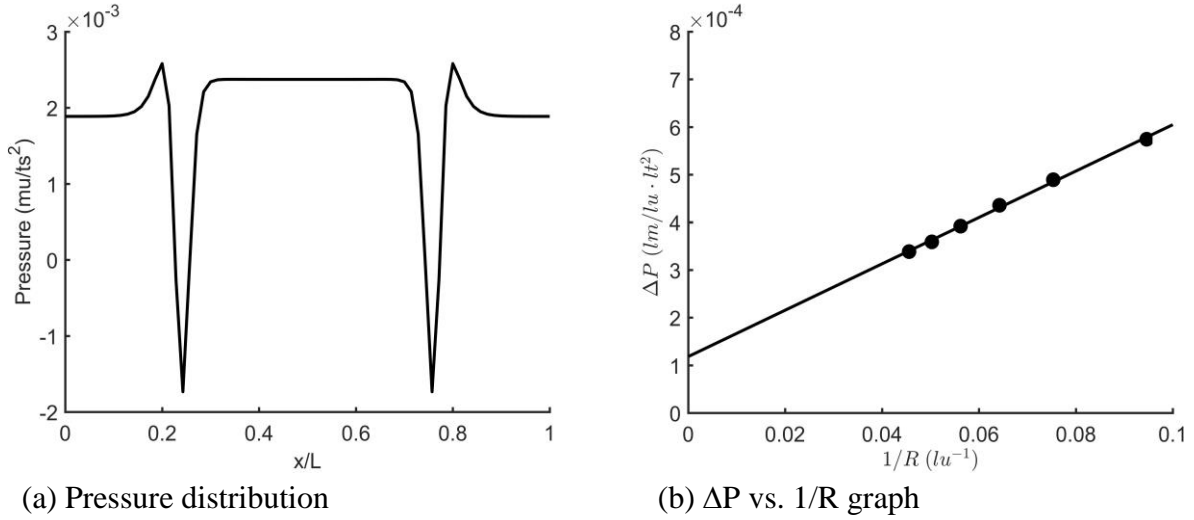


**Figure 17. (a) Typical pressure distribution throughout the domain of a bubble (b) A linear fit to the pressure difference vs. inverse radius graph**

#### 4.3.2 Contact Angle

The contact angle is controlled by the adhesion coefficient,  $G_{adh}$ . Once again, the effect of  $G_{adh}$  on the contact angle is not explicitly given by the EOS and should be measured. To do so fluid droplets are initialized on plates with varying adhesion coefficients in a  $101 \times 101 \times 71$  computational domain. The contact angle between the droplet and the plate is then measured. This is done via Eq. 22.

$$\theta = 2 \cdot \text{atan}(h/r) \quad (22)$$

Where  $\theta$  is the contact angle,  $r$  is the radius of the part of the droplet in contact with the plate, and  $h$  is the maximum height of the droplet. The contact angle as a function of  $G_{adh}$  is then plotted. This data is shown in Fig. 18. It can be seen that  $G_{adh}$  is related to the contact angle by  $\theta$

= 681.4Gadh + e53.3Gadh + 86.1. This relationship is in excellent agreement with the literature [9].

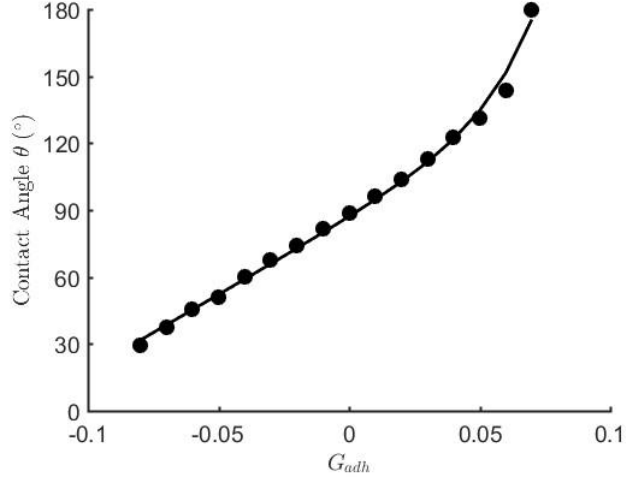


**Figure 18. Contact angle vs. Gadh for droplets on a flat plate**

#### 4.3.3 Capillary Intrusion

The code is verified for capillary action by simulating capillarity in a circular pore of radius 20. The procedure will closely mimic that used in [8]. The capillary will exist in a  $71 \times 71 \times 201$  computational domain. The height of the liquid-gas interface is tracked as a function of time, and compared to the Bosanquet equation. The liquid-gas interface is tracked by fitting a hyperbolic tangent function to the vertical density distribution. The interface is considered as the location where the concavity of the curve changes sign. In the absence of gravity, the Bosanquet equation is given by Eq. 23.

$$\rho h \frac{d^2 h}{dt^2} + \frac{8\mu(h + h_+)}{r^2} \frac{dh}{dt} + \frac{1}{4}\rho \left( \frac{dh}{dt} \right)^2 = \frac{2\sigma \cos(\theta)}{r} \quad (23)$$

Where  $h$  is the height of the gas-liquid interface as measured from the liquid surface outside the tube,  $h_+$  is the length of the submerged part of the tube,  $r$  is the radius of the tube,  $\rho$  is the density of the liquid part,  $\mu$  is the dynamic viscosity of the liquid part,  $\sigma$  is the surface tension of the liquid part, and  $\theta$  is the contact angle between the liquid part and the tube wall. This equation can be made dimensionless by substituting  $h = h_0 h^*$ ,  $t = t_0 t^*$ , and  $r = h_0 r^*$  where  $h_0 = \mu^2 / \rho \sigma$  and  $t_0 = \mu^3 / \rho \sigma^2$ . Doing so results in Eq. 24.

$$h^* \frac{d^2 h^*}{dt^{*2}} + 8 \frac{h^* + h_+^*}{r^{*2}} \frac{dh^*}{dt^*} + \frac{1}{4} \left( \frac{dh^*}{dt^*} \right)^2 = \frac{2 \cos(\theta)}{r^*} \quad (24)$$

Usually, it is assumed that the reservoir the tube is placed in is large enough to ensure that  $h_+$  is constant. However, due to computational constraints the reservoir in this simulation is only slightly larger than the tube itself. This means there is a large downward shift in  $h_+$  as fluid enters the capillary. The relationship between  $h$  and  $h_+$  was measured empirically and, for this

particular simulation, found to  $h_+^* = -0.269h^* + 32.332$  be. This quantity can be substituted into Eq. 24 as a correction term for this simulation. The results of this simulation, as compared to the Bosanquet equation, are shown in Fig. 19.

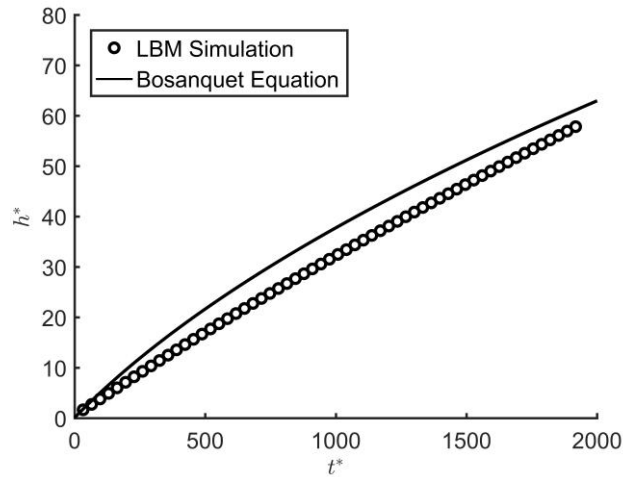


**Figure 19. Simulation and analytic results for capillary rise in a tube of radius 20**

We see that the simulation provides results that are in good agreement with the theoretical solution. The results also agree well with those measured in [8].

#### 4.4 Substrate Simulation

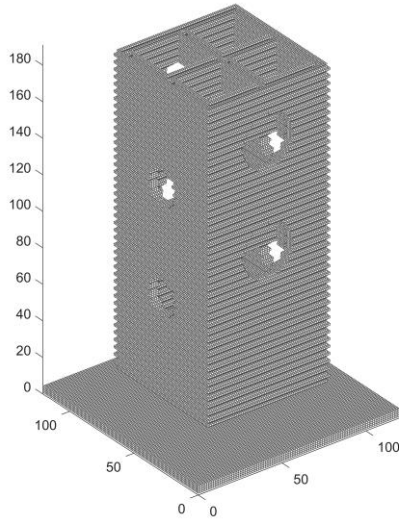
The primary goal of the simulations that follow is to assess the effectiveness of hydrophobic air channels at preventing complete saturation of the substrate. There is a strong suspicion that even with a hydrophobic coating around the edge of the air channel, fluid will simply form a column going through the channel without touching the walls of the channel. To test whether this will actually be the case, the fluid flow through a square capillary array with hydrophobic air channels is simulated.

##### 4.4.1 Geometry

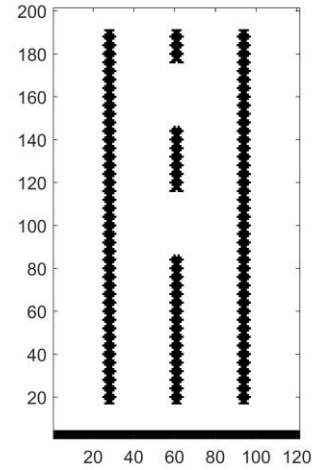
The geometry used is shown in Fig. 20. An array of four square capillaries is generated within a  $121 \times 121 \times 201$  computational domain. The capillary array is given an adhesion coefficient of  $G_{adh} = -0.06$ , which corresponds to a contact angle of  $53^\circ$ . A 3 lattice unit thick base is put at the bottom of the domain to prevent fluid from entering the top of the array (recall that the boundaries are periodic). The base is given an adhesion coefficient of  $G_{adh} = -0.01$  to ensure that the fluid does not stick to it (while ensuring that fluid is not repelled away either). The base of the capillary array is located 18 lattice units above the bottom of the domain.

Four circular air channels are created at varying heights along the capillary array. Two of the channels have a radius of 10 lattice units and the other two channels have a radius of 15 lattice units. Around the air channels the adhesion coefficient of the capillary material is changed to

$G_{adh} = 0.06$ , which corresponds to a contact angle of  $151^\circ$ . This simulates the application of a hydrophobic coating to the air channels. This geometry can be seen in Fig. 20a.



(a) Square capillary array geometry



(b) Cross-sectional view

**Figure 20. Simulated capillary array geometry**

Each of the square tubes has an average perimeter of 112 lattice units. The perimeter fluctuates between 106 lattice units and 120 lattice units as a function of height. This approximates the geometry created when the substrate is 3D printed. This geometry can be seen in Fig. 20b. The simulation is initialized with an initial density distribution of  $\rho(x,0) = 0.28$  if  $z \leq 56$  and  $\rho(x,0) = 0.03$  if  $z > 56$ . No initial velocity is given.

The results of the simulation for the first 17,000 time steps can be seen in Fig. 21. In each image the red semi-circles represent the locations of the hydrophobic air channels. Due to the symmetry of the simulation all four capillaries are mirror images of each other. Thus, only one capillary tube will be shown.



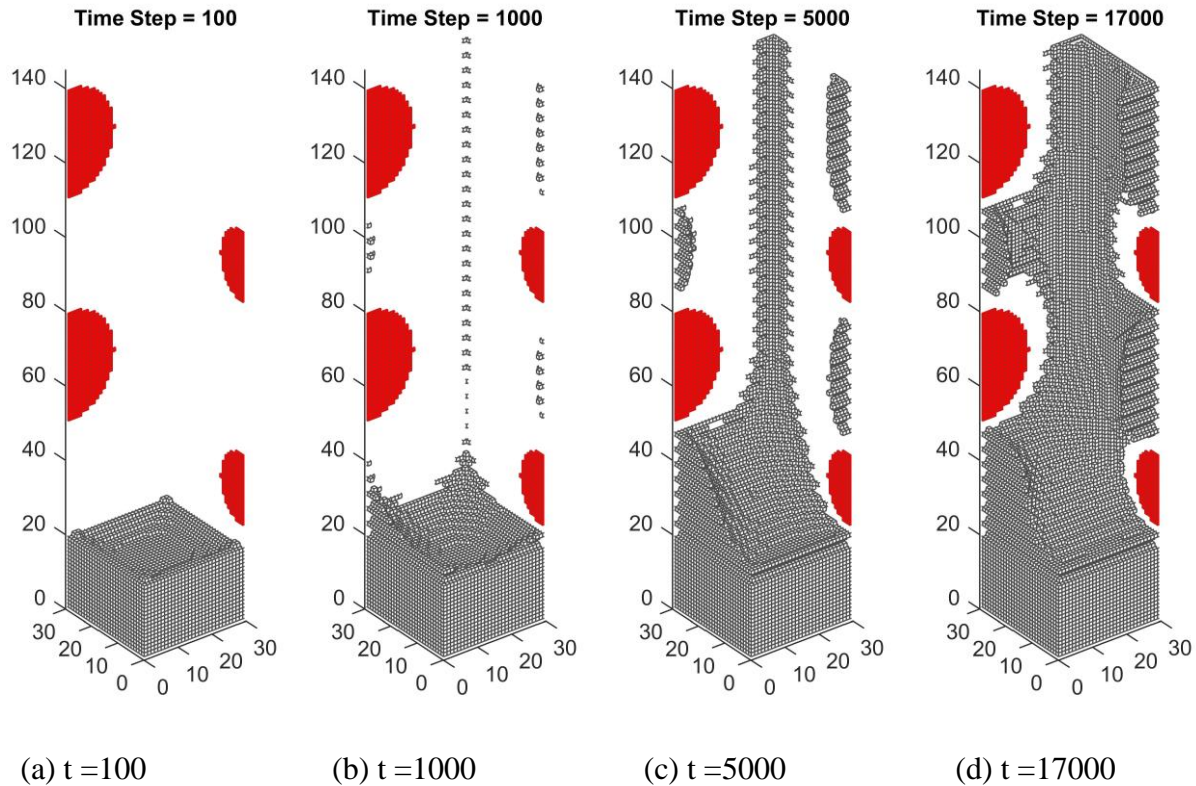


**Figure 21. Fluid rise in a square capillary with rough walls and hydrophobic air channels**

Figure 21a shows the initial state of the fluid in the pore before any capillary action has occurred. In Fig. 21b the beginnings of condensation can be seen in the corners of the capillary. This is because the corners contain fluid nodes that are surrounded almost entirely by solid nodes. This results in a very large adhesive force that causes the gas to spontaneously condense. Between  $t = 1000$  and  $t = 5000$  liquid rapidly enters the capillary with further condensation happening in the corners. At this point the furthest corner has made contact with the bulk fluid and is rapidly pulling fluid into it. At  $t = 17000$  the capillary is still uptaking fluid, however the rate has slowed significantly.

From the simulation data shown in Fig. 21d it can be seen that the hydrophobic air channels have successfully prevented fluid from oversaturating the pore. Despite earlier concerns about the performance of the hydrophobic coating, no water columns have formed in the channels themselves.

## 5 Plants

### 5.1 Germination

After initial attempts to germinate seeds on Kimwipes or on the blocks covered by Kimwipes, it was determined that Kimwipes did not maintain sufficient moisture to germinate the seeds. Seeds were first successfully germinated on germination paper, kept in sealed boxes or plastic bags to

maintain the moisture during germination. Similarly, seeds of sufficient size to not fall through the pores in the blocks were placed directly on the blocks, with germination paper on top to allow for germination on the blocks (removing the need for transplanting). Plants have successfully grown in the blocks after being transplanted from germination paper as well as from being germinated directly on top of the blocks, also using germination paper. One anomaly wheat plant successfully grew for a time after it germinated in the bottom of a block (fell through the holes during attempted germination) and germinated in the nutrient solution reservoir.

## **5.2 Plant Growth**

Testing plant growth in the 3D printed blocks began in November 2017. The initial tests done attempted to determine which plants would successfully grow in the blocks (requirements for different pore sizes and air holes) as well as to determine which germination methods would be most reliable and replicable. After a number of initial growth tests, a large variety of seeds were purchased and all attempted growth (by germination on paper method). From this initial trial, it was decided that further, focused testing would be continued using spinach, arugula, and lettuce. Each USU team member working on plant growth was assigned one species to focus on and began separate growth tests to look at growth of these three species in the different block designs and under varying factors influencing growth.

## **5.3 Potential Issues**

With the first block designs, the team discovered an issue of overflowing the roots of the growing plants. The capillary action of the substrate drew too much water to the root zones, and insufficient oxygen, killing the plants relatively early in growth. The team decided to pursue different substrate block designs, changing how nutrient solution and oxygen were delivered to the plant roots. After speaking with the NASA scientists, the team was also concerned about temperature and humidity shock. Most of the seeds were transplanted to the substrate after germination in relatively humid environments, as described above. To mitigate this, the USU team began germination directly on the substrate blocks, and the UA team enclosed the growing space with plastic wrap after transplantation to the substrate.

## **5.4 Water and Nutrient Delivery**

Nutrients were obtained from Dr. Bruce Bugbee for growth of plants at USU. A mix of Hydrosol (at 1 g/L) and calcium nitrate (0.5 g/L) were added to water to form the nutrient solution. The USU team initially just placed blocks straight into a reservoir of nutrient solution, allowing it to wick up the substrate. Nutrient build up was observed on multiple blocks after having been in the nutrient solution for weeks. To try and counteract this, a method was attempted of washing the blocks in fresh water each day, then submerging the block in nutrient solution and placing under growth lights without a reservoir. The plants switched to this method, however, quickly died. Further testing by the USU team has all been performed using the reservoir method. The goal is to develop a system which will allow the blocks to pull needed water from a reservoir bag

through a membrane or sintered plate, purely due to the matric potential caused by the depletion of water as it is used by the plants.

In the testing conducted by the UA team, blocks were placed on felt wetted with the same nutrient solution.

## **5.5 Hydrogels/Agar**

A hydrogel layer was initially proposed to make germination of seeds on the top of blocks feasible and successful, thus eliminating the need for any interaction with the block once germination has begun. A germination layer was researched, but no make-up was decided upon which would provide the needed elements in such a way that could be used with the blocks and used in space. An alternative to a hydrogel layer was proposed, using agar to create a growth area for the roots of the plants. The agar control (in petri dishes) successfully germinated and allowed plants to begin to grow. The blocks which were specifically created for agar germination (with small divots in the top), did not see any growth when the seed-impregnated agar was placed under lights. However, when the block was kept covered during germination, growth was seen on the blocks.

## **5.6 Pore Geometry**

The geometry of the pores was chosen to be triangles by the previous USU X-Hab team, as it was determined that the triangle would provide the maximum amount of water wicking within the block. Equilateral triangles were used, for ease of modeling and printing, and varying sizes were tried to determine what size best supported root growth. Although plants grew successfully to a harvestable size in any of the triangle sizes, the 2.5 mm triangles seemed to choke the roots, and ultimately the lettuce plant, which was growing well, harvested itself from lack of sufficient root support. Due to the determined water retention of the nylon blocks, the possibility of varying triangle sizes as the block goes up has been considered to maintain the matric potential desired.

## **5.7 Seed Planting Procedure**

For the seeds which were germinated on germination paper independent of the blocks, seedlings were transplanted two to four days after initial germination was observed. The plants seemed to hook onto the blocks and thrive if transplanted at an optimal size, not too young but also not too developed. The seedlings were threaded into one of the capillaries, either by simply sliding into place or by use of a floss threader. The blocks were wetted with nutrient solution prior to transplanting; and directly following transplanting, were placed in a reservoir under growth lights.

## **5.8 Schedule**

All three members routinely fed their specific plant each day. The individual feeding schedules were determined by the members and their plants. However, over spring break and holidays, one

member that was in town would come and feed all the plants while the other members were absent. During most meetings, the team discussed how the plants were doing and what could be improved.

## **5.9 Growth Chamber/Housing**

For housing, we used a box pipe structure to house the plants. We then used 11x11x4cm plastic boxes that housed two to four blocks at a time. Furthermore, two 28.5x28.5cm white LED lights were hung from the top of the box pipe structure.

## **5.10 Optimal Substrate Design**

The substrate that grows best depends on the plant. So far, the best substrate to grow spinach in is the microchannel substrate. The microchannel substrate produced more spinach plants than any other design. This substrate had no roots growing on the outside of the block, contrary to the other substrate designs used. For the assorted salad, the best substrate to grow in is the air channel design.

# **6 Housing Design**

## **6.1 Manufacturing Plan**

The housing design was something above and beyond the proposal that was initially given to us at the beginning of the year. We decided we wanted to tackle the housing unit as a part of our project because of the detailed external specificities that were going to become important to the design of the substrate to make it successful. The requirements to sustain the passive system that the 3D substrate characterizes are crucial to ensure that the right amount of nutrient solution at any given time can successfully supply the plant. The requirements of the housing structure that we felt were necessary to implement include providing a location where the 3D substrate can be securely placed, providing a passive system to consistently transfer the nutrient solution to the 3D substrate, utilizing some sort of membrane to disperse the nutrient solution to all parts of the substrate, and keeping the nutrient solution in contact with the bottom of the pores of the 3D substrate at all time.

These requirements were met in the final design, but unfortunately did not receive any further testing because of time restraints. A prototype was built to ensure that the parts would fit together and the engineering logic behind the design was intact. The housing design described can only be applied to a 3D substrate block base that is 41 mm × 36 mm, which is currently the triangle size of 3 mm if it is exposed in a 10 × 10 matrix. Unfortunately, because of this specificity, this does not have the ability to warp to other designs easily. If the project will be continued, we would encourage the making of a similar design which would be able to adjust to different block measurements if needed.

We decided that it would be beneficial to also have the substrate housing made out of 3D printed material. This will ensure that it can be fixed if it were to break on the ISS. This was not the top

priority while designing the housing unit, but it played a big role in designing pieces of the housing to accommodate being built using a 3D printer.

The housing unit contains various parts that will be discussed, including the materials used and the reasoning behind why we chose each one. SolidWorks designs, assemblies, and challenges that were needed to overcome are also discussed.

## **6.2 Check Valve**

A check valve can be used to create a negative pressure in the substrate. The opening pressure of the check valve corresponds to how much suction will be maintained at the base of the substrate. As the substrate drains, either due to evaporation or from the plant uptaking fluid, the substrate will actively try to draw fluid into itself (suction). From the WRCs it is known what volumetric water content corresponds to what suction. When the substrate creates enough suction, the check valve will open and allow fluid into the substrate until the suction is low enough for the valve to close.

The primary limiter to using a check valve to maintain negative pressure in the substrate is the strength of the spring inside. The smallest commercial check valves have an opening pressure of 6 cm of head, whereas our substrates require around 1 cm of head to achieve 50% volumetric water content. In other words, current check valves do not contain springs weak enough to maintain the proper suction in the substrate. It is expected, however, that in microgravity the WRCs will be shifted upwards. The total amount is unknown, but it is possible that they may shift enough to make commercial check valves viable. Finally, it is also important to note that both the substrate and the check valve exhibit hysteresis. For example, a check valve normally closes at 20% less pressure than it opens at. This should be accounted for in future designs that are striving for a passive solution.

## **6.3 Sintered Porous Plate**

A sintered plate is used to maintain a consistent and evenly distributed suction on the base of the substrate. The sintered plate is made of stainless steel and has a pore size of 10 microns. The plate is used in conjunction with the check valve to maintain negative pressure in the water supply line. The sintered plate serves two purposes. The first is that it acts as a wick; fluid in contact with the plate is evenly distributed through the entire plate. Second, the sintered plate serves as a pressure membrane that ensures the entirety of the fluid near the plate can be kept at (potentially) large negative pressures without allowing air into the system.

## **6.4 Reservoir**

There are two nutrient solution reservoirs employed in our design: a local reservoir and an exterior reservoir. The local reservoir sits directly beneath the sintered plate. The only goal of the local reservoir is to maintain fluid continuity between the exterior reservoir and the entirety of the sintered plate. The local reservoir is 1/8" thick because it is formed entirely by the thickness of the sealing gasket located underneath the sintered plate.

In microgravity the proposed exterior reservoir utilizes a collapsible bag. This reservoir is connected to the local reservoir via 1/16" tubing, with the check valve located in the middle. The bag is prefilled with nutrient solution in such a way that it is completely full; there should be no air bubbles in the reservoir. By using a collapsible bag, it can be ensured that no air bubbles enter the system and break fluid continuity. The only requirement for such a reservoir is that the material is weak enough for the pressures involved to actually collapse it.

It is important to note that a collapsible reservoir presents technical challenges on Earth. As fluid is drawn out, the total height of fluid in the reservoir will fall. This results in the suction applied to the substrate increasing over time, unless the reservoir is shifted up to compensate. On earth this problem can be resolved by using a Mariotte Bottle instead of a collapsible bag. A Mariotte Bottle allows for large quantities of fluid to be supplied to the substrate without change in the suction.

## **6.5 SolidWorks Design**

We considered a circular unit but decided to go with a rectangular unit to ensure that the 3D substrate will cover the entire surface of the sintered plate. No air pockets should be allowed into the sintered plate, to ensure that only the appropriate amount of water is transferred; air pockets in the sintered plate membrane will destroy the passive system. Since the block is rectangular shaped, we made the housing rectangular shaped.

The housing unit contains two 3D printed parts that compress together to secure the sintered plate and nutrient water reservoir inside. The top of the housing unit has an opening in the middle for the 3D substrate to sit inside. The bottom of the housing unit has a few openings and layered lips. The cut out circle in the middle on the underside is an opening for tubing to be inserted. This is where the nutrient solution will be transferred from the check valve, which will be connected to a nutrient bag. The opening on the top of the bottom piece of the housing is made to carry materials that the 3D substrate will be sitting on top of. The materials include the sintered plate, which will sit in between two rubber rectangular gaskets. When the two 3D printed parts are compressed together, a latch on the right side of the housing unit is available for the check valve to be secured. The check valve needs to be consistently locked in at the same latitude location as the bottom of the sintered plate. By latching the check valve onto the housing unit, it will ensure that the check valve will stay in the same place consistently throughout the growing process.

Figure 22 shows the design with the 3D printed parts as a transparent view, so the other parts inside of the housing can be seen. There are labels on the figure to show where specific parts are located relative to each other.

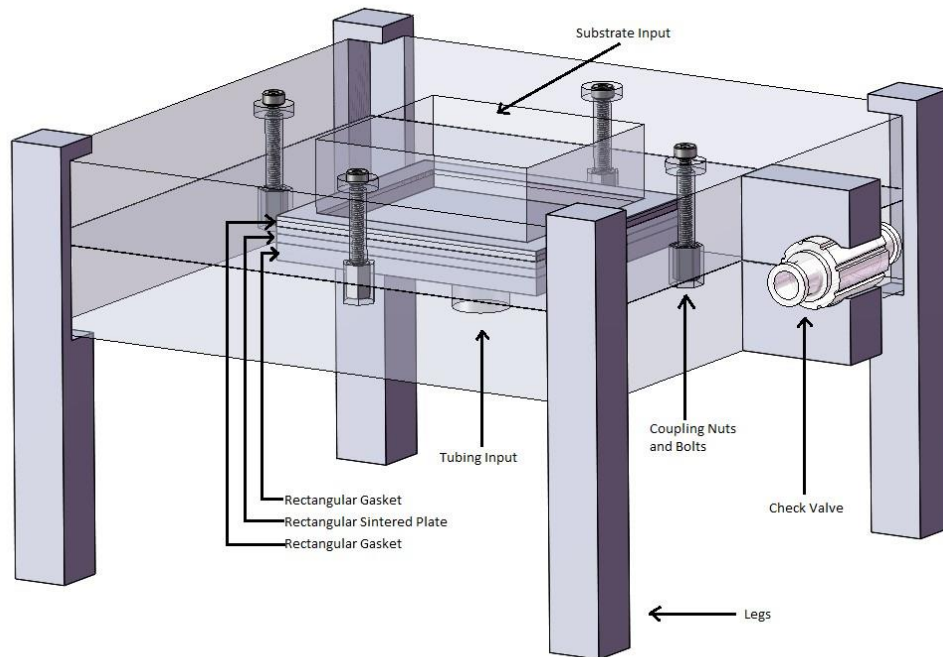


**Figure 22. Labelled housing diagram**

Figure E.1 shows the SolidWorks drawing of the housing as a whole unit. This particular view is when it is all compressed together. Figure E.2 shows the SolidWorks drawing of the bottom of the 3D printed housing unit. Figure E.3 shows the SolidWorks drawing of the top of the 3D printed housing unit.

The design utilizes the sintered plates and the pulling of water to supply the plant as it needs it. The negative potential that the plants will create when they are in need of nutrients will pull on the water from the bottom of the substrate. This will cause a reaction to the check valve, which will release more nutrient solution from the nutrient bag.

## 6.6 Material Chosen

The team decided to print the housing in Polylactic acid (PLA). This is because PLA does not warp on the bed of the printer compared to other materials such as ABS and Nylon. This ensures that the parts printed will be closer to the designed tolerance level.

To ensure that no air pockets got trapped into the membrane, we used rubber gaskets to seal the reservoir inside of the housing unit. Allowing air pockets inside of the interior of the housing unit will destroy the sintered plate mechanism, which is the only transfer system to get the nutrient solution from the nutrient bag into the 3D printed substrate.

There are coupling nuts and bolts that are used in the design. This is to keep the two 3D printed parts of the design in compression so that the substrate will continually be touching the sintered plate membrane. This will also ensure that no air bubbles will get into the interior of the housing unit.

## 6.7 Prototype

The prototype was made using the PLA material. The parts were all printed separately, including the top of the housing, the bottom of the housing, and the four legs. The coupling nuts and bolts were used to compress the design together.

## 6.8 Acquisition of Parts

A lot of the parts were obtained from previous projects that happened at Utah State University and professors who had spare parts. The few parts that we did purchase are included on the project budget section of the report. In particular, the check valves were ordered from Smart Products Inc., the sintered plates are from Mott Corp., and the coupling nuts and screws are off the shelf from local stores.

## 6.9 Future Manufacture of Components

Although keeping the housing structure 3D printed allows for repairs to happen directly on the space station, it may become more feasible to create the housing structure out of another material that has better tolerances and can be manufactured repeatedly with more accuracy.

## 6.10 Assembly

The complete assembly of the housing structure is shown in Fig. 23.

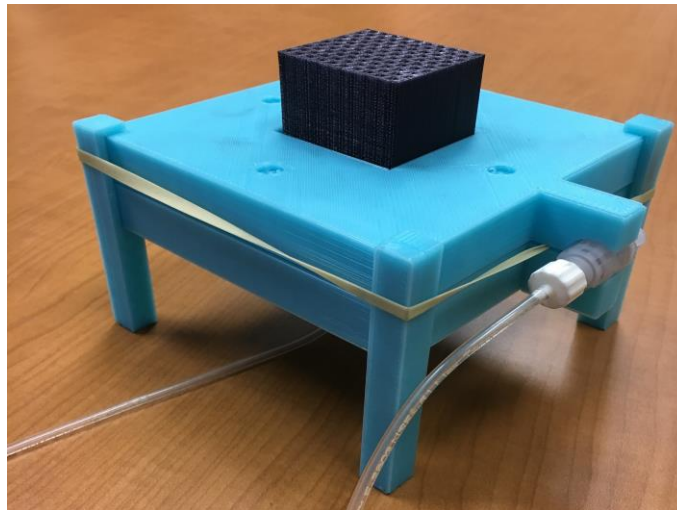


**Figure 23. Prototype housing**

## 6.11 Specific Challenges

Throughout the whole housing structure process, the team did not know what the final design was going to look like. It was only in the last few months of the project that the housing structure became a feasible idea based on the information collected regarding water retention and how to implement that concept into the substrate in a passive way.



This housing design is very specific to one type of dimensioned block. Other sizes are not accounted and would need to be adjusted if this were to happen.

## 6.12 Future Work

We need some way of measuring how much water is actually going into the block at one time when the plants are being grown in the substrate. We do have the check valve but that does not give us any information regarding what the plants are intaking. To improve the system or make any adjustments, we would need a system to be able to read the pressure differences occurring in the tubing when the check valve opens and closes. This would give us information regarding whether or not the plants are uptaking the maximum, or minimum, water available based on the water potential each part of the block possesses.

Future additions to the housing unit include adding hooks to each end of the housing structure, and creating a place for the nutrient bag to sit. By adding hooks to either end of the housing structure, an opportunity to stack multiple housing structures together in one unit becomes available. If multiple housing structures are close to each other, they could share the same nutrient bag. This would increase its space efficiency and utilize the resources available. The nutrient bag in the current design would just sit on the table next to the housing unit. This may be dangerous to be disconnected from the housing unit, because there is a possibility that the nutrient bag could fall off or be punctured, which would destroy the housing unit altogether. On the ISS station, there is a possibility that the nutrient bag could float off and take the housing unit with it. This would also cause destruction to the unit created and the plants inside.

## 6.13 Schedule

The schedule for the design of the housing can be found in Fig. 24.

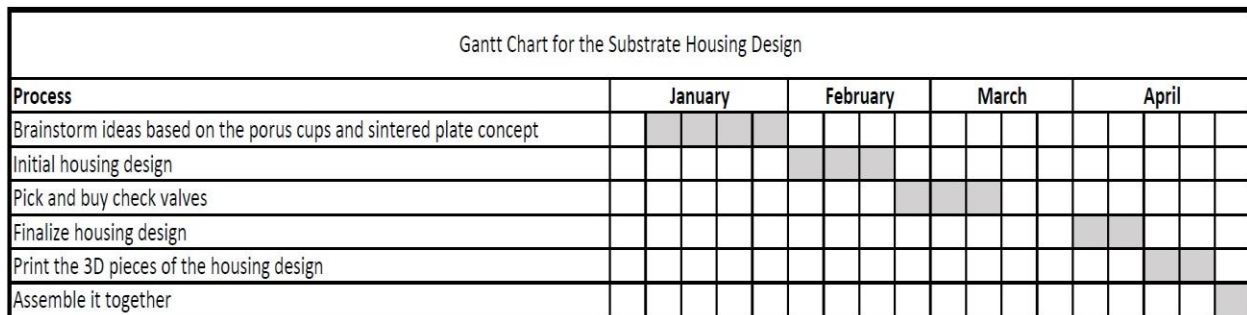


Figure 24. Housing design schedule

# 7 Low Gravity Testing

## 7.1 Purpose

After finalizing multiple 3D substrate block designs, it was necessary to determine their feasibility in a microgravity environment. The ideal situation would have been to use a drop tower test, however, there are no drop towers available around the USU or UA campuses. With

this in mind, the team began designing a way to emulate a drop tower test without the actual drop tower. This led to the team's current system for low gravity testing.

The team decided that the best way to simulate a drop tower was to actually drop the 3D substrate. Since the acceleration of the substrate would be comparable regardless of the apparatus the substrate was dropped in, the team settled on utilizing a drone and airfoil-like drop box. By designing an airfoil shaped drop box, the team would be able to limit the drag felt by the drop box while simultaneously leaving enough space inside the airfoil to place our substrate and a camera. This allowed us to view the capillary action inside the substrate during the fall, which gave us insight into how the substrate would behave in a low-to-microgravity situation.

## 7.2 Airfoil Design

To start with, the airfoil was designed to be symmetric. The operation outline of the low gravity testing assumed that the airfoil would be dropped straight down, which meant a zero-degree angle of attack. We didn't want to generate any lift on the airfoil, so a symmetric airfoil was used. Symmetric airfoils do not generate lift at a zero-degree angle of attack [16]. Symmetric airfoils are also slightly easier to model using 3D modelling software, so the choice was relatively straightforward.

Next, we needed to ensure that there would be enough space between the edges of the airfoil shape to house the GoPro we purchased and the substrate we wished to test. Using the formula for symmetric airfoils to determine the maximum thickness (Eq. 25),

$$t_m = 0.18c \quad (25)$$

Where  $c$  is the chord length and  $t_m$  the maximum thickness, the best fit for the airfoil design was determined to be a NACA 0018 airfoil with a chord length of 14 inches. This airfoil was modeled in SolidWorks and is shown in Fig. 25.

## 7.3 Airfoil Material

Once the airfoil was design, the team created a 3D print of it. The team wanted to use 3D prints of the airfoil for all the drop tests; however, 3D printing of the airfoil took at least a week for a single print, and the team required at least 8 of the airfoil prints. Since time was an issue, the team decided to find a different route to create the airfoils. The team purchased high density Styrofoam and a hot knife to construct the airfoils with. Using the 3D printed airfoil as a stencil, we cut out the airfoil shape from the Styrofoam. This was both faster and more cost effective.

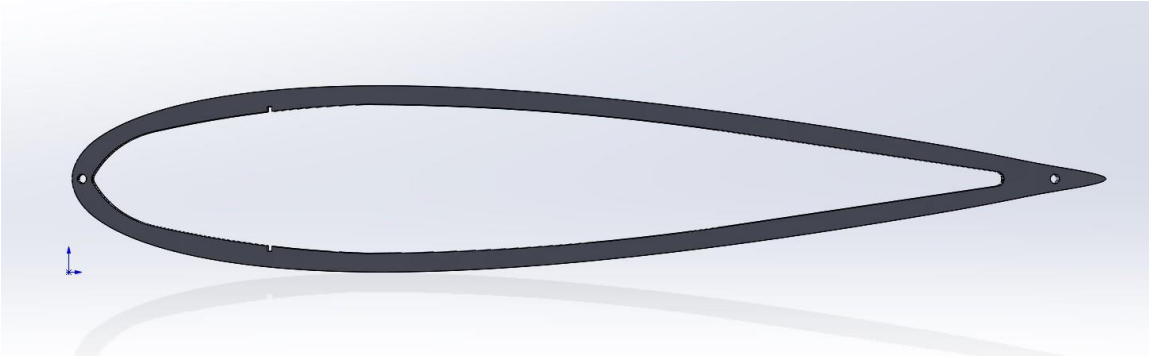


**Figure 25. NACA 0018 airfoil design in SolidWorks**

Using the Styrofoam cut-outs, the airfoil drop box was constructed with wooden struts to hold the Styrofoam together and a thin plastic glued over the edge of the airfoil shape to maintain a smooth outer surface. Notches were cut into the Styrofoam to hold a platform that the GoPro and the 3D substrate could rest on during testing. The completed drop box is shown in Fig. 26.



**Figure 26. Completed drop box for low gravity testing**

#### **7.4 Filming**

After the airfoil design was complete, the team needed a to purchase a small camera to fit inside the airfoil. We decided on the GoPro Hero 6. This camera was small enough to fit within our airfoil while also providing high quality video footage of the 3D substrate in low gravity. The videos were saved as a mp4 file and could easily be accessed using any media software interface. We also purchased a parachute to be placed inside the drop box. This would allow us to drop the system from a large height without damaging the GoPro significantly.

#### **7.5 Drone**

A Yuneec Typhoon H was selected as the lift vehicle for drop testing. This drone was chosen for three reasons: a high lifting capacity, a pair of retractable landing gear, and a low price. With the included camera removed, the Typhoon H is capable of lifting weights in excess of 1.5 kg. The total weight of the drop box is not expected to exceed 1 kg, so the aircraft is fully capable of lifting the payload with a modest factor of safety.

The Typhoon H also features retractable landing gear. This feature can be used as a payload release mechanism. The retraction mechanism of the landing gear is strong enough to break weak thread. By attaching the drop box to the thread, the drop box can be dropped in a smooth manner when the landing gear is retracted. This reduces overall complexity in the system because it is no longer necessary to design a special release mechanism.

## **7.6 Reservoir and Test Blocks**

The reservoir that was used during the drop test to supply the substrate with the appropriate amount of water is shown in Fig D.2. The reservoir was made in such a way that the bottom of the testing block would always be submerged in water even if the test block columns become completely saturated.

The assembled reservoir and test block design is shown in the SolidWorks drawing in Fig. D.1. The bottom half of the reservoir is shown in a SolidWorks drawing in Fig. D.4. The top half of the reservoir is shown in a SolidWorks drawing in Fig. D.3. A breakdown of each part is shown in Fig. 27. The assembly of these parts is done by using plastic bonder. The interior of the reservoir is consistently 0.6 mm thick. This is not explicitly shown in the SolidWorks drawing. This is to ensure that the water does not seep through the 3D plastic material.

The test block design shown in the reservoir drawing is labeled with triangles that have 3 mm length sides and represent one of the control blocks. This specific block is shown in a SolidWorks drawing in Fig. D.2. Other test blocks that were created specifically for the drop test include other control blocks of triangle sizes 2 and 2.5 mm. A rendition of the crosshatch block design of triangle size 3 mm was also created. Each block was designed at 50 mm tall so that there would be enough room for the water to travel up the columns of the design and give us accurate data of the water motion the block would experience.

The test blocks only had two rows of capillary tubes and were printed in Bridge Nylon 680, which is a clear material. The thinner cross-section allowed for enough light to pass through the test block. Green food coloring was added to water to visibly observe the water motion as it traveled through the capillaries in the test block. A small inlet tube on top of the reservoir was added to allow air to replace the water that was originally in the reservoir.

## **7.7 Testing Procedure**

The reservoir and GoPro were attached to the airfoil using Gorilla Glue brand double-sided tape. The reservoir was then filled with 13 ml of green water to ensure the base of the capillaries were covered. The airfoil was attached with string and thin, velcro straps to the landing gear of the drone. The drone was flown to 200 feet above ground and the landing gear retracted, which broke the string and dropped the airfoil.

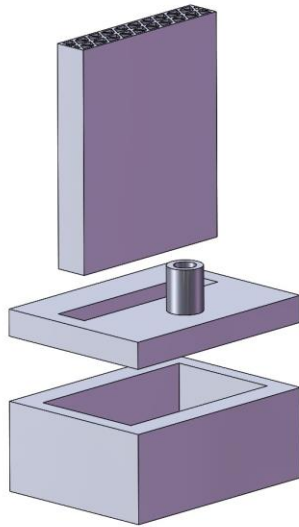


**Figure 27. SolidWorks view of low gravity testing assembly**

## 7.8 Data

The data collected from our drop tests was inconclusive. Windy test days and our inability to drop the drop box straight down consistently led to the airfoil moving laterally and occasionally flipping over completely. The few videos that were useful showed high velocity capillary action through our substrates, but the spacing of the water in the blocks was inconsistent.

Though the data turned out to be unhelpful in testing our design, the team believes we are on the right track to finding a suitable replacement for an actual drop tower. With a few tweaks, the drop test system will be able to give us more conclusive data.

**Table 4. Drop test schedule**

Date	Block Type
April 14, 2018	2.5 mm control
April 14, 2018	3 mm control
April 21, 2018	2 mm control
April 21, 2018	2.5 mm control
April 21, 2018	3 mm control
April 21, 2018	3 mm with air holes

## 8 Outreach

### 8.1 Outreach Overview

The focus was on reaching out to high school students around the Cache Valley area. Table 5 shows which high schools the team was able to reach. A poster was created to summarize the interesting parts of the project that could be presented to the students at these schools. This Poster can be found in Appendix F.

**Table 5. The scheduled outreach events**

School Name	Event Type	Event Date	Event Time	Location Address	Volunteer Captain
Ridgeline High School	Booth	4/11/18	11:00	180 N 300 W, Millville, UT 84326	Adreann Peel
Sky View High School	Booth	4/16/18	11:30	520 S 250 E, Smithfield, UT 84335	Camren Hansen
Intech Collegiate High	Booth	4/17/18	12:00	1787 Research Park Way, Logan, UT 8434	Camren Hansen

To promote unity and to include on various social media platforms, a photo was taken of the students participating in the research. This can be seen in Fig. 28. These efforts along with the written press release were done to promote the project to the community and to increase the interest of upcoming students to become involved in future research.

### Outreach to Students

#### 8.2

The team attended high schools during their lunch hour to talk to students about the project and about engineering. The three schools attended were Ridgeline High School on April 11, Sky View High School on April 16, and Intec High School on April 17. During the lunch hour, the team was able to talk to approximately 50 students at each school who were interested in our project endeavors. Many students were drawn to the table by the swag and the NASA logo. Students were excited to hear about our project even if they expressed little interest in engineering. The team felt that the outreach effort was successful in sharing our research, and more importantly helping others to see the opportunities associated with space travel.

### 8.3 Social Media

Iren Bencze, as our team mentor, technical writer, and manager, encouraged the team to develop professional skills while working on our project. Each team member obtained a LinkedIn account and kept each of our networks informed of the endeavors we were pursuing. Facebook became a tool that was utilized as well to spread the word about our project and outreach opportunities we wanted to create. The Facebook page can be found at <https://www.facebook.com/USU.UA.XHabTeam/>. Social media was a great way for us to reach out beyond the boundaries of the University.

On Facebook, we have 27 followers, with posts reaching just over 480 people. On LinkedIn, a post was shared 6 times, liked over 50 times, commented on 3 times, and viewed over 1000 times. The post is shown in Fig. 29.

#### **Figure 29. Social media post**

Overall the team felt that outreach was effective in reaching the community. We want to thank NASA for being so generous in their outreach donation. It was a great addition to have handouts while talking to kids who were interested in our project and research endeavors. The hope is that having something from NASA will remind them of our project and encourage them to go to college, work on a similar project, or maybe one day work for NASA. The bookmarks, paper assembly rockets, and ISS stickers were a big hit.

## **9 Conclusion**

### **9.1 Lessons Learned**

Integrating a team with students from different geographical locations was a new experience for everyone involved. All meetings involving coordination between students at USU and at the UA were done through Skype, so we could see each other and communicate about the project endeavors. It took time to adjust to the physical disconnection; and to rely only on the virtual connection. It is almost incredible that we were able to create working relationships between the University of Alabama and Utah State University without ever physically seeing each other.

We learned that it is important to be proactive with these kinds of team-based designs. With more than 20 individuals working on the project throughout the year, it was easy to fall into the mentality that “someone else will take care of it” when it came to doing research or brainstorming ideas for further exploration. We learned that it is crucial to be accountable not only to the team, but also to ourselves individually. Taking initiative on various parts of the project – although sometimes may seem like a small deed – contributed immensely to the overall success of the project, because as a team we started moving in the right direction. We also learned that any goals made initially needed to be revisited throughout the year. This would have removed some of the stress and hardship when the end of the academic year rapidly approached.

Frequently an issue in industry as well, we also found that management and communication did not occur at the optimal level. While we organized ourselves into task-related subgroups along the main objectives of the project, there was so much overlap in the smaller tasks that the work breakdown structure was found to be not defined well enough with respect to the overall project goals. In the future it would be beneficial to have an overall project manager and teams that are more clearly defined in relation to the project goals. Furthermore, an overall systems engineer would be necessary to ensure that design requirements are met and that systems integrate together properly.

In terms of communication efficiency, we suffered a shock from ¼-th of the overall team having graduated in December 2017, and needing to integrate a new set of students in January 2018. With the project deadline approaching rapidly, subgroup reorganization did not formally take place, and this created a sense of randomness regarding who is in charge of what and is reporting to whom. As a takeaway for the future, we need to make sure that defined structure and goals set from the beginning are maintained throughout the project – regardless of personnel change and the perceived length or difficulties of the onboarding process – to ensure that everyone is working on something pertaining to the project, and that they feel a sense of belonging and responsibility towards the team.

### **9.2 Societal Impact**

C3PO is a pioneering project that will be beneficial not only to space exploration, but here on earth. With the increasing dangers of climate change, the growing number of droughts, C3PO



could provide drought stricken communities without topsoil with a substrate that could provide plants with the nutrients they need here on earth. Many other benefits are currently unforeseen in the domain of 3D printed substrates, but the future is not just defined to space exploration.

### **9.3 Guidelines for the Next Iteration**

Suggestions for future teams who may continue this endeavor are included in this section. These are things that we would have liked to accomplish, but did not have enough time.

Some of the variability of the water retention curves could have been from the fact that each block was a different volumetric size. The smaller blocks did not pull out as much water compared to the bigger blocks because they physically could not hold as much water. This was a confounding variable that added to the difference in block designs that may have caused skewness in the data. Only testing one variable at a time can significantly increase the accuracy and repeatability of the test completed.

Only having one block tested for each data set could have also contributed to the variability of the data collected. Statistically, only having one test per data set is not enough to signify whether something is statistically significant or not. Providing more than one sample per data set would increase the accuracy of the data collected by catching outliers and predicting patterns.

The last week of the project we were able to produce a block that gradually moved from a 2 mm triangle size to a 3 mm triangle size. This was newly created intelligence for the team, but unfortunately we were not able to do anything about it. The testing of this block would be beneficial not only for the water retention curves, but also for growing plants using the passive system we created.

### **9.4 Substrate**

Although a confident pattern was not necessarily found, there is a specific direction that we feel future endeavors could explore. By gradually moving from a 3 mm triangle to a 2 mm triangle, the energy potential in the block can be monitored during each phase of the plant growth. The parameters have been determined by the water retention curve data. Although no testing has been done on the final block, we are confident that this is a good direction to go for future endeavors.

### **9.5 Simulation**

In this report computational fluid dynamics software utilizing Lattice Boltzmann methods has been developed. The software was used to test key design features of several of the proposed substrate designs. In particular, hydrophobic air channels were tested to see if they provided sufficient retarding of the fluid uptake rate. The development of this software was motivated primarily by the lack of a specific feature set in existing open-source solutions. In particular, there is no easily identifiable way to simulate things like hydrophobic coatings with the open-source alternatives.

The software was validated in two ways. The first was by comparing bubble formation to the Young-Laplace equation. It was shown that the pressure difference between the inside and

outside of the bubble followed the equation. Second, capillary rise in a circular tube was simulated. The results were in agreement with the exact solution, and the literature. The relationship between the adhesion coefficient and contact angle was also characterized. A simulation was run for a square capillary array with rough walls and hydrophobic air channels. The simulation showed that hydrophobic air channels are sufficient to significantly lower the maximum volumetric water content in the substrate.

The most exciting prospect moving forward is the ability to measure the water-retention curves of the substrate in software. There are two potentially viable ways of accomplishing this. The first method would be to apply a pressure boundary to the bottom of the domain and an open boundary to the top of the domain. The pressure boundary would likely need to change in both space and time as the saturation of the substrate changes, which would be an interesting programming challenge. The open boundary could be implemented using Grad's approximation [17]. The second way would be to apply increasingly large gravitational forces to the substrate. There is also work to be done in improving simulation accuracy. In particular, the method of calculating the cohesion force acting on a node near a wall could be improved. The cohesive force relies on the density of all the surrounding nodes. When a fluid node is near a wall, several of the necessary densities won't exist because they will be in the wall itself. Currently, these values are approximated by calculating the weighted averages of all fluid nodes surrounding the solid node in question. This approach is naive, however, because it ignores density gradients in the vicinity of the node. In the next iteration of the software, a more sophisticated approach to approximating these values should be implemented.

Additional future work could also include moving to a more sophisticated approach to the relaxation time [18]. Currently, a single relaxation time approach is implemented. Once again, this is a naive approach because it assumes all particles collide at the same time, even when they are moving at different velocities.

## **9.6 Plants**

Successful growth of a variety of plants was maintained in the blocks from this project. The plants did not get as large as controls grown under similar parameters, but in a hydroponic soil substitute, suggesting stunted growth. The harvested lettuce from the blocks was quite bitter, likely due to a lack of nutrients and/or water received. In order to efficiently grow palatable plants in the 3D printed blocks, adjustments will have to be made in how the water and nutrients are delivered and taken up by the plants. For plants with a root crown, a divot in the block would likely best be employed to provide some protection—mimicking soil—for the root zone.

## **9.7 Low Gravity Testing**

The low gravity testing, though it was ultimately a failure, allowed us to think outside the box on how to test our design. We believe that, with more effort into perfecting our drop test, we will be able to validate our design with real data.

## **9.8 Housing**

The housing 3D structure could become a great place to test plant growth within the boundaries of utilizing energy potential and nutrient uptake as discussed. Unfortunately, the housing design only accommodates for only one size of block containing 3 mm triangles. If later it is concluded that a different base size would be appropriate to ensure success of the plant growth, a modified housing structure will need to be made.

## **9.9 Outreach**

The outreach to the local and online communities was successful. The team enjoyed being able to share what they have been working on and help high school students get excited about the opportunities available to them in the future. The online outreach will be continued on since some members of the team will continue to test and work on the project throughout the upcoming academic school year 2018-2019.

## References

- S. Baldwin, K. Carr, D. Crane, D. Froerer, T. Holyoak, Z. Jensen, E. Madsen, T. Marlar, P. Mortola, T. Rupp, E. Sherman, N. Stacey, and M. Turner, “EDEN: A Novel Approach to Plant Growth in Space,” rep., 2016.
- A. K. Datta, *Heat and Mass Transfer: A Biological Context*. Boca Raton, FL: CRC Press, 2017.
- B. Lajos, “Soil science,” 2008. [Online]. Available: [www.tankonyvtar.hu](http://www.tankonyvtar.hu). [Accessed: 26-Apr-2018].
- M. M. Weislogel and S. Lichter, “Capillary flow in an interior corner,” *Journal of Fluid Mechanics*, vol. 373, pp. 349–378, 1998.
- A. Ponomarenko, D. Quéré, and C. Clanet, “A universal law for capillary rise in corners,” *Journal of Fluid Mechanics*, vol. 666, pp. 146–154, 2011.
- M. M. Weislogel, “Compound capillary rise,” *Journal of Fluid Mechanics*, vol. 709, pp. 622–647, 2012.
- M. C. Sukop and D. T. Thorne, *Lattice Boltzmann Modeling: An Introduction for Geoscientists and Engineers*. Berlin: Springer, 2007.
- P. Raiskinmäki, A. Shakib-Manesh, A. Jäsberg, A. Koponen, J. Merikoski, and J. Timonen, “Lattice-Boltzmann Simulation of Capillary Rise Dynamics,” *Journal of Statistical Physics*, vol. 107, no. 1-2, pp. 143–158, Apr. 2002.
- S. Son, L. Chen, Q. Kang, D. Derome, and J. Carmeliet, “Contact Angle Effects on Pore and Corner Arc Menisci in Polygonal Capillary Tubes Studied with the Pseudopotential Multiphase Lattice Boltzmann Model,” *Computation*, vol. 4, no. 1, p. 12, 2016.
- Palabos. [Online]. Available: <http://www.palabos.org/>. [Accessed: 26-Apr-2018].
- OpenLB: Open Source Lattice Boltzmann Code. [Online]. Available: <http://optilb.org/openlb/>. [Accessed: 26-Apr-2018].
- P. L. Bhatnagar, E. P. Gross, and M. Krook, “A Model for Collision Processes in Gases. I. Small Amplitude Processes in Charged and Neutral One-Component Systems,” *Physical Review*, vol. 94, no. 3, pp. 511–525, Jan. 1954.
- X. Shan and H. Chen, “Lattice Boltzmann model for simulating flows with multiple phases and components,” *Physical Review E*, vol. 47, no. 3, pp. 1815–1819, Jan. 1993.
- P. Yuan and L. Schaefer, “Equations of state in a lattice Boltzmann model,” *Physics of Fluids*, vol. 18, no. 4, p. 042101, Apr. 2006.

Y. Su, X. Tang, F. Wang, X. Li, and X. Shi, “Three-Dimensional Cavitation Bubble Simulations based on Lattice Boltzmann Model Coupled with Carnahan-Starling Equation of State,” *Communications in Computational Physics*, vol. 22, no. 02, pp. 473–493, Jan. 2017.

J. D. Anderson, *Fundamentals of Aerodynamics*. New York, NY: McGraw-Hill Education, 2017.

S. S. Chikatamarla, S. Ansumali, and I. V. Karlin, “Grads approximation for missing data in lattice Boltzmann simulations,” *Europhysics Letters (EPL)*, vol. 74, no. 2, pp. 215–221, 2006.

K. Mattila, “Implementation Techniques for the Lattice Boltzmann Method,” thesis, 2010.

# Appendices

## A Gantt Chart

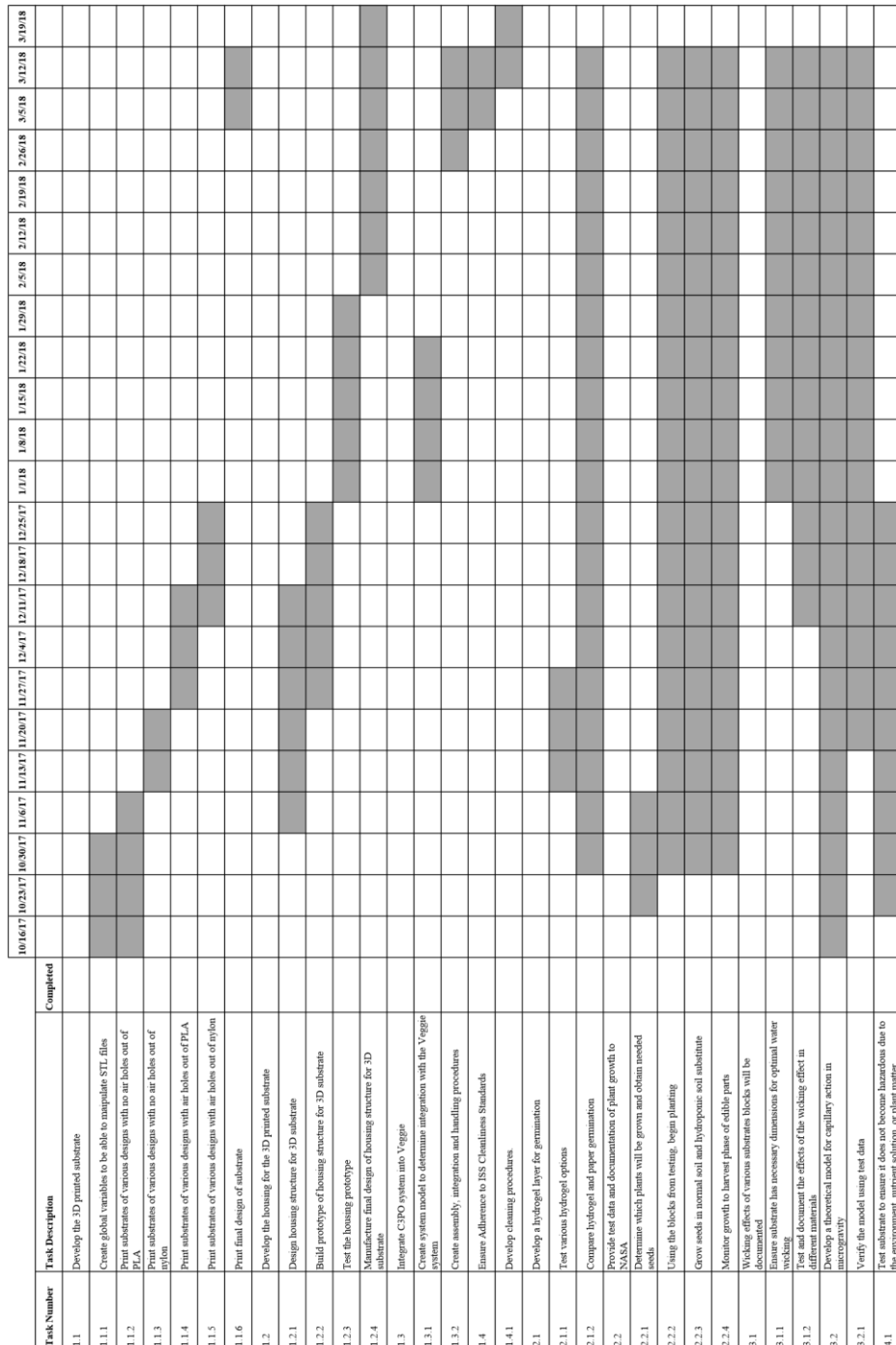
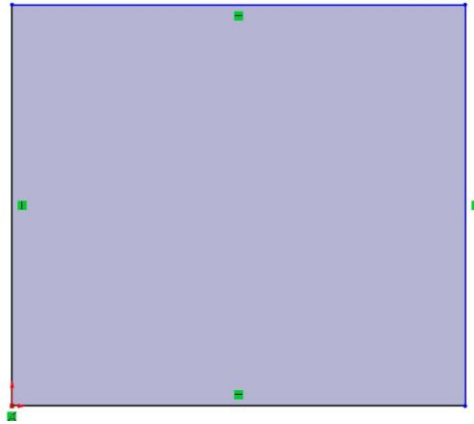


Figure A.1. Gantt chart

## B How To Make A 3D Substrate With Global Variables

1. Open the SolidWorks program. Create a box using the line tool with horizontal and vertical constraints. Do not make any other dimension constraints shown in Fig. B.1.



**Figure B.1. Global variables step 1**

2. Create more horizontal lines inside of the box to create how many rows you want in your substrate. Make sure the nodes of the lines are connected on opposite sides of the box, again with no dimension constraints. Start making diagonal lines to start making your matrix. You can make as many columns and rows as you would like. For this example, a 3 x 3 matrix is made, so eventually there would be 9 full triangles. It is a little tricky to tackle how many diagonal lines you need. Play around with it until you start seeing the triangles come to life shown in Fig. B.2.

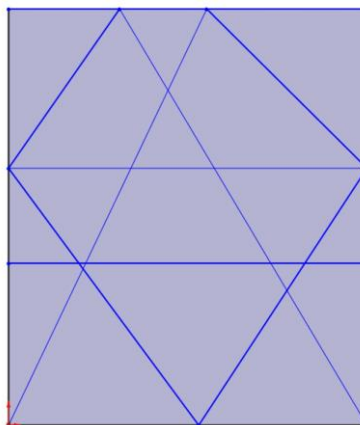


**Figure B.2. Global variables step 2**

3. Make 60 degree angles on two of the triangles. With two lines locked in (make sure they are going in opposite directions), make all of the other diagonal lines parallel to those lines. Adjust the horizontal lines so that they are intersecting where the diagonal lines are intersecting shown in Fig. B.3.

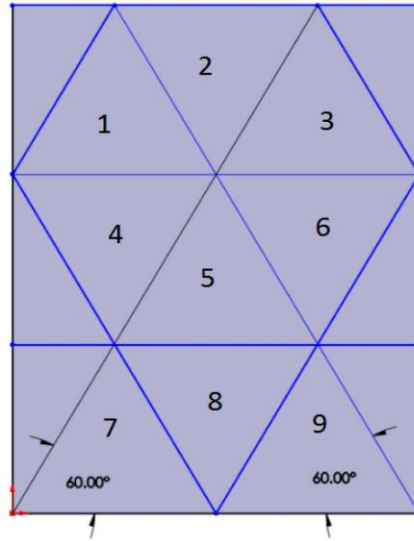


**Figure B.3. Global variables step 3**

4. Make all lines inside of the box “construction lines” by right clicking on the line and clicking the button shown in Fig. B.4.

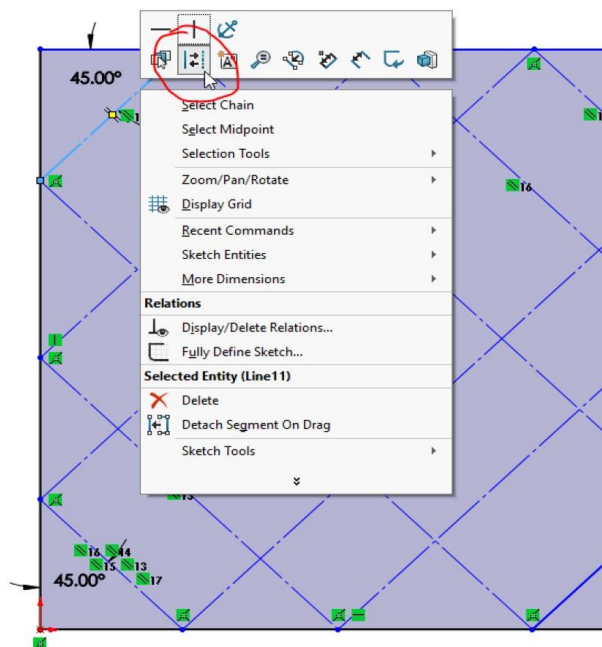


**Figure B.4. Global variables step 4**

5. Make sure the outside of the box still has solid lines and ONLY the inside of the box has construction lines shown in Fig. B.5. Try moving one of the outside box lines up and down. The rest of the lines should follow your movement because of the constraints. This is what is wanted as you create the triangles.



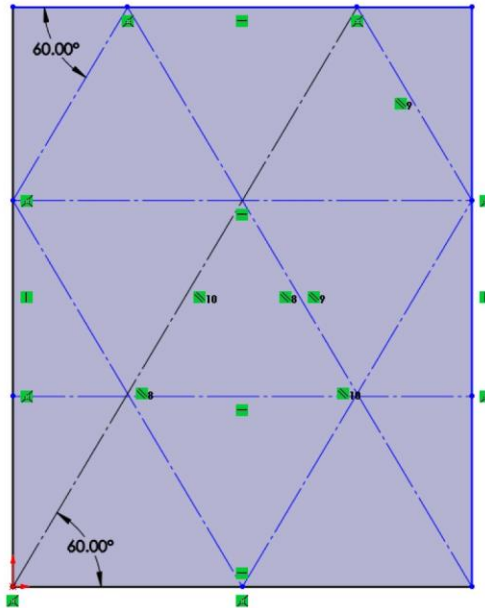


**Figure B.5. Global variables step 5**

6. Start on the bottom row and start making triangles as shown in Fig. B.6. Make sure the base of the triangle has a horizontal constraint. The other sides of the triangles do not matter quite yet.

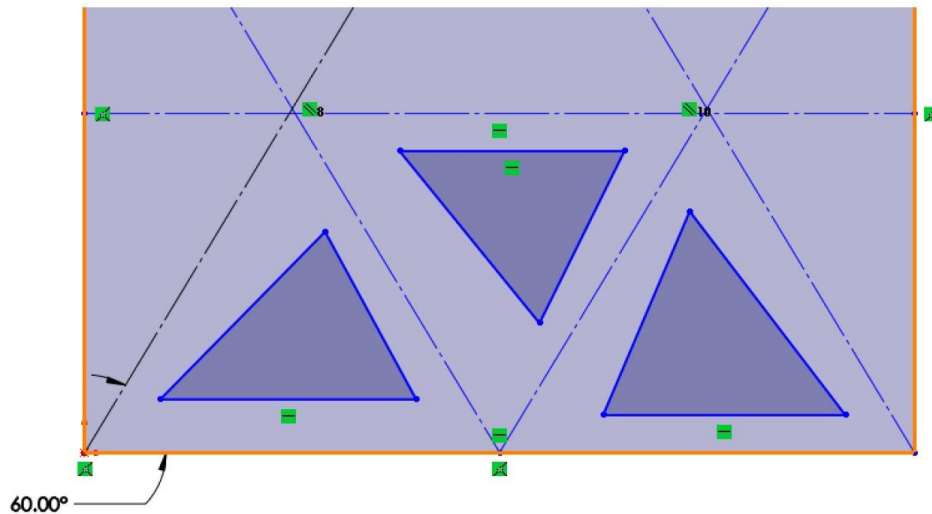


**Figure B.6. Global variables step 6**

7. Take the first triangle on the left side and make the far left angle equal to 60 degrees using the “Smart Dimensions” tool. Make all other triangle lines that are in that same direction parallel to that line. Do the same thing for the angle on the right side of the first triangle. Make all other triangle lines that are in that same direction parallel to that line. The top of the triangle should automatically have an angle of 60 degrees. This is shown in Fig. B.7.

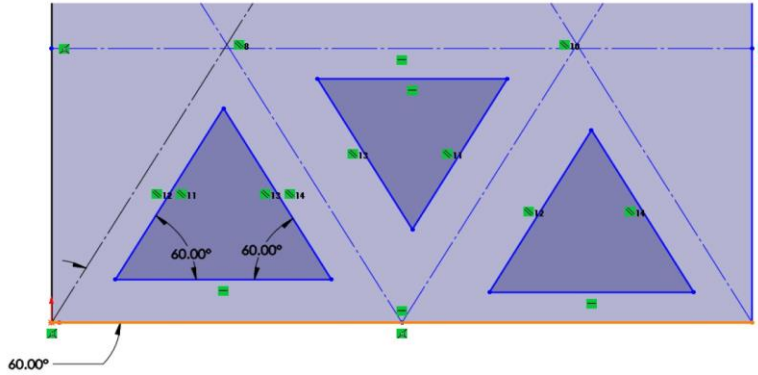


**Figure B.7. Global variables step 7**

8. Create a variable that will specify the distance from each triangle side to the construction lines. To create a global variable that can be used over and over again, click on “Tools” on the top menu, then “Equations” on the drop down menu. A menu should pop up as shown in Fig. B.8.

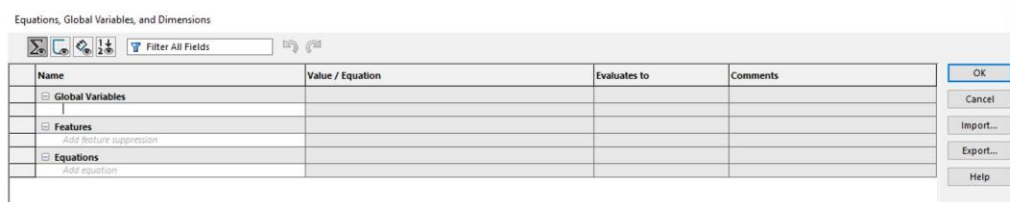


**Figure B.8. Global variables step 8**

9. In the “Name” column under “Global Variables”, write a variable name. Make sure to put the variable in quotation marks. In the “value” column, write down the value that you want the variable to always have. In the drop down menu that appears after the value is created, pick the units that are associated with the value. Click the check mark and the “Evaluates to” column will fill in automatically. Click “OK”. An example is shown below in Fig. B.9.

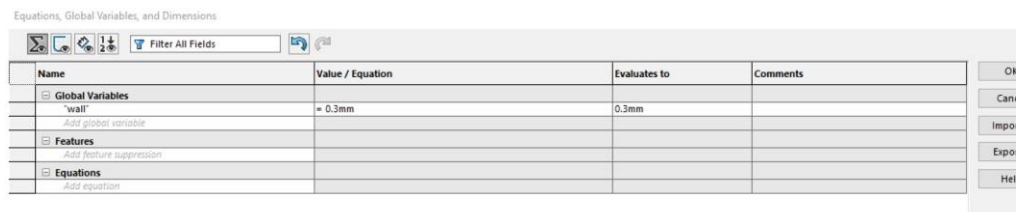


**Figure B.9. Global variables step 9**

10. The first variable in this example, as mentioned, will be the distance between the triangle sides and the construction lines. In the figure, the variable is named “wall”. Use the “Smart Dimensions” tool and click on one of the sides of the first triangle and then click on the construction line closest to it. In the dimension box, put the “=” sign, click “Global variables”, and click on the global variable that was specified just a moment ago. In this case it is “wall” as shown in Fig. B.10.

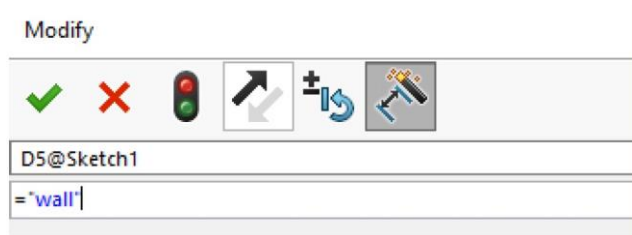


**Figure B.10. Global variables step 10**

11. Do this for every side of the triangles that you created on the bottom row. When a global variable is used it will be signified by a red summation sign as seen in Fig. B.11.

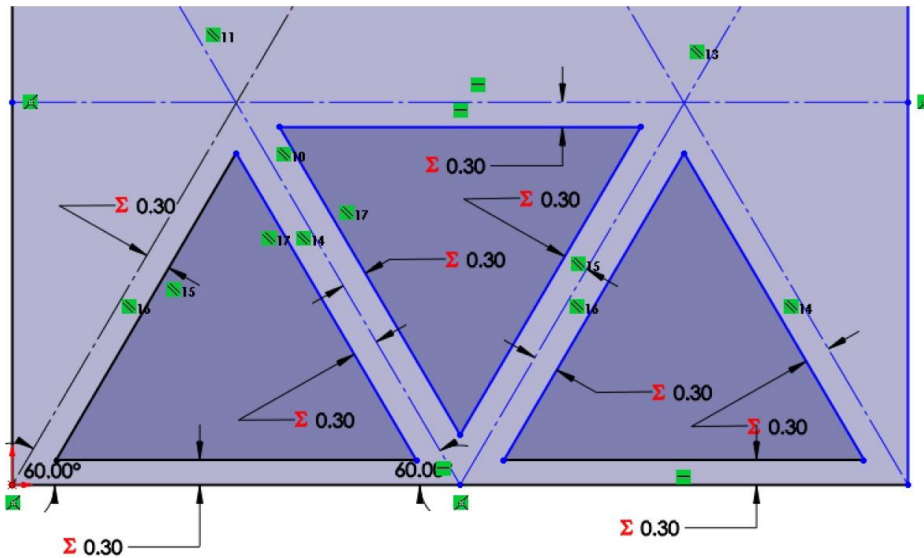


**Figure B.11. Global variables step 11**

12. Create another global variable that will represent each side of the triangle. The second variable name in this example is called “side” with a dimension of 3 mm as shown in Fig. B.12.

Equations, Global Variables, and Dimensions

Name	Value / Equation	Evaluates to	Comments
Global Variables			
"wall"	= .3mm	0.3mm	
"side"	= 3mm	3mm	
Add global variable			
Features			
Add feature suppression			
Equations			
"D5@Sketch1"	= "wall"	0.3mm	

**Figure B.12. Global variables step 12**

13. Define each triangle side with this newly created variable. (At least the ones that will not over constrain the design.) SolidWorks will let you know when this happens. Simply do not define that side. Most likely there are other constraints that Solid Works already put in because it is trying to help. Most of the time SolidWorks is helpful. There are a few times that you have to override it.

Do not worry about overriding any constraints for this application. This is shown in Fig. B.13.

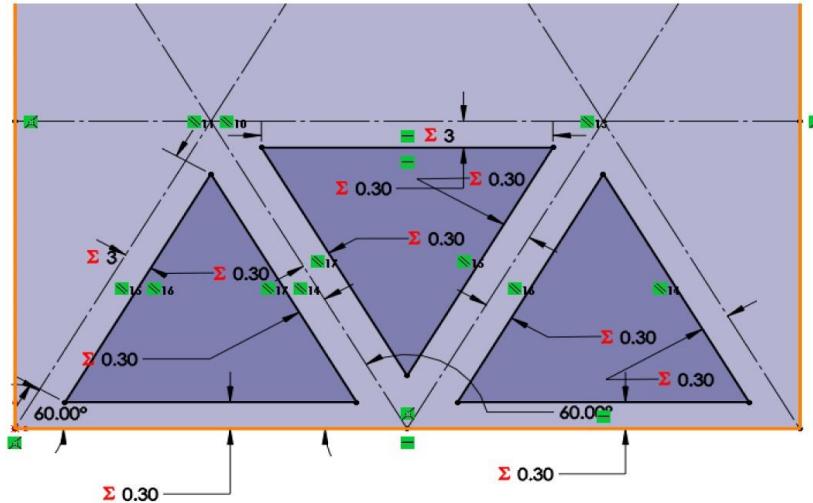


**Figure B.13. Global variables step 13**

14. Use the “Mirror Entities” function and mirror all of the triangles that were just created about the first horizontal construction line above the first set of triangles. Make sure that all of the triangles as a whole are selected. If you click in the middle of each triangle, it should capture all the lines that the triangle contains and all of the constraints that were previously included. In the “Entities to mirror” option, make sure all of the triangle sides are included. In the “Mirror about” option, click the horizontal construction line just about the first row of triangles. A preview of what the triangles will look like will be shown as a yellow outline shown in Fig. B.14. Click the green check mark in SolidWorks to solidify the preview.

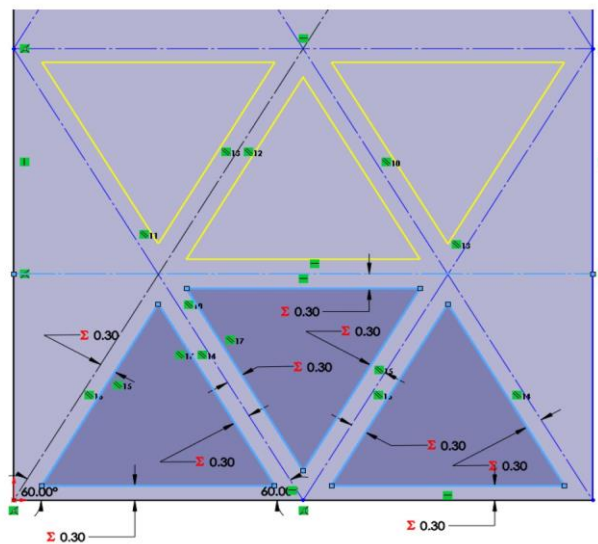


**Figure B.14. Global variables step 14**

15. Do this again by selecting the newly created row of triangles and mirror it about the next horizontal line about that row of triangles so that it creates another row of triangles on the very top of the box. All nine triangles should be created at this point shown in Fig. B.15.

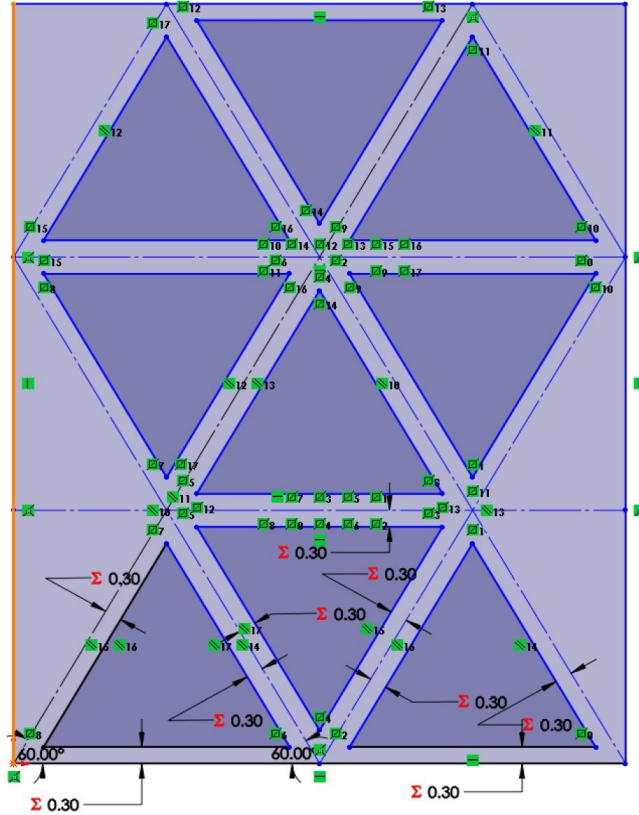


**Figure B.15. Global variables step 15**

16. Create the last two triangles on the bottom row that will be half as big as the other triangles. Put the triangles on both ends of the design. These can also be mirrored upward to fill in the void space of the box. Repeat steps 14 and 15 to mirror the last two triangles. The final product is shown in Fig. B.16.

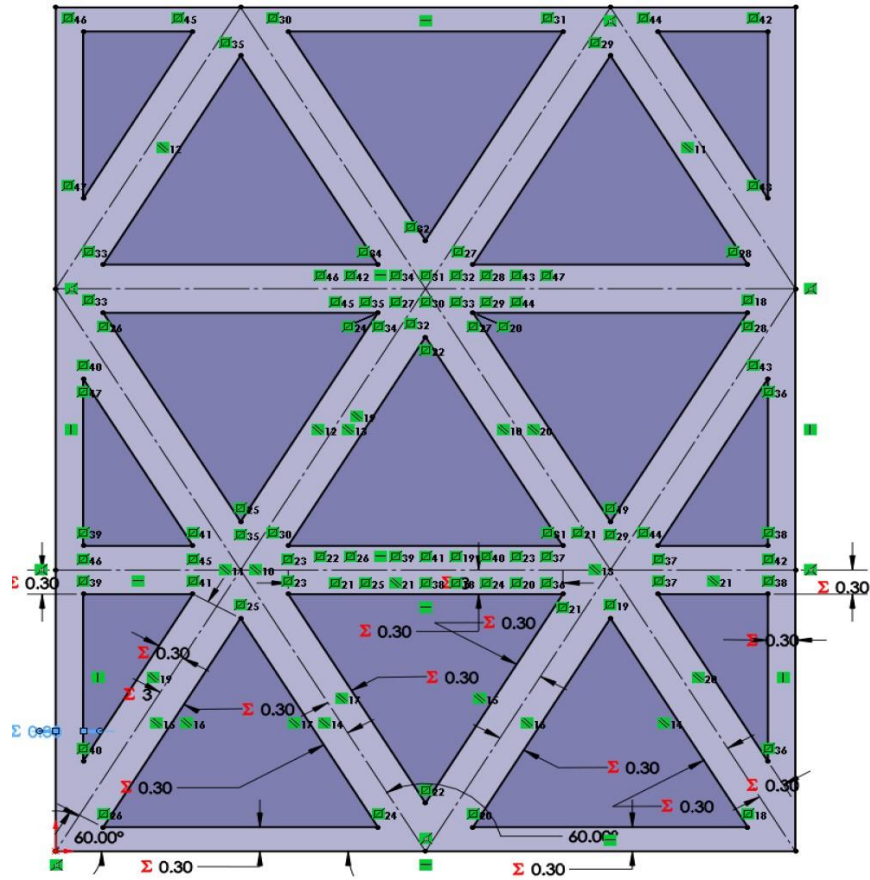


**Figure B.16. Global variables step 16**

17. Create another box around the design that has already been created and make the distance between the new box and the old box equal to the “wall” variable that was defined earlier. This is to ensure that the outside of the substrate is just as thick as the walls on the inside of the substrate. The structure of the substrate will be stronger if the outside walls are thicker than 0.6 mm. Make the old lines that created the old box construction lines. This is shown in Fig. B.17.

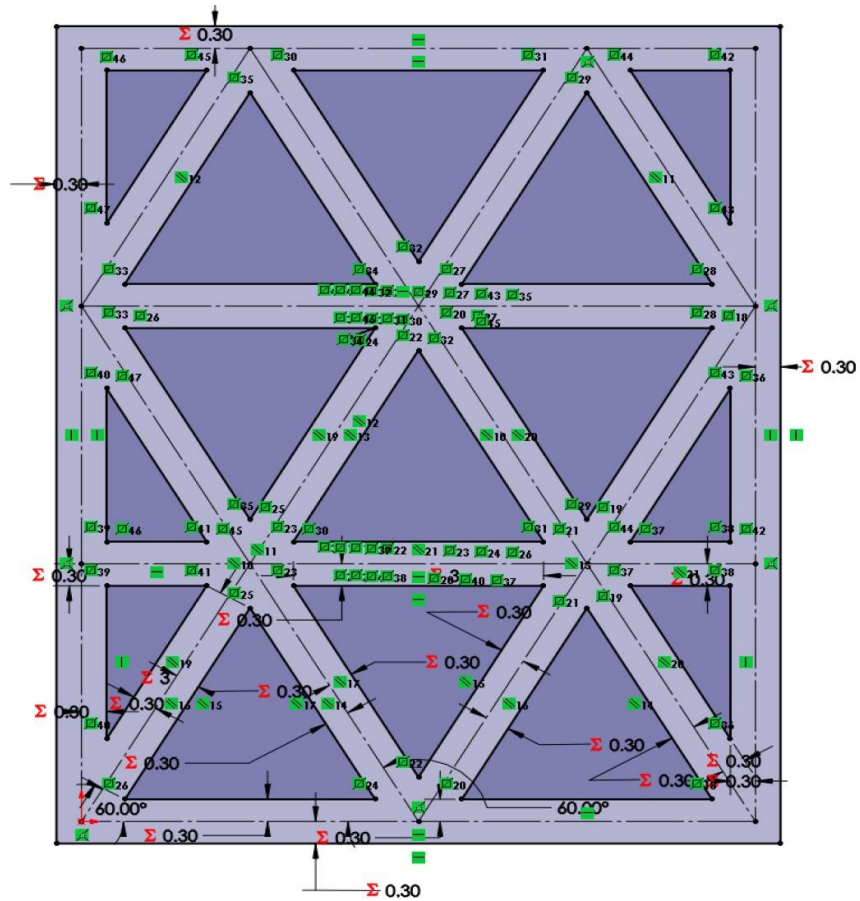


Figure B.17. Global variables step 17

18. Create another variable that will be used to adjust the height of the design when it is extruded. In this example, the variable name is called “height” with a dimension of 20 mm as shown in Fig. B.18.

Equations, Global Variables, and Dimensions

Name	Value / Equation	Evaluates to	Comments
Global Variables			
"wall"	= .3mm	0.3mm	
"side"	= 3mm	3mm	
"height"	= 20mm	20mm	
Add global variable			
Features			
Add feature suppression			
Equations			
"D5@Sketch1"	= "wall"	0.3mm	
"D6@Sketch1"	= "wall"	0.3mm	

Figure B.18. Global variables step 18

19. Use the “Extruded Boss” tool and click on the region with all of the construction lines so that the triangles continue to stay holes in the design. Make the “depth” dimension is equal to the variable that was just created. The final product as an extruded substrate is shown in Fig. B.19.

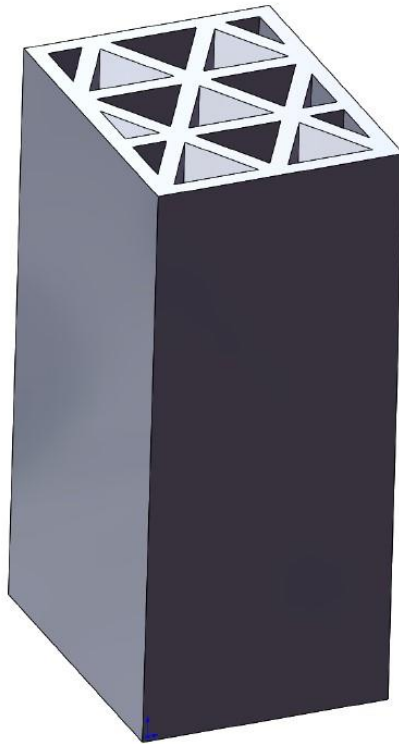


**Figure B.19. Global variables step 19**

20. Play around with it! Go to “Tools”, then “Equations”, and then change the global variables that you created. The substrate will change instantaneously when you click “okay”.



# C Substrate Drawings

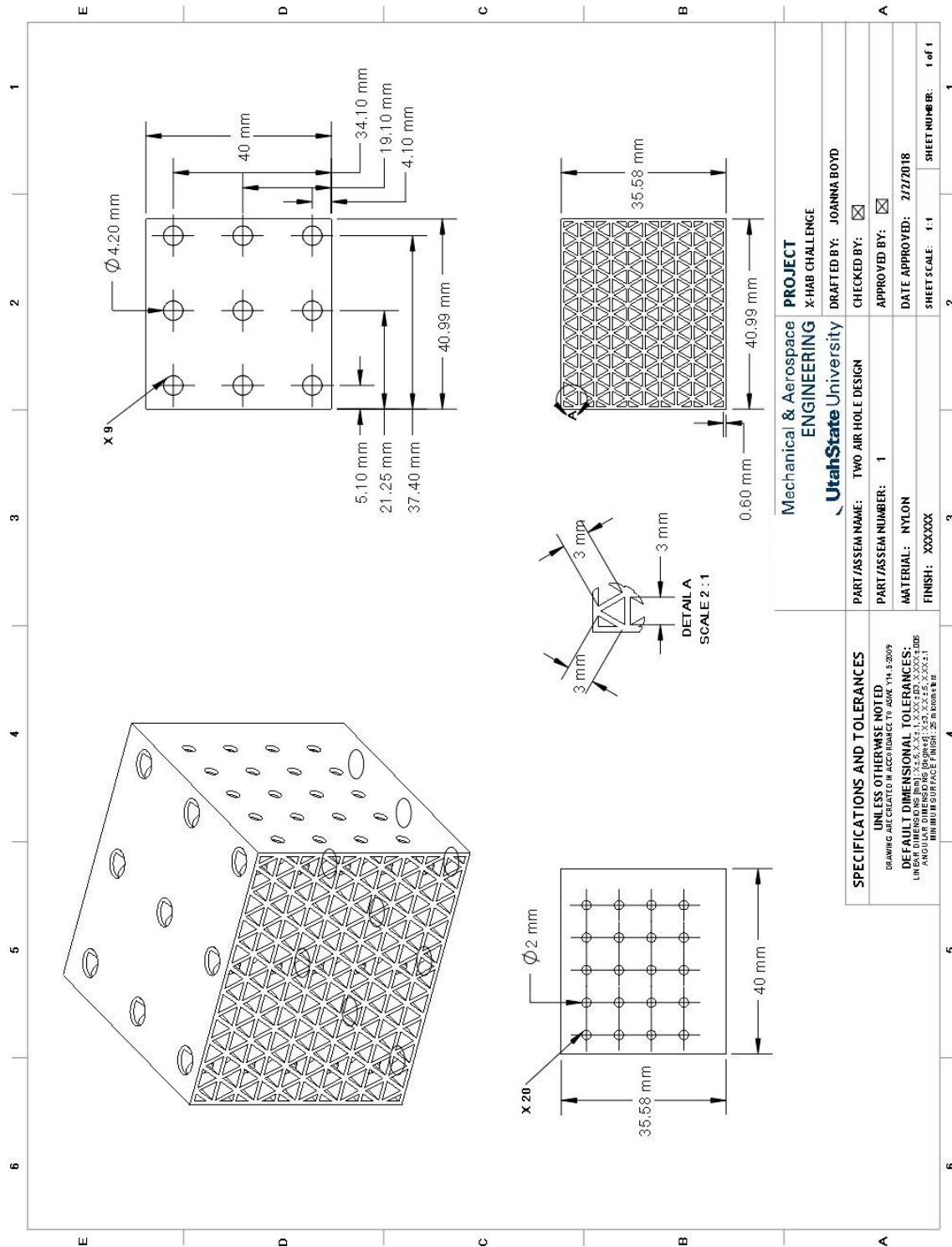
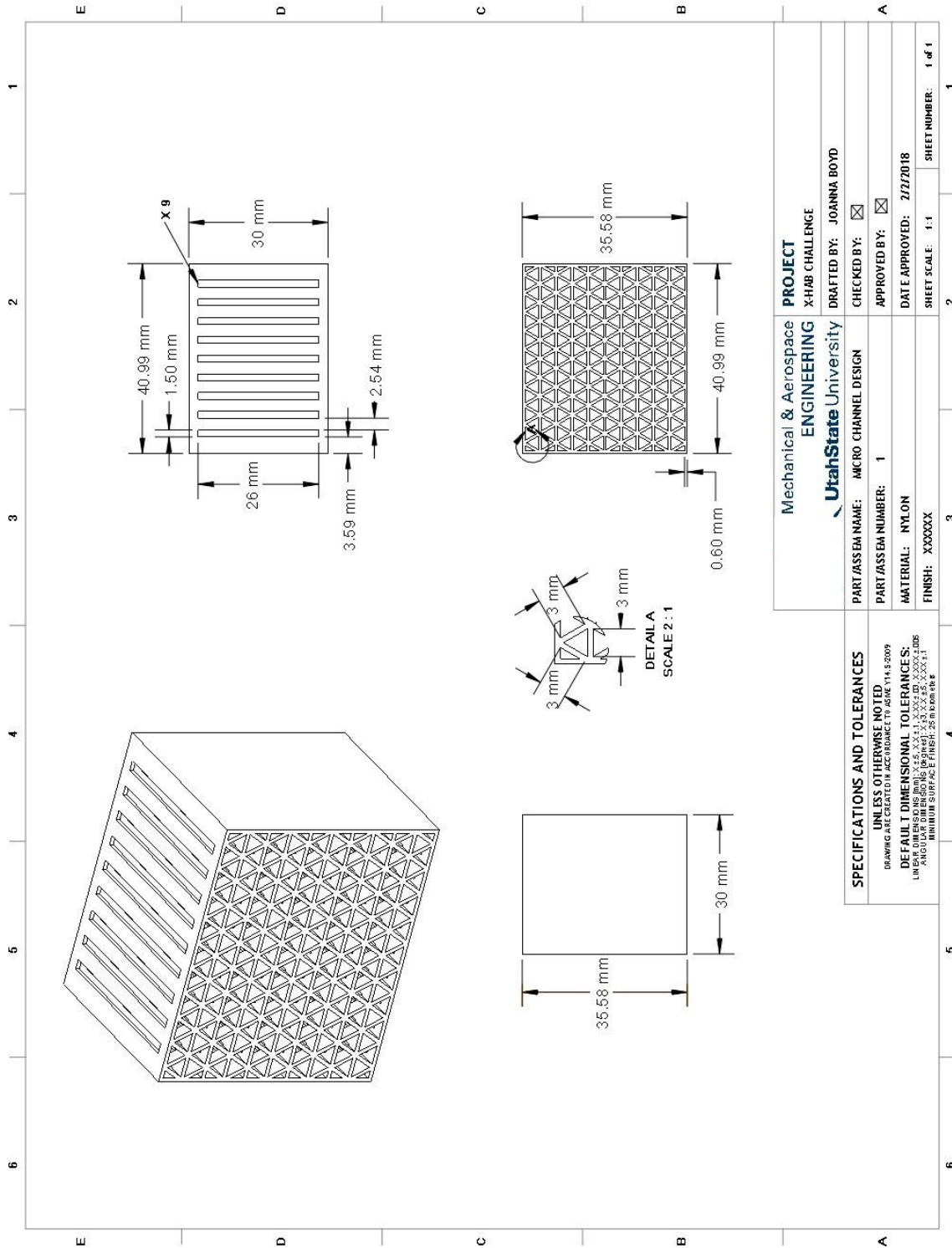


Figure C.1. Crosshatched design





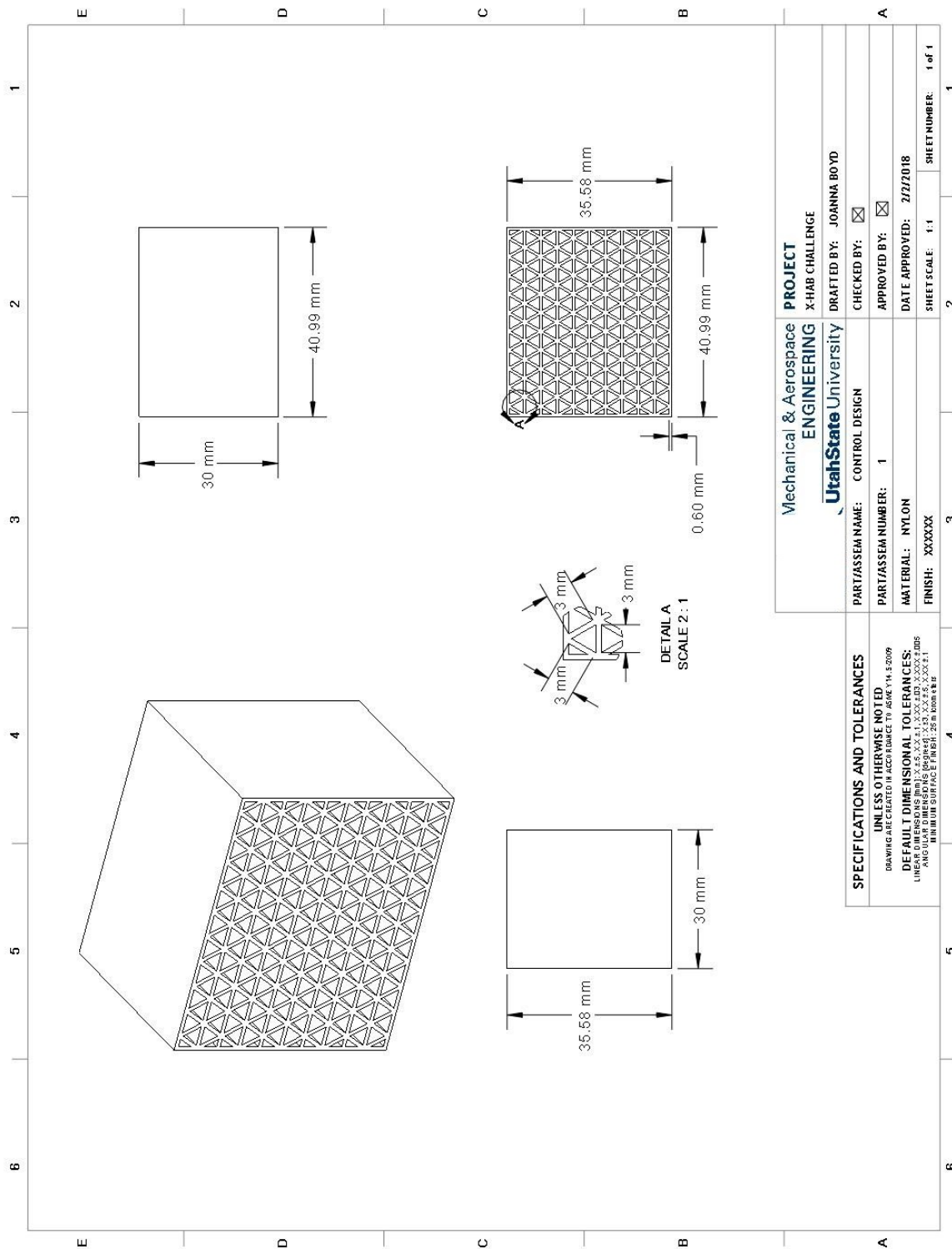
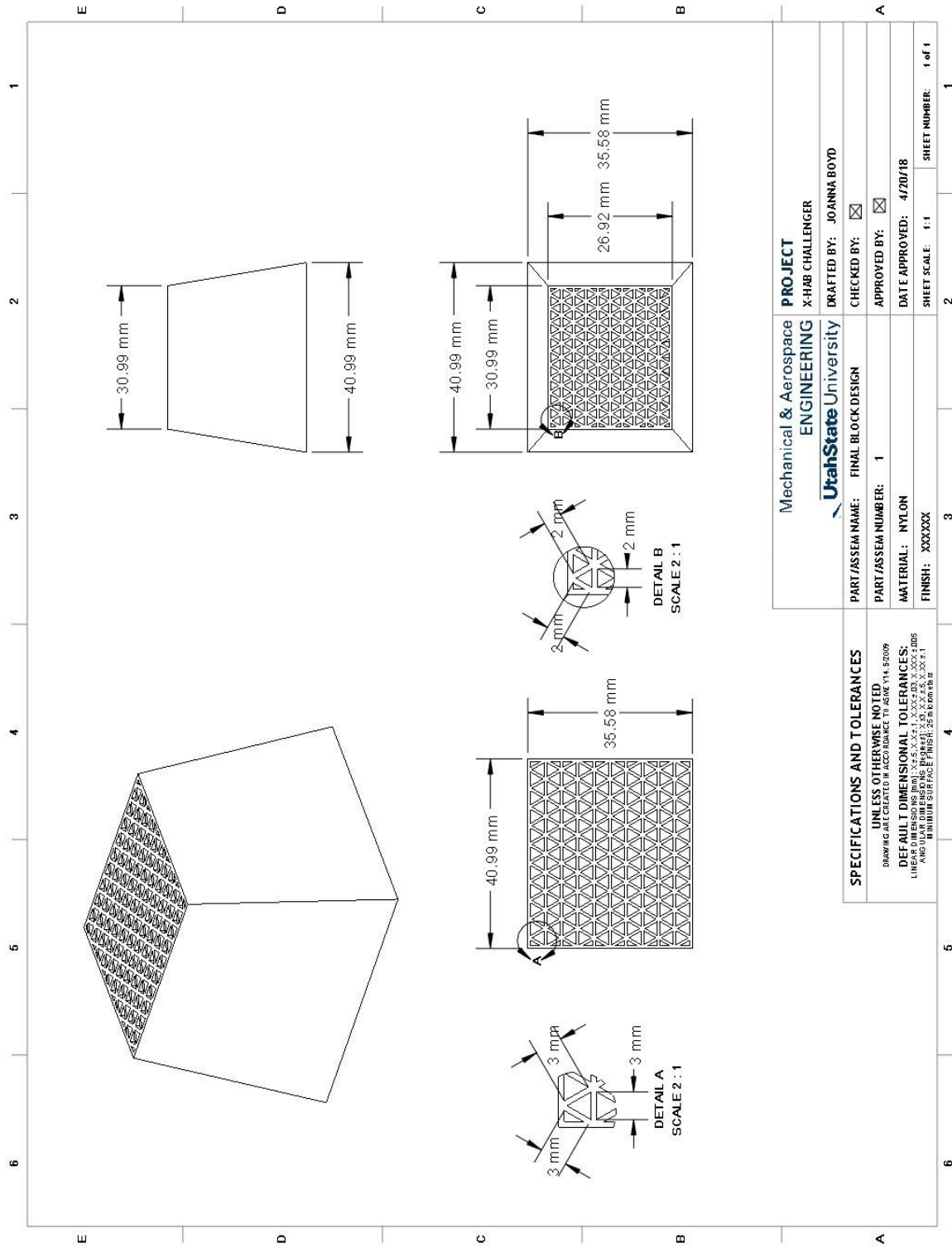


Figure C.4. Control design

Mechanical & Aerospace ENGINEERING		PROJECT X-HAB CHALLENGE	
UtahState University		DRAFTED BY: JOANNA BOYD	
PART/ASSEMBLY NAME:	CONTROL DESIGN	CHECKED BY:	<input checked="" type="checkbox"/>
PART/ASSEMBLY NUMBER:	1	APPROVED BY:	<input checked="" type="checkbox"/>
MATERIAL:	NYLON	DATE APPROVED:	2/7/2018
FINISH:	XXXXXX	SHEET SCALE:	1:1
SPECIFICATIONS AND TOLERANCES		SHEET NUMBER: 1 of 1	
UNLESS OTHERWISE NOTED			
DRAWING ARE CREATED IN ACCORDANCE TO ASME Y14.3-2009			
DEFAULT DIMENSIONAL TOLERANCES:			
LINEAR DIMENSIONS (mm): ±.25, ±.125, ±.0625, ±.03125, ±.015625, ±.0078125			
ANGULAR DIMENSIONS (DEG): ±.5, ±.25, ±.125, ±.0625, ±.03125, ±.015625, ±.0078125			
HOLE SURFACE FINISH: 32 IN. RMS OR BETTER			



# D Drop Test Drawings

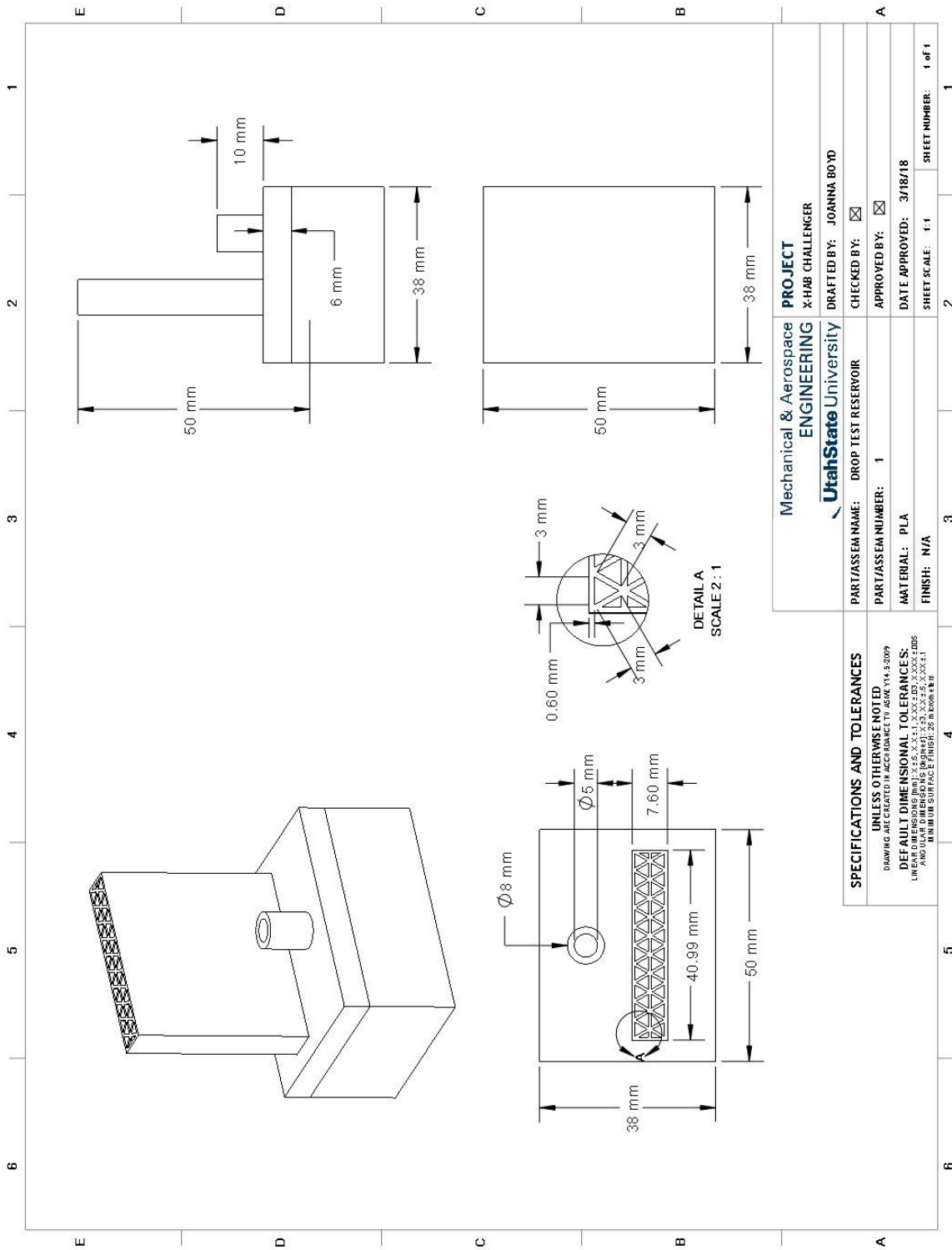


Figure D.1. Drop test assembly

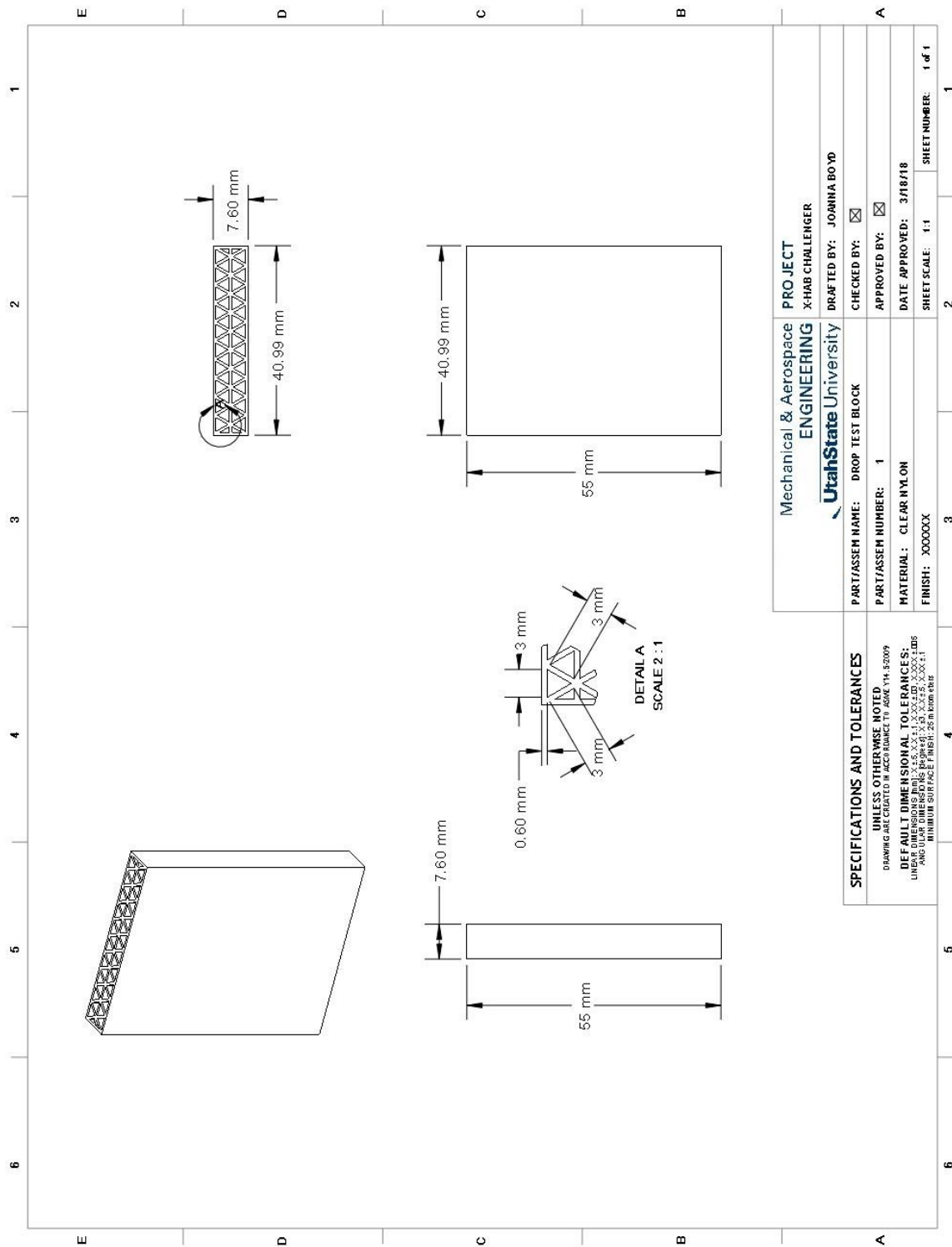


Figure D.2. Drop test sample

Mechanical & Aerospace ENGINEERING		PROJECT X-HAB CHALLENGER	
UtahState University		DRAFTED BY: JOHANNA BOYD	
PART/ASSEMBLY NAME: DROP TEST BLOCK		CHECKED BY: <input checked="" type="checkbox"/>	
PART/ASSEMBLY NUMBER: 1		APPROVED BY: <input checked="" type="checkbox"/>	
MATERIAL: CLEAR NYLON		DATE APPROVED: 3/18/18	
FINISH: XXXXXXX		SHEET SCALE: 1:1	
		SHEET NUMBER: 1 of 1	

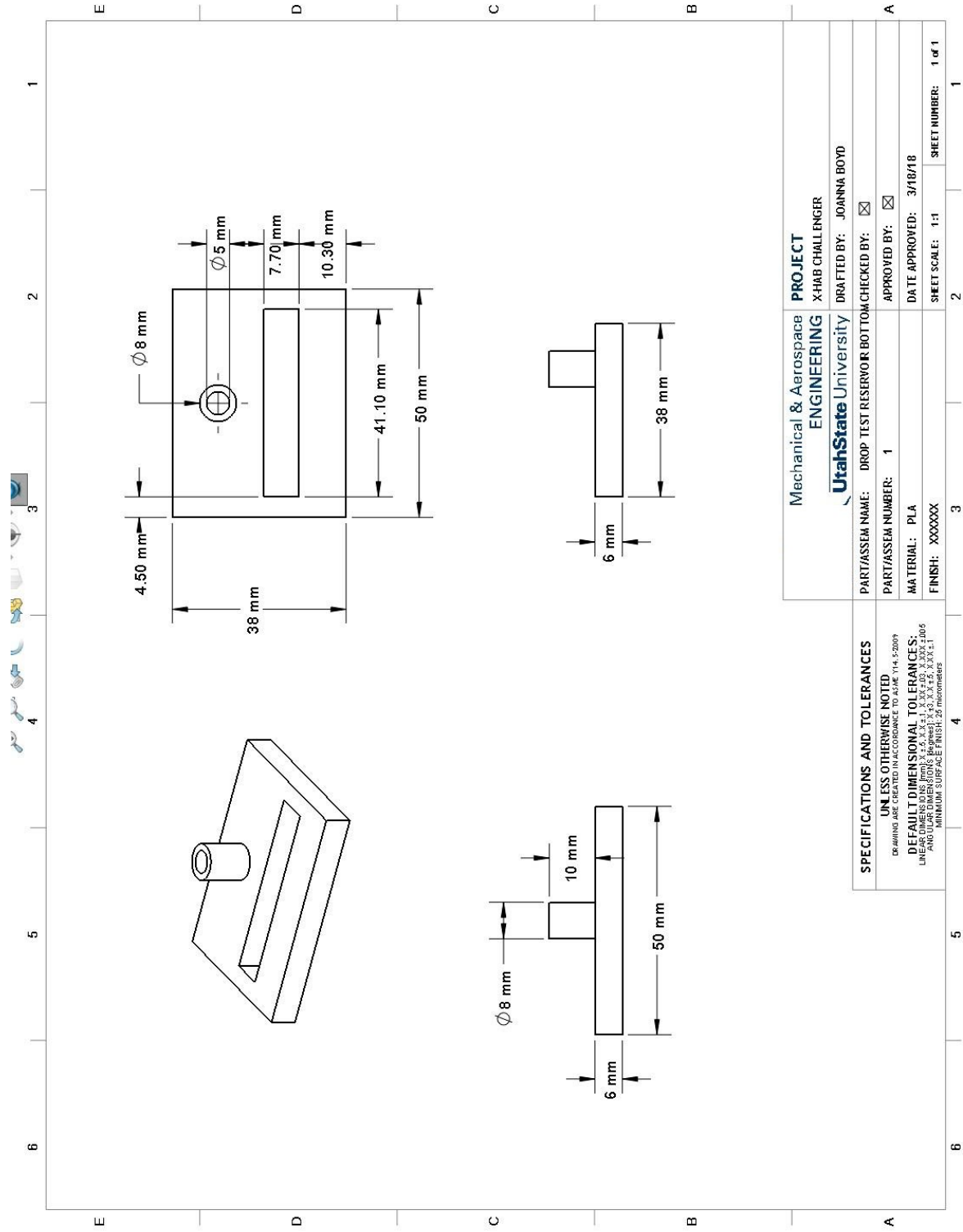


Figure D.3. Drop test reservoir



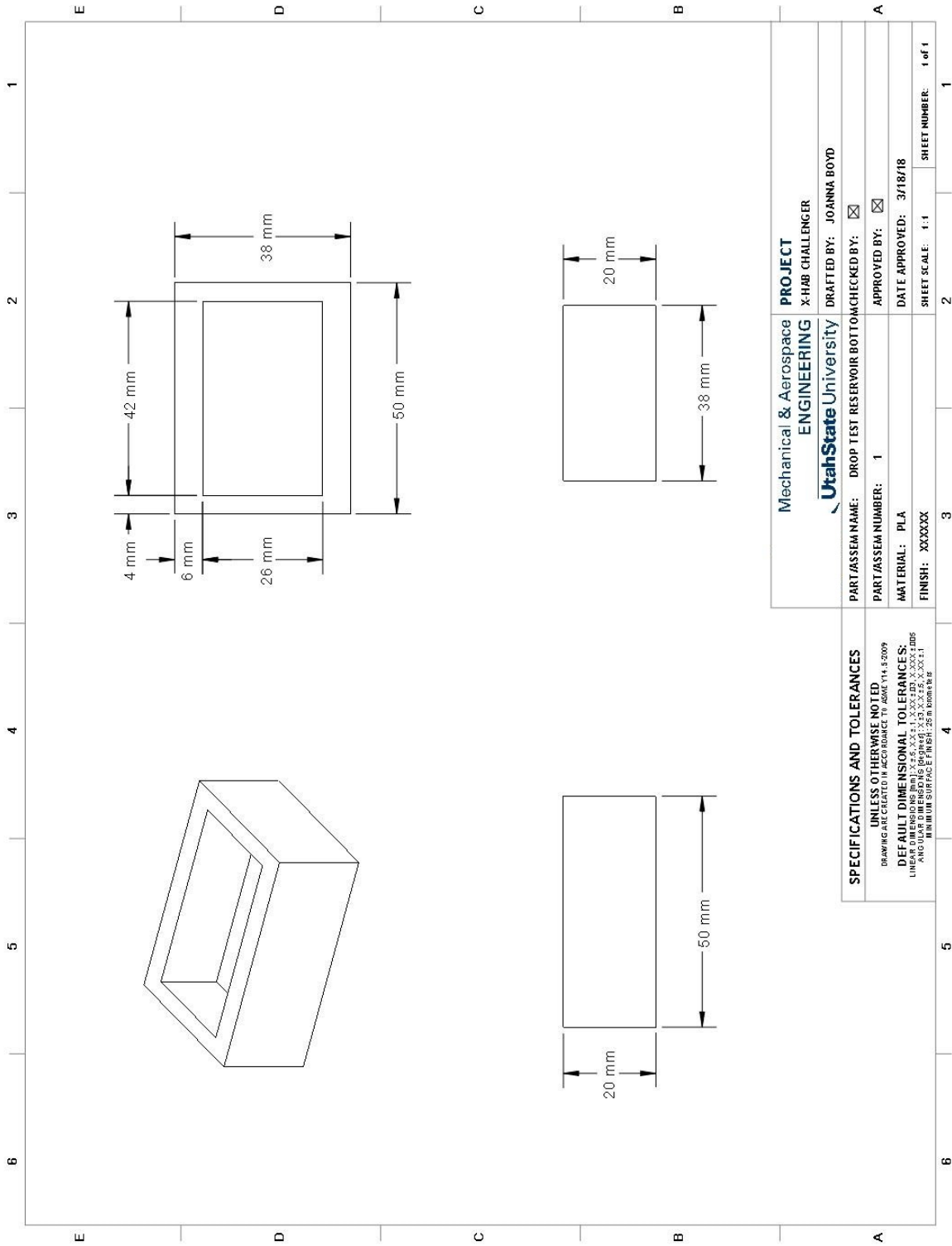


Figure D.4. Drop test reservoir

# E Housing Drawings

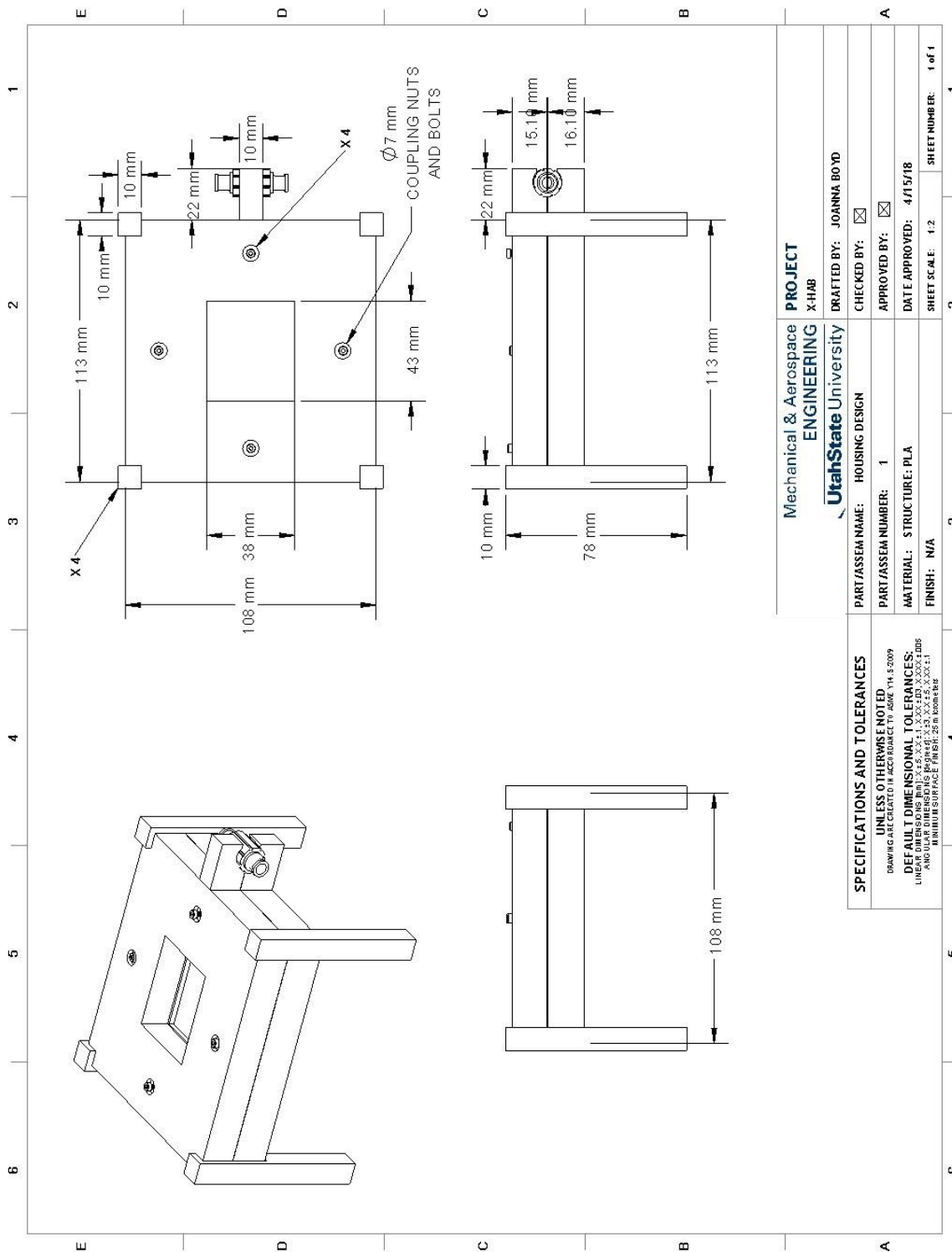


Figure E.1. Housing

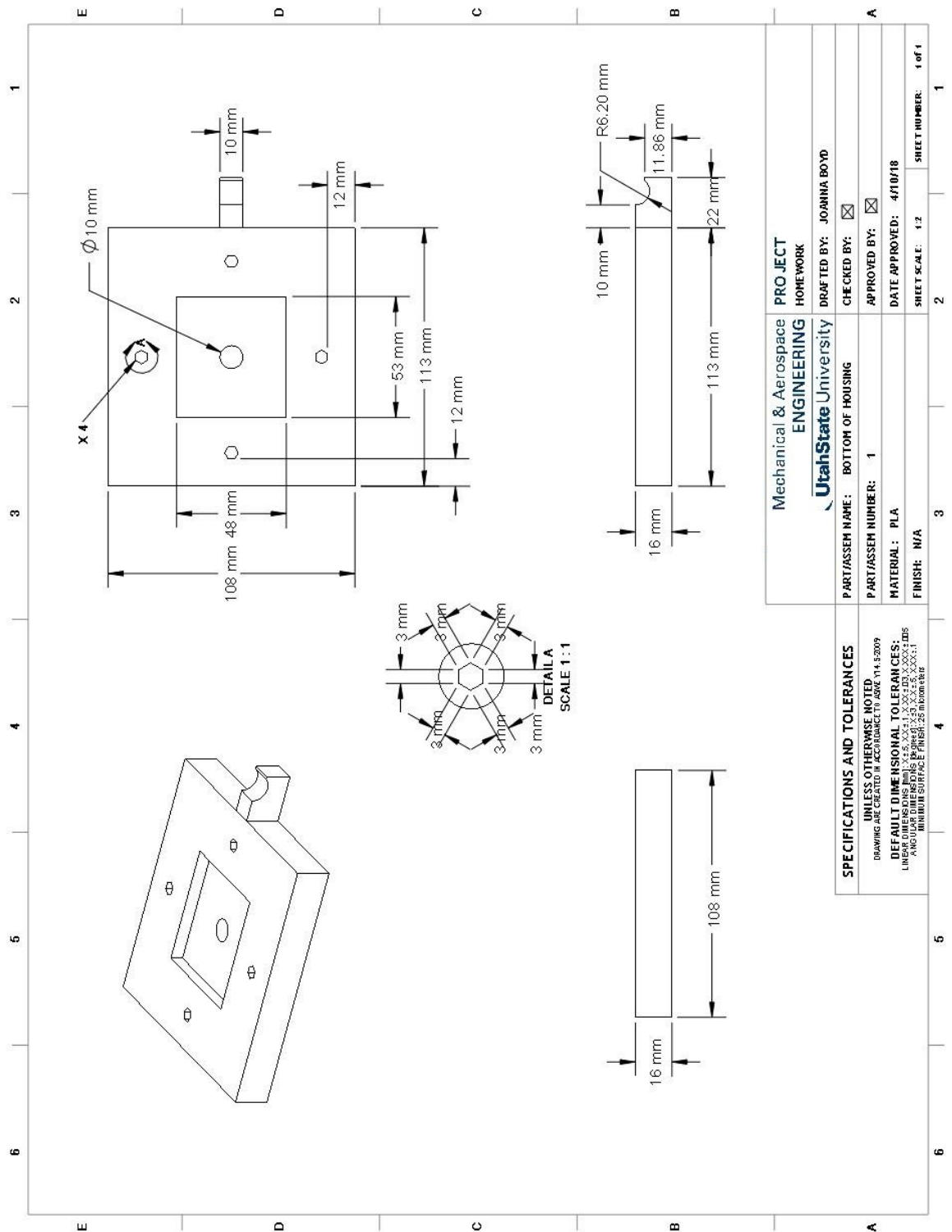


Figure E.2. Bottom housing

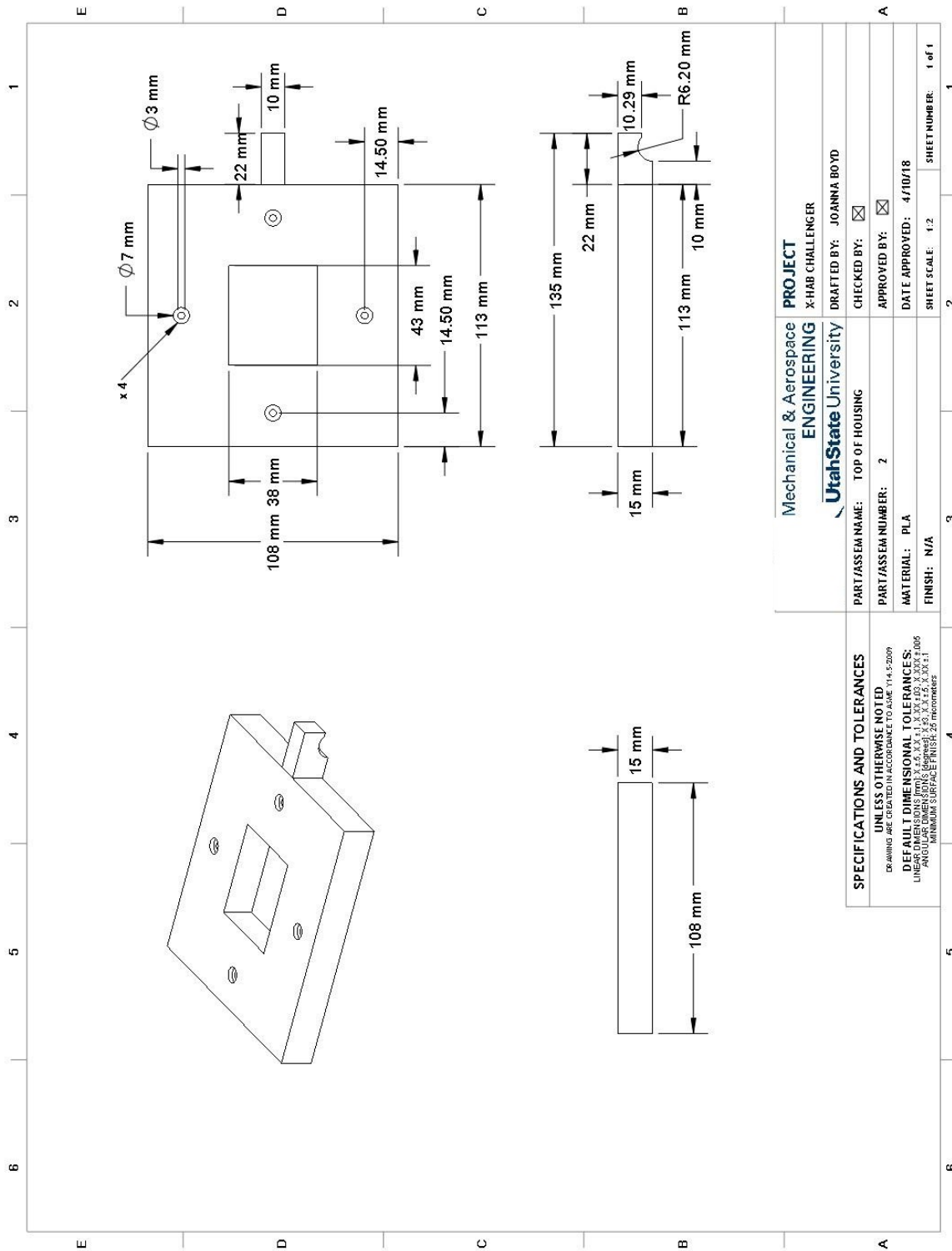


Figure E.3. Top housing

Mechanical & Aerospace ENGINEERING		PROJECT X-HAB CHALLENGER	
Utah State University		DRAFTED BY: JOANNA BOYD	
PART/ASSEMBLY NAME: TOP OF HOUSING		CHECKED BY: <input checked="" type="checkbox"/>	
PART/ASSEMBLY NUMBER: 2		APPROVED BY: <input checked="" type="checkbox"/>	
MATERIAL: PLA		DATE APPROVED: 4/10/18	
FINISH: N/A		SHEET SCALE: 1:2	
SPECIFICATIONS AND TOLERANCES		SHEET NUMBER: 1 of 1	
<p>UNLESS OTHERWISE NOTED DRAWING ARE CREATED IN ACCORDANCE TO ASME Y14.5-2009</p> <p>DEFAULT DIMENSIONAL TOLERANCES: LINEAR DIMENSIONS (mm): X .6, X .4, X .3, X .2, X .15, X .1, X .075, X .05, X .025 ANGULAR DIMENSIONS (DEG): X .5, X .3, X .2, X .15, X .1, X .075, X .05, X .025 MINIMUM SURFACE FINISH: 32 microinches</p>			

## F Outreach Poster

# X-Hab C3PO Project

eXploration Systems and Habitation (X-Hab) 2018 Academic Innovation Challenge Creative 3D Plant Optimization

Irene Beneze, Shelby Berrett, Carter Bodnar, Joanna Boyd, Jake Brockwell, Rebecca Brown, Emily Burgett, Kaitlin Burnash, Logan Crawford, Camille Daniels, Amanda Dennis, Brandon Furman, Datin Givida Jackson, Jackson Graham M.S, Camren Hansen, Scott Jones PhD, Cameron LeBaron, Nicholas Narrell, Ty Nicholas, Adreann Peel, Ryan Summers PhD, Timothy Taylor PhD, Joshua Wallace, Spencer Wendell M.S.

### Plant Growth in Space

“With the long-duration missions aboard the International Space Station (ISS), it has become clear that more emphasis needs to be placed on improving human habitability. The Vegetable Production System (Veggie) provides a means to supply crews with a continuous source of fresh food and a tool for relaxation and recreation.

Veggie can support a variety of experiments used to determine how plants sense and respond to gravity. The plants are harvested for further investigation and consumed by the crew members.” [1]

The Veggie is shown in the middle and 3D printed blocks are on either side.

Water floating on the ISS.

### 3D Printing

When astronauts are on the Space Station and something breaks, they may go months without access to new materials and parts to replace it. That is why a 3D printer is so useful. Within a few hours, a new part can be printed and in use. We decided to use a 3D printer to create our plant growth matrix to ensure it can be maintained and replaced by existing technology on the Space Station. Currently we are printing Nylon because of the hydrophilic properties.

A 3D Printer and the blocks to be used in the Veggie.

### Design using Capillary Action

Capillary action can be observed when water moves up a straw past the water level in the cup. The forces present between water molecules and the surface of the straw as well as intramolecular forces cause this movement up the straw. We decided to take advantage of this property of water and create a system that would use capillaries to draw water from the bottom of the Veggie to the plants sitting on top. A block with triangular tubes was created. The addition of channels going horizontally through the blocks was necessary to allow air to reach the plant roots.

### Water Properties in Microgravity

Looking at the water bubble sitting on a leaf shows some of the oddities found in microgravity. “The air bubble doesn’t rise because it is no lighter than the water around it -- there’s no buoyancy. The droplet doesn’t fall from the leaf because there’s no force to pull it off. It’s stuck there by molecular adhesion.

Sticky water. No buoyancy. These are some of the factors spacefarers must take into account when they plan the future. Suppose one sprays water onto the base of the plant. Will it trickle down to the roots? More likely it will stick to the stem or adhere the substrate in which the plant grows... Nevertheless, plants can flourish in spaceships. Recent experiments onboard the ISS prove it.” [2]

### Drone Drop

In order to get an idea of how our design will work in microgravity, it is necessary to minimize the effect of gravity. Using a drone, we are going to fly the blocks up to 300 ft in an air foil device. The blocks and an attached GoPro will then drop, reaching close to terminal velocity. This free fall will simulate conditions given in space travel and we will gather the data from the video.

Download - NASA Science Investigations: Plant Growth or SSI: Plants

## References

- Water and Astronaut: [https://www.nasa.gov/images/content/112515main\\_exp10\\_image\\_009hires.jpg](https://www.nasa.gov/images/content/112515main_exp10_image_009hires.jpg)
- Water on Leaf: [https://www.nasa.gov/audience/forstudents/5-8/features/space\\_gardens\\_feature.html](https://www.nasa.gov/audience/forstudents/5-8/features/space_gardens_feature.html)
- Smith, T. (2018, February 28). Vegetable Production System. Retrieved March 28, 2018, from [https://www.nasa.gov/mission\\_pages/station/research/experiments/383.html](https://www.nasa.gov/mission_pages/station/research/experiments/383.html)
- Drone: [https://www.yuneec.com/en\\_GB/camera-drones/typhoon-h/overview.html](https://www.yuneec.com/en_GB/camera-drones/typhoon-h/overview.html)
- Dunbar, B. (n.d.). The Physics of Space Gardens. Retrieved March 28, 2018, from [https://www.nasa.gov/audience/forstudents/5-8/features/space\\_gardens\\_feature.html](https://www.nasa.gov/audience/forstudents/5-8/features/space_gardens_feature.html)
- Veggie System: [https://www.nasa.gov/sites/default/files/thumbnails/image/iss054e054071\\_0.jpg](https://www.nasa.gov/sites/default/files/thumbnails/image/iss054e054071_0.jpg)
- 3D Printer: <http://www.zdnet.com/article/promising-trend-for-innovators-3d-printer-prices-are-falling/>

Figure F.1. Outreach poster